OXIDATIVE STRESS-INDUCED EPIGENETIC TRANSCRIPTIONAL MEMORY AS A MECHANISM OF PROGRAMMED ENDOTHELIAL DYSFUNCTION IN LARGE FOR GESTATIONAL AGE NEWBORN OF WOMEN WITH OBESITY

DISSERTATION ZUR ERLANGUNG DES DOKTORGRADES DER NATURWISSENSCHAFTEN (DR. RER. NAT) DER FAKULTÄT FÜR BIOLOGIE UND VORKLINISCHE MEDIZIN DER UNIVERSITÄT REGENSBURG

Vorgelegt von

Ivo Carrasco Wong

aus

Iquique – CHILE

im Jahr
2019

Das Promotionsgesuch wurde eingereicht am: 10.01.19

Die Arbeit wurde angeleitet von:

Prof. Dr. Paola Casanello, Pontificia Universidad Católica, Santiago, Chile

Prof. Dr. Gernot Längst, Universität Regensburg

Unterschrift:

Die vorliegende Arbeit mit dem Titel

OXIDATIVE STRESS-INDUCED EPIGENETIC TRANSCRIPTIONAL MEMORY AS A MECHANISM OF PROGRAMMED ENDOTHELIAL DYSFUNCTION IN LARGE FOR GESTATIONAL AGE NEWBORN OF WOMEN WITH OBESITY

vorgelegt von Ivo Carrasco Wong

entstand unter der gemeinsamen Betreuung

der Universität Regensburg

und

der Pontificia Universidad Católica de Chile

im Rahmen des internationalen Promotionsprogramms *iP*UR

als Doppelpromotion

ACKNOWLEDGEMENTS

My deepest gratitude to all those who supported me in this process.

FUNDING

This thesis was funded by the Chilean National Fund for Scientific and Technological Development, FONDECYT #1171406 and #11209281

TABLE OF CONTENTS

FIGURES INDEX

CHAPTER I

CHAPTER II

CHAPTER III

TABLE-INDEX

ABBREVIATIONS

5hmC	5-hydroxymethylcytosine
5mC	5-methylcitosine
ARE	Antioxidant response element
ATP5F	ATP synthase peripheral stalk-membrane subunit b
AUC	Area under the curve
BACH	BTB domain and CNC homolog
Brd4	Bromodomain-containing protein 4
CBP	CREB Binding Protein
CDK9	Cyclin-dependent kinase 9
C-HUAEC	HUAEC isolated from control newborn
CpG	Dinucleotide CG
CRMs	*cis*-regulatory modules
CTCF	CCCTC DNA element binding factor
CTD	RNAPII carboxy-terminal domain
DHFR	dihydrofolate reductase
DNMT	DNA methyl transferase
DOHaD	Developmental origin of health and disease
DSIF	DRB-Sensitivity-Inducing factor
E1	Enhancer 1
E2	Enhancer 2
EC_{50}	Half-maximal effective concentration
ECs	Endothelial cells
eNOS	Endothelial nitric oxide synthase
eRNAs	RNA transcribed at enhancer regions
ETM	Epigenetic transcriptional memory
FOXO3A	Forkhead Box O3
GCLM	Glutamate-Cysteine Ligase Modifier Subunit
GPX1	Glutathione peroxidase 1

GSH	Glutathione
H_2O_2	Hydrogen peroxide
H3K27me3	Tri-methylation of lysine 27 of Histone 3
H3K4me1	Mono-methylation of lysine 4 of Histone 3
H3K4me2	Di-methylation of lysine 4 of Histone 3
H3K4me3	Tri-methylation of lysine 4 of Histone 3
H3K9ac	Acetylation of lysine 9 of Histone 3
HB_2	Dihydrobiopterin
HB_4	Tetrahydrobiopterin
HDAC1	Histone Deacetylase 1
HMOX1	Heme oxygenase 1
HO•	Hydroxyl anion
HUAEC	Human umbilical artery endothelial cell
IL2	Interleukin 2
IUGR	Intrauterine growth restriction
Keap1-Cul3/Rbx1 complex	NRF2 ubiquitin ligase complex
LGA	Large for gestational age
LGA-HUAEC	HUAEC isolated from LGA newborn
lncRNA	long non-coding RNA
MAF	Avian Musculoaponeurotic Fibrosarcoma
MBD	methyl-CpG-binding domain
MeCPs	methyl-CpG-binding proteins
MEF cells	Mouse Embryonic Fibroblasts
MLL	mixed lineage leukemia
ncRNA	non-coding RNA
Neh domain	Nrf2-ECH homology domain
NELF	Negative elongation factor
NF-E2 p45	Nuclear Factor, Erythroid-Derived 2 45 KDa
NO	Nitric oxide
NOX	NAD(P)H oxidase

NQO1	NAD(P)H Quinone Dehydrogenase 1
NRF1	Nuclear Factor, Erythroid 2 Like 1
NRF2	Nuclear Factor, Erythroid 2 Like 2
NRF3	Nuclear Factor, Erythroid 2 Like 3
NURD/Mi-2/CHD	Nucleosome Remodeling Deacetylase complex
$O2•-$	Superoxide anion
OM	Obese mother
$ONOO^-$	Peroxynitrite
ORAC	Oxygen radical absorbance capacity
OxS	Oxidative stress
OxS-ETM	ETM induced by oxidative stress
P/T	Primed and Treated
P/UT	Primed and Untreated
P	Primed
P300	E1A-Binding Protein, 300kD
p66shc	SHC Adaptor Protein 1
p90	percentile 90^{th}
PIC	Pre-initiation complex
PMA/I	Phorbol-Myristate-Acetate and Ionomycin
PRDX3	Peroxiredoxin 3
PRDX6	Peroxiredoxin 6
pS5-RNAPII	RNAPII phosphorylated at serine 5 of CTD
P-TEFb	Positive transcription elongation factor-b
RISC	RNA-induced silencing complex
RNAPII	RNA polymerase II
RNS	Reactive nitric species
RO•	Alkoxyl anion
RO2•	Peroxyl anion
ROS	Reactive oxygen species

RPLP0	Ribosomal Protein Lateral Stalk Subunit P0
RPLP2	Ribosomal Protein Lateral Stalk Subunit P2
RUNX2	Runt Related Transcription Factor 2
S.E.M	Standard error of the mean
SEC	Super elongation complex
SOD	Superoxide dismutase
tBHP	tert-Butyl Hydroperoxide
tBHQ	tert-Butyl Hydroquinone
TBP	Tata binding protein
TET	ten-eleven translocation
TF	Transcription factor
TFII	General transcription factors
TSS	Transcription start site
TXNDR	Thioredoxin reductase
UP/T	Unprimed and Treated
UP/UT	Unprimed and Untreated
UP	Unprimed
y.o.	Years old

RESUMEN

La obesidad es un problema de salud pública mundial. Contrariamente a la idea general de que los resultados de un estado de obesidad solo afectan al mismo individuo, ahora está claro que existe una asociación directa entre la obesidad materna y un aumento de los riesgos cardiometabólicos en la progenie. En varias enfermedades cardiovasculares, la disfunción endotelial suele ser el evento más temprano que se presenta, mucho antes de que se pueda evidenciar clínicamente la hipertensión. En las arterias placentarias y umbilicales de recién nacidos grandes para su edad gestacional y de madres obesas (LGA-OM, su acrónimo en inglés), se ha descrito una disfunción endotelial relacionada con una alteración en la respuesta antioxidante y niveles elevados de marcadores oxidativos circulantes. Sin embargo, no hay evidencia, hasta el momento, que muestre el posible efecto del ambiente pro-oxidante inducido sobre la maquinaria antioxidante de células endoteliales umbilicales de recién nacidos LGA-OM; incluyendo el desconocimiento de cómo la alterada fisiología perinatal presente a lo largo del desarrollo fetal, puede alterar el rendimiento vascular. En esta tesis, se probó la hipótesis de que el estrés oxidativo crónico inducido por la obesidad materna puede modular la fisiología vascular fetal mediante una modificación en el rendimiento de la maquinaria antioxidante. Al usar una sonda fluorescente sensible al H_2O_2, se evidenció una mayor capacidad antioxidante cuando se indujo un desafío oxidativo exógeno en células endoteliales de la arteria umbilical humana (HUAEC) aisladas de recién nacidos LGA-OM. Esta condición no solo estaba relacionada con una expresión basal del gen *HMOX1* elevada; sino también, con una transcripción exacerbada del gen *GPX1*; asociado a un estado abierto de la cromatina en el promotor, de este último, sugiriendo la participación de mecanismos epigenéticos. Por lo tanto, propusimos que posiblemente una activación constante del gen *GPX1* debido al estrés oxidativo ambiental podría inducir el rendimiento de respuesta exacerbada mediante la adquisición de una memoria transcripcional epigenética (ETM, su acrónimo en inglés). Para evaluar esta idea, aplicamos un protocolo de "doble impacto" a las células de control HUAEC y EA.hy926. Al contrario de lo que se esperaba, solo el gen *HMOX1* mostró una respuesta similar a la ETM. En dicho gen, el primer desafío oxidativo indujo un estado abierto de cromatina tanto en su promotor proximal como en el enhancer 2 (ubicado a 9 kilobases río arriba); los que se asociaron, respectivamente, a un

enriquecimiento de RNAPII pausada y al factor de transcripción NRF2. Todos los datos obtenidos en esta tesis indican que el estrés oxidativo, por sí mismo, podría actuar como un factor que puede modular la futura respuesta del gen *HMOX1*; pero, que no es suficiente para modular otros genes antioxidantes como *GPX1*. Como perspectiva, proponemos que ETM podría ser parte del mecanismo involucrado en la programación fetal de la disfunción endotelial *in vivo*; Aunque, aún es necesario encontrar la señalización específica.

ABSTRACT

Obesity is a worldwide public health problem. Contrary to the general idea that the outcomes from an obesity state only affect to the individual, it is now clear that a direct association between maternal obesity and an increased cardiometabolic risks in the progeny. In several cardiovascular diseases, endothelial dysfunction is usually the earliest event present, much before hypertension can be clinically evidenced. In placental and umbilical arteries from large for gestational age newborn from obese mothers (LGA-OM), endothelial dysfunction has been described, related to an alteration in the antioxidant response and to elevated levels of circulating oxidative markers. However, there is no evidence at the time showing the possible effect of the pro-oxidant environment induced in LGA-OM on the antioxidant machinery in umbilical endothelial cells; including how the altered perinatal physiology present throughout fetal development, can alter the vascular performance. In this thesis, the hypothesis that maternal obesity-induced chronic oxidative stress can modulate the fetal vascular physiology by a modification on the antioxidant machinery performance was tested. Using an H_2O_2-sensitive fluorescent probe an increased antioxidant capacity when exposed to exogenous oxidative challenge was evidenced in human umbilical artery endothelial cells (HUAEC) isolated from LGA-OM. This condition was not only related to an elevated basal *HMOX1* gene expression but also to an over-responsive *GPX1* gene transcription; associated to an open state of the chromatin in the promoter, suggesting the involvement of epigenetic mechanisms. Thus, we proposed that possibly a constant activation of the *GPX1* gene due to the environmental oxidative stress could induce the over-responsive performance by the acquisition of an epigenetic transcriptional memory (ETM). To evaluate this idea we applied a double hit protocol to control-HUAEC and EA.hy926 cells. Contrary to what was expected only *HMOX1* gene showed an ETM-like response. However, when induced by the first oxidative challenge, an open state of chromatin in both its proximal promoter and enhancer 2 (located 9 kilo base upstream) were associated to an enrichment of paused-RNAPII and NRF2 transcription factor, respectively. All the data indicate that oxidative stress, by itself, could act as a factor that can modulate the future response of *HMOX1* gene, but it is not sufficient to modulate other antioxidant genes and *GPX1*. As perspective, we propose that ETM could be part of the mechanism involved in the fetal programming of endothelial dysfunction *in vivo*; although, still is necessary to find the specific signaling.

CHAPTER 1

GENERAL INTRODUCTION

THE MOLECULAR BASES OF VASCULAR PROGRAMMING IN LARGE FOR GESTATIONAL AGE NEWBORN FROM WOMEN WITH PREGESTATIONAL OBESITY

GENERAL INTRODUCTION

THE MOLECULAR BASES OF VASCULAR PROGRAMMING IN LARGE FOR GESTATIONAL AGE NEWBORN FROM WOMEN WITH PREGESTATIONAL OBESITY

Introduction

Developmental origin of health and diseases (DOHaD), also known as fetal programming, is the field of medical sciences that studies how certain conditions in susceptible periods of development can modulate the physiology of an individual at birth and throughout life. Many epidemiological reports have described that maternal nutritional status, as well as some obstetrical conditions, can increase cardiometabolic risk in the offspring.

Obesity is a global epidemic[1], and an important public health issue due to the elevated risk of developing chronic, non-communicable diseases[2] such as type 2 diabetes, obesity, hypertension, among others. Chile is not far from this situation and the last national health survey showed that 31,2% of the adult populations presents obesity[3]. Near 31% of women in reproductive age begin their pregnancy with obesity[3]. Maternal obesity is one of the leading causes of infant obesity and an elevated risk of cardiometabolic disease[4].

When neonatal weight is greater than p90 for a determined gestational age, that newborn is classified as large for gestational age (LGA)and macrosomic, when the birth weight is ≥ 4 kg.[5–7]. The elevated cardio-metabolic risk in individuals born LGA from women with pregestational obesity has been described through all ages: as early as the neonatal period[8], childhood[9,10], adolescence[9], and adulthood[11].

Big efforts have been done to try to understand how vascular physiology changes during the intrauterine period. In humans, the earliest time window to obtain fetal vascular samples are the placenta and umbilical cord collected at delivery. In placental chorionic arteries, isolated from LGA newborn, endothelial dysfunction was described [8,12]. These findings indicate that the altered nutritional status of the mother influences the setting of vascular physiology of the offspring actually begins during fetal life.

The main aim of this thesis is to find the molecular/epigenetic mechanisms that underlie the altered antioxidant defense associated with endothelial dysfunction in large for gestational age newborn (LGA) from obese mothers. Primary cell culture of human artery endothelial cell (HUAEC) isolated from control and LGA newborn was used as a model to find basal differences, and those unveiled after an acute oxidant stimulus, on the antioxidant capacity at the cellular and molecular level. Additionally, EA.hy926 endothelial cell line was used to evaluate if pro-oxidant agents can induce epigenetic transcriptional memory (ETM).

In order to offer a better understanding of the results and discussion showed in the following chapter, the general topics of endothelial cell physiology, epigenetic and gene expression regulatory mechanism are briefly reviewed.

Programming of vascular dysfunction

The relationship between birthweight and cardiovascular performance during life has been previously indicated. Maternal obesity has been associated with cardiovascular-related diseases such as angina, stroke and peripheral vascular disease in the offspring in adulthood[13]. Endothelial cells (ECs) are central in vascular function,[14] modulating smooth muscle tone,[15] immune cell adhesion, and activation and its altered function is an early event in

arteriosclerosis[16], hypertension[17] and diabetes[18]. Endothelial dysfunction is defined as "*an imbalance between vasodilating and vasoconstricting substances produced by (or acting on) endothelial cells*"[19], and vascular programming has been broadly studied during fetal life. In 150 days old mice progeny from dams fed a high-fat diet, showed an altered endothelium-dependent relaxation, induced by low levels of nitric oxide (NO), Endothelium-Derived Hyperpolarizing Factor (EDHF) or prostacyclin PGI2, together with increased systolic pressure[20]. It has been evidenced that the setting of vascular performance starts during development, *in utero*. Schneider et al. evidenced endothelial dysfunction in chorionic arteries isolated from IUGR and LGA newborn and suggested that oxidative stress was at least one of the components of the abnormal vascular tone and NO-dependent relaxation observed[8].

Oxidative stress (OxS)

Oxidative stress occurs when reactive oxygen species (ROS) and reactive nitrogen species (RNS) surpass the antioxidant defense capacity in a cell or organism[21]. The term ROS describes O_2-derived free radicals such as superoxide anion (O2•−), hydroxyl (HO•), peroxyl (RO2•) and alkoxyl (RO•); as well, O_2-derived free nonradicals such as hydrogen peroxide (H_2O_2)[22]. In endothelial cells, high superoxide and NO production induce the formation of peroxynitrite ($ONOO^-$)[27], which nitrates tyrosine residues to form nitrotyrosine in proteins[28]. In general, ROS and their derivates can attack most of the functional molecules in the cell including lipids[29], proteins[30], and DNA[31].

To deal with pathophysiological levels of ROS/RNS, cells possess complex interconnected antioxidant enzymatic and non-enzymatic systems. Members of the enzymatic system are SOD, catalases, glutathione peroxidases (GPx), thioredoxin and peroxiredoxin[32]. The non-

enzymatic system includes glutathione (GSH), vitamin C, bilirubin, vitamin E, carotenoids and flavonoids[33]. In parallel, several oxidative stress-induced transcription factors (TF) like SP1[34], Oct-1[35], FOXO[36], PPARγ[37], HIF1α[38], and NRF2[39] transactivate antioxidant enzymes coding genes.

The influence of maternal obesogenic diet on redox status and antioxidant coding-protein gene expression in the offspring has been already demonstrated. Wistar rat pups from cafeteria-diet-fed dams showed a reduced oxygen radical absorbance capacity (ORAC) and catalase activity in blood together with an elevated plasma hydroperoxide, carbonyl protein levels, and SOD activity[40]. Reduced gene expression of hepatic *Sod1*, *Sod2*, *Gpx1* was reported in the offspring of dams fed with high-fat diet during gestation and lactation[41]. In humans, high levels of catalase and SOD activities were found in cord blood of macrosomic newborn from obese mothers, together with elevated levels of oxidative stress markers in both peripheral bloods of mother and fetus[42].

NRF2, the oxidative stress sensor at a cellular level

NF-E2 related- factor 2 (NRF2) has been named a master transcription factor since its ability to transactivate a plethora of antioxidant- and anti-xenobiotic-protein-coding genes[43]. NRF2 is a leucine zipper transcription factor and, together with NRF1, NRF3, NF-E2 p45, and BACH belong to the Cap'n'Collar transcription factor family[44].

The transactivation of the gene targets of NRF2 occurs mainly by its stabilization[45.] In a steady-state cell, NRF2 is constantly polyubiquitinated by the KEAP1-CUL3/RBX1 complex[46]; thus, the half-life of NRF2 is between 15 mintutes[45] to 3 hours[46]. A direct attack to cysteine residues in KEAP1 by ROS can interrupt NRF2-KEAP1 interaction inducing NRF2 release[47]. Similarly, the phosphorylation of serine 40 of NRF2, among other post-

translational modifications, has been observed generating the same effect[48]. Once NRF2 is released, it translocates to the nucleus[49]; where it heterodimerizes with small MAF protein G or K (sMAF-G/K) that is already bound to antioxidant response elements (ARE) [50] which consensus sequence is 3´-RTKAYnnnGCR- 5´[51,52], located upstream of genes that respond to OxS[53]. For a complete activation, NRF2 is acetylated by CBP/p300 acetyl-transferase[54,55]. Interestingly, BACH1 also binds to ARE elements but induces repression of the gene expression (Figure 1)[56].

Mainly from cancer studies, the suggestion that the NRF2-ARE pathway can be altered by epigenetic mechanisms has emerged. In a human cell model of lung cancer, H3K27 tri-methyltransferase EZH2 binds to NRF2 promoter inducing its repression[57]. Likewise, changes in TET-dependent DNA methylation pattern in *NRF2,* and the upregulation of *NRF2* and *HMOX1* mRNA were associated with an increase in tumor resistance to the chemotherapeutic agent, 5-FU[58]. Those reports suggest that antioxidant coding genes transcribed by NRF2 could be controlled by epigenetic mechanisms in pathologies as obesity.

Epigenetic regulation of gene expression

Currently the term epigenetic refers to two different fields of study: 1) To explain how diverse phenotypes are inherited without a change in DNA sequence; and 2) To study how multiple cellular differentiation occurs from a single cell during development[59]. Almost all the epigenetic mechanisms that control the expression of genes occurs in the chromatin, which is the multimeric structure formed by nucleosomes. It has been described that nucleosomes are 145-147 bp of DNA wrapping histones, an octamer protein complex[60].

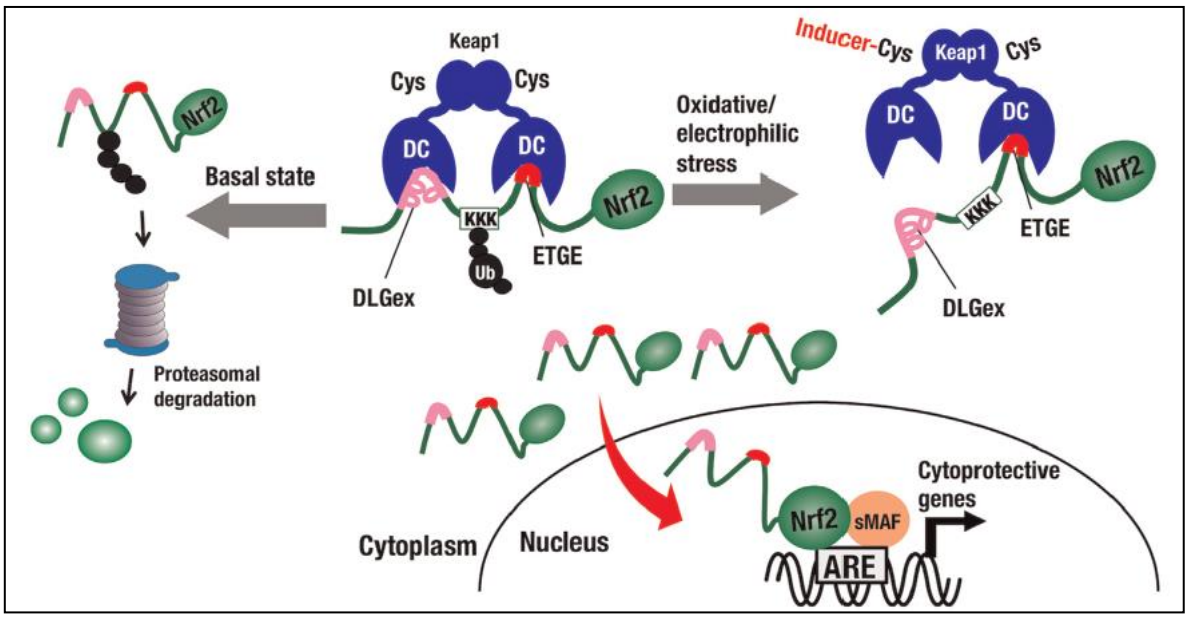

Figure 1. Schematic model of the NRF2–KEAP1 signalling pathway. Under unstressed conditions, NRF2 is degraded in a KEAP1-dependent manner via the ubiquitin (Ub)–proteasome pathway. The KEAP1 homodimer binds to single NRF2 molecules by means of two-site binding utilizing DLGex and ETGE motifs. Both motifs individually bind to a pocket in the DC (double glycine repeat and C-terminal) domain of KEAP1. Lysine (K) residues that reside between the two motifs are the targets of ubiquitination. In response to oxidative and electrophilic stresses, NRF2 inducers inactivate KEAP1 via the modification of cysteine residues (Cys), and NRF2 is stabilized, and de novo synthesized NRF2 translocates into the nucleus. NRF2 heterodimerizes with small Maf proteins (sMaf) and activates target genes through binding to the antioxidant response element (ARE), exerting cytoprotective effects against various noxious insults[61].

DNA methylation

Methylation refers to a transference of a methyl group from an S-adenosyl-L-methionine, SAM, (donor) to the position 5´of a cytosine which is located beside guanine (dinucleotide called CpG), generating a 5-methylcytosine (5mC)[62]. CpG methylation is associated with gene repression, which is inherited through cell division[63]. Mainly by a reduction of transcription factors biding when regulatory elements in DNA include a methylable CpG[64] or by recruitment of gene repressor protein complex[65–68].

Three methyltransferases in mammalian cells, DNMT1, DNMT3a and DNMT3b[62] have been described. From those, DNMT1 is the only one that reproduces a CpG methylation pattern in a new DNA strand during cell division[69]. Both DNMT3a and DNMT3b generate de novo methylation, thus leading to a new methylation pattern during gametogenesis, embryo development, and cellular differentiation[70,71].

The finding that the methyl group from cytosine can be transformed and, thus, eliminated changed all the paradigm of CpG methylation as a permanent modification. The elimination Ten-eleven translocation (TET) family enzymes are crucial enzymes for the remotion of the methyl group in cytosine because they can oxidize 5mC producing 5-hydroxymethylcytosine (5hmC)[72].

Post-translational histone modification

The nucleosome-forming histones, named H2A, H2B, H3, and H4[73], have a C-terminal globular domain and an N-terminal flexible tail, by which they bind to each other and interact actively with DNA, respectively[64]. The post-translational modification of the histone tails includes arginine (R) methylation; lysines (K) methylation, acetylation, ubiquitination and sumoylation; and serine (S) and threonine (T) phosphorylation[74,75]. Although the histone modifications act in a complex manner a "histone code" model has been proposed, describing

that a specific histone modification pattern is related to a chromatin state induced by recruitment of non-histone proteins[76]. Of them, the histone acetylation occurs in lysine residues and is associated with gene expression[77,78.] Acetylated lysine residues can be deacetylated by histone deacetylase (HDAC) [78]. The histone deacetylation is related to gene repression; even more, methylated DNA recruits HDAC and methyl-CpG-binding proteins (MeCPs)[65,79,80]. The methylation in K4, K36, and K79 of H3 and K20 of H4 are associated with gene expression; meanwhile, histone 3 K9 and K27 methylations are related to gene repression[64]. Also, the methyl group added to histone tails can be removed by the action of histones demethylases (HDM) [81].

Histones variants

Histone variants differ in a small number of amino acids in comparison with canonical histones[82]. Using the D. melanogaster model, H3.3 variant was found to be incorporated into chromatin in a DNA-replication-independent manner, showing a preferential enrichment in actively transcribed chromatin[83]. H2A.X variant is enriched in transcription start site of genes and present a negative correlation with 5mC; even more, its phosphorylation strongly marks DNA double-strand breaks in DNA[82]. It has been evidenced that dedicated machinery that recognizes select histone variant is able to induce a rapid exchange of histone variant in chromatin, as the H2A.Z variant exchange by SWR1 chromatin remodeling complex[84].

ATP-dependent chromatin remodeling complexes

Those complexes are energy-driven multiprotein machineries, that allow the access to specific histones or DNA regions by altering nucleosome positions[85]. It has been proposed that ATPase-remodeling complexes act first by a partial releasing of DNA from histones (Looping) allowing histone movement (Sliding)[86]. Other authors have indicated that complete eviction of histones can also occur[87]. At the moment 4 families of ATPase-

remodeling complex have been identified: SWI/SNF[88], ISWI[89], NURD/Mi-2/CHD[90], and INO80[91].

Non-coding RNAs (ncRNAs)

In human cells, the most studied short ncRNA are miRNA; which, after several processes from its genesis, end up as RNAs of 21 nucleotides of length that are loaded in RNA-induced silencing complex (RISC) and used as a guide to repress mRNA translation[92]. In the other hand long-non-codings RNAs (lncRNAs) basically, seem to have 3 main functions: 1) To shape nuclear organization[93–95], 2) to capture miRNAs[96] and 3) to modify gene expression. For the last, an example is the lncRNA RMST that regulates the correct localization SOX2 transcription factor binding in neurogenesis[97].

Epigenetic mechanisms have been defined as crucial during development. In that period critical processes such as dosage compensation[98], genes imprinting[99], and protection against transposable elements ocurrs[100]. However, epigenetic mechanisms also participate in the inheritable fine-tuning of gene expression, such as epigenetic transcriptional memory.

Epigenetic Transcriptional Memory (ETM)

It has been described that some inducible genes are expressed faster and stronger when they are previously transcribed, several cell cycles before. The fact that the first gene transactivation is "remembered" by the chromatin has been called epigenetic transcriptional memory (ETM).[101,102,103,104,105]. The events and mechanisms that control ETM have been studied mainly in eukaryotic cells, in both yeast and human cells. This memory can be maintained for four or five cell divisions, without any re-stimulation in the meantime[103,105,106]. The features that characterize ETM can be summarized in 1) a second gene induction is faster and stronger compared to non-treated cells[101]; 2) the "memory" is maintained for four to five cell divisions[105]; 3) the locus of genes that acquire ETM are

recruited to nuclear boundary during gene transcription and they stay there for 4 to 12 hours after gene expression[101]; 4) an open state of the chromatin at the gene proximal promoter[103]; 5) a long-range interaction between gene promoter and *cis*-regulatory modules (CRMs) sustained by cohesines[107], forming a chromatin loop; 6) incorporation of histone variants H2A.Z to proximal-promoter chromatin regions[101,104]; 7) enrichment of H3K4me2 histone modification and poised-RNAPII during the "resting period" after first activation[102,106] (Figure 2).

Mechanisms that regulate gene transcription

For better understanding, some of the mechanisms of gene transcription regulation are exposed bellow, with special focus in paused-RNAPII.

Transcription initiation

Classically, gene transcription cycle has been divided into three phases; initiation, elongation and termination[108,109]. Initiation of transcription is a highly regulated process, which includes sequential events. First, the binding of specific activators, as transcription factors (TF), to specific sequences induces the recruitment of chromatin remodeling complexes in order to make the core promoter accessible to transcriptional machinery[110,111]. Then, the pre-initiation complex (PIC) is formed by the assembly of general transcription factors (TFII—A, -B, -D, -E, -F and –H) and RNAPII[112]. TFII-H generates the TSS DNA melting and one strand is loaded into RNAPII cleft, forming the open promoter complex[113]. TFII-B helps RNAPII find the TSS starting the productive elongation phase, called promoter clearance[114]. Initiation factors stay at the core promoter, forming the promoter-bound scaffolds, which facilitate the re-initiation of another RNAPII[108].

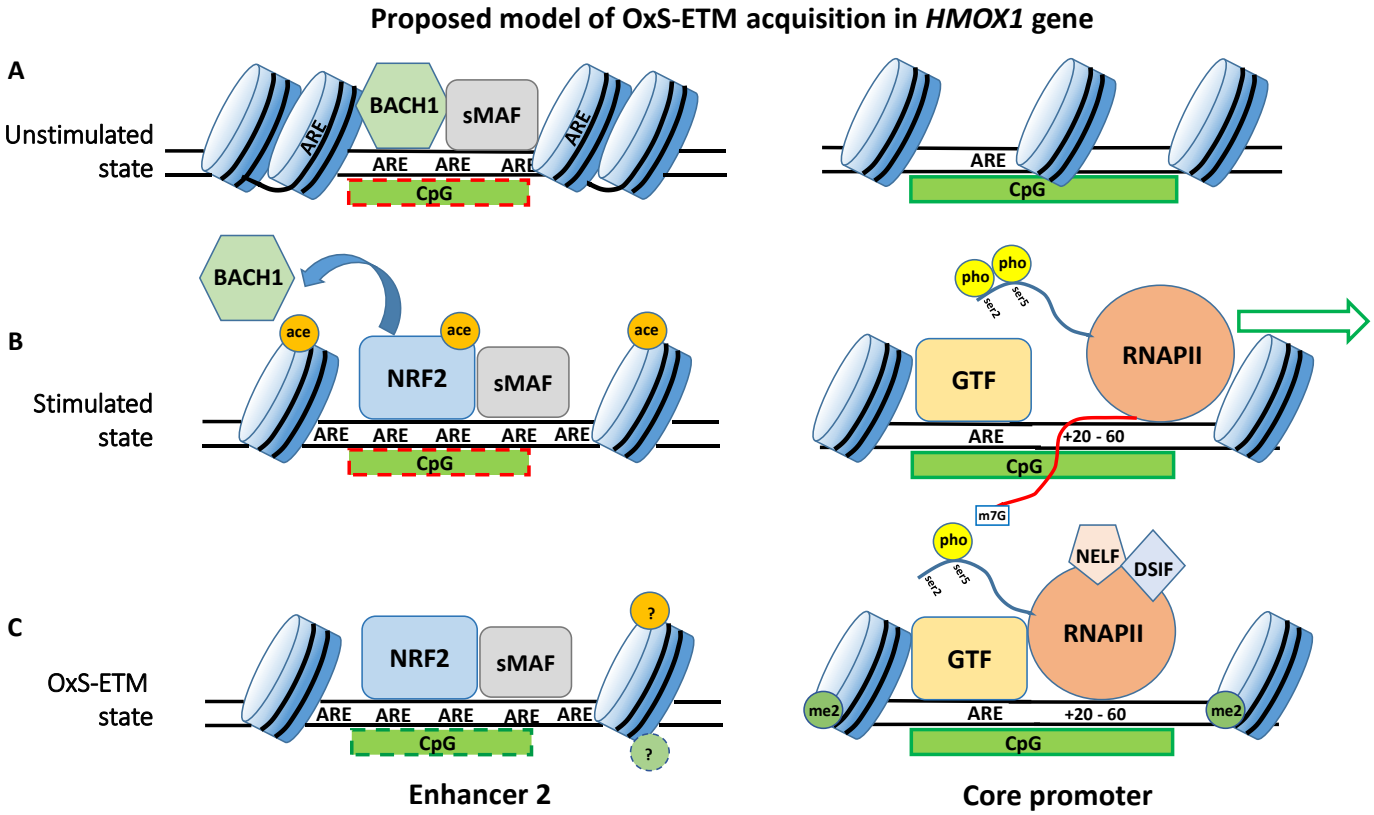

Figure 2. Proposed model of oxidative stress-ETM acquisition in the *HMOX1* gene. A) In an unstimulated state, Enhancer 2 has a closed-state of the chromatin (represented by ARE elements found in the nucleosome wrapping DNA), and BACH1 co-binding with sMAF proteins on non-canonical ARE sites; CpG could be methylated favoring closed chromatin in that region. Although the gene has a basal activity, the proximal promoter is represented as closed, with completely unmethylated CpG Islands. B) In a stimulated state, with gene expression, at Enhancer 2 the chromatin structure becomes more relaxed; BACH1 is released allowing NRF2 binding to sMAF protein on ARE; CBP/P300 acetyltransferase (not showed) acetylate histones nearby and NRF2 for full activation. Relaxed chromatin at the proximal promoter allows the binding of general transcription factors (GTF) and RNAPII. During the initiation step, serine 5 of RNAPII is phosphorylated by TFIIH kinase (not showed); the productive elongation step is induced by recruitment of P-ELFb (not showed), which phosphorylates serine 2. C) In the OxS-ETM state, Enhancer 2 maintains an open state of chromatin where NRF2 is enriched with sMAF co-activator protein. CpG demethylation in non-canonical ARE sites could facilitate NRF2 enrichment. At proximal promoter paused-RNAPII is enriched, maintained at pausing region (+20-60 pb) by NELF and unphosphorylated DSIF; H3K4dimethylation (ETM hallmark in pro-inflammatory ETM model) could be present; CpG island pattern remains without changes.

Carboxy-terminal domain (CTD) RNAPII phosphorylation

RNAPII holoenzyme is formed by a core complex of 12 subunits and a sub-complex of two subunits[115]. In human, Carboxy-Terminal Domain (CTD) of subunit 1 (Rpb1) is formed by a 52 tandem repetitions of a heptapeptide sequence Tyr1-Ser2-Pro3-Thr4-Ser5-Pro6-Ser7 (YSPTSPS)[116]. Different phosphorylation of serine residues into CTD has been associated with the different phases of the transcription cycle, so-called CTD code[117]. Thus, phosphorylation of serine 5 (pS5) by cyclin-dependent kinase 7 (CDK7) happened at the initiation phase, and its level decreases as RNAPII moves into the gene body[118–120]. Serine 2 phosphorylation by ctk1[121] occurs during productive elongation phase, and it is de-phosphorylated at the end of transcription associated with RNAPII re-cycling[118,122,123]. Serine 7 phosphorylation occurs at the beginning of the transcription and is maintained until the end[124].

RNAPII pausing

It has been indicated that high accumulation of RNAPII at the proximal promoter region (i.e. 30-60 nucleotides downstream of TSS), occurs in both developmental and inducible genes[125,126]. After initiation pS5-RNAPII reach stalling site, pausing is induced by binding of negative elongation factor (NELF) and DRB-Sensitivity-Inducing factor (DSIF) to RNAPII[127,128]. After the stimulus, positive transcription elongation factor-b (P-TEFb) complex, that includes cyclin T1 and Cyclin-dependent kinase 9 (CDK9), phosphorylates Ser2 at CTD of RNAPII, NELF (inducing its release) and DSIF, transforming it into a positive elongation factor[125,126,129], starting productive elongation phase of RNAPII.

Enhancers in gene transcription regulation

It is known that core promoter of genes is sufficient to recruit the RNAPII machinery; however, the robustness of gene transcription can be increased by genomic regions located far away from the transcription start site (TSS). These elements are termed enhancers or *cis*-regulatory modules (CRMs)[130]. A big amount of TF binding motifs are located there, allowing that the recruitment of activating or repressive TF and co-regulators modulate the activity of the enhancers[130]. Enhancers have been classified as inactive, poised, primed and active[131]. Inactive enhancers have compacted chromatin, with the absence of TF[131] and, mainly, H3K4me1 and H3K4me2 modifications[132]. Additionally, H3K27me3, a repression-associated mark, indicates a poised enhancer[133]. Active enhancers are featured by H3K27ac modification[133] and the presence of an active RNAPII[134]. Just in the middle, primed enhancers contain H3K4me1 and H3K4me2 modifications but lack histone acetylations[133]. They are posed closely bound to transcription factors, maintaining a nucleosome-free region[135] which is hypersensitive to DNase I[136].

Since the enhancer can be located at several hundred kilobases from gene promoter, a long range of interactions are maintained by mediator complexes[137] and cohesines[138]. It has been showed that for gene transcription, the recruitment of RNAPII not only occurs at the TSS but also at enhancers themselves inducing the active expression of Enhancer RNAs (eRNAs)[139]. The experimental evidence suggests that eRNAs play a pivotal role in RNAPII promoter escape[140].

Hypothesis

Considering the background set in the introduction, the hypothesis of this thesis is that *the previous exposure to oxidative stress induces an epigenetic transcriptional memory in the*

HMOX1 gene in HUAEC from large-for-gestational-age (LGA) offspring of women with pre-gestational obesity, which can be mimicked in vitro in an endothelial cell line.

General and Specific Aims

General aim. To determine the presence of an epigenetic transcriptional memory (ETM) in the *HMOX1* gene associated with a previous exposure to oxidative stress in LGA-HUAEC, and in a human endothelial cell line.

Specific aim 1. To characterize the potentiated *HMOX1* mRNA expression by pro-oxidant stimuli in LGA-HUAEC.

Specific aim 1.1. To determine if the pro-oxidant priming induces changes in the levels and timing of the *HMOX1* mRNA in LGA-HUAEC.

Specific aim 1.2. To determine if the changes in the *HMOX1* mRNA levels are due to the stability of *HMOX1* mRNA in LGA-HUAEC.

Specific aim 1.3. To determine if the treatment with a pro-oxidant agent induces changes in the methylation pattern at the *HMOX1* proximal promoter from LGA-HUAEC.

Specific aim 2. To determine the acquisition of ETM in the *HMOX1* gene by pro-oxidant stimuli, in the endothelial cell line, EA.hy926.

Specific aim 2.1. To standardize a model of ETM induced by a pro-oxidant stimulus in the *HMOX1* gene in EA.hy926.

Specific aim 2.2. To determine the presence of a poised-RNAPII at the *HMOX1* gene proximal promoter in an ETM cell model in EA.hy926.

Specific aim 2.3. To evaluate the state of the chromatin at the proximal promoter of the *HMOX1* gene proximal promoter in an ETM cell model in EA.hy926.

Specific aim 2.4. To characterize the kinetics of the post-transcriptional modifications of histones during the basal, gene activation and post-activation cycle in an ETM cell model in EA.hy926.

In the second chapter of this thesis, the mechanisms that define how endothelial antioxidant machinery from LGA newborn works under exogenous oxidative challenge are shown. In summary, the results show that LGA-HUAEC has a pro-oxidant environment, characterized by a reduced GSH:GSSG ratio and a high H_2O_2 tone. The latter was associated with a diminished level of superoxide anion and an increased SODs activity. In response to a new H_2O_2 challenge, LGA-HUAEC showed a robust global antioxidant machinery; tolerating higher concentrations of exogenous H_2O_2 and showing least efficient oxidation kinetics and a faster reduction rate of an H_2O_2-induced fluorescent probe. Although candidate antioxidant proteins levels in cell culture were not different compared to control cells, the *in situ* protein levels of NOX4 and SOD1 were increased. The basal mRNA level of *NRF2* and *HMOX1* were reduced and elevated, respectively, in the primary cell culture model. Interestingly, when LGA-HUAEC cells were stimulated with H_2O_2 for 3 hours, *GPX1* mRNA was overexpressed. A concurrence of an open chromatin state at *GPX1* core promoter pointed to plausible epigenetic mechanisms.

Considering the original hypothesis, an ETM mechanism could answer the question left by chapter two. ETM implies epigenetic modifications at the promoter of inducible genes, left in the promoter by a first stimulus, called gene priming. This priming favors an over-expression of the gene when cells are stimulated for a second time[141]. The *in vivo* oxidative

stress in LGA newborn of obese mothers could act as a first priming factor in the *GPX1* gene in HUAEC, being unmasked by a second *in vitro* challenge.

In the third chapter of this thesis, the question if oxidative stress itself is necessary and sufficient to lead to epigenetic modifications in antioxidant coding-protein genes in an ETM manner. Using a pro-oxidant double hit protocol in primary control-HUAEC, EA.hy926 or HeLa cells, among several antioxidant-coding genes, *HMOX1* gene acquired an ETM state. The ETM was characterized by an open chromatin state at the core promoter and enhancer 2 (located at -9 kb from TSS) of *HMOX1*, together with a paused RNAPII and NRF2 enrichment at the core promoter and enhancer 2, respectively.

The fourth chapter comprises is a general discussion of redox status alterations on endothelial cell physiology; as well as the possible molecular/epigenetic mechanisms that could be involved in the programming of vascular function.

This thesis shows the first evidence that maternal obesity is associated with changes in the antioxidant capacity of endothelial cells of LGA-offspring and proposes epigenetic transcriptional memory in the *HMOX1* gene as a specific mechanism.

References

1. Hamann, A. Aktuelles zur Adipositas (mit und ohne Diabetes). *Diabetologe* **13,** 331–341 (2017).
2. WHO. Global status report on noncommunicable diseases 2014. *World Health* 176 (2014). doi:ISBN 9789241564854
3. MINSAL. Primeros y segundos resultados de ENS 2016-2017. (2018). at <http://epi.minsal.cl/resultados-encuestas/>
4. Adamo, K. B., Ferraro, Z. M. & Brett, K. E. Can we modify the intrauterine environment to halt the intergenerational cycle of obesity? *International Journal of Environmental Research and Public Health* **9,** 1263–1307 (2012).
5. Baeten, J. M., Bukusi, E. A. & Lambe, M. Pregnancy complications and outcomes among overweight and obese nulliparous women. *Am. J. Public Health* **91,** 436–440 (2001).

6. Ehrenberg, H. M., Mercer, B. M. & Catalano, P. M. The influence of obesity and diabetes on the prevalence of macrosomia. in *American Journal of Obstetrics and Gynecology* **191,** 964–968 (2004).
7. Bhattacharya, S., Campbell, D. M., Liston, W. A. & Bhattacharya, S. Effect of Body Mass Index on pregnancy outcomes in nulliparous women delivering singleton babies. *BMC Public Health* **7,** (2007).
8. Schneider, D. *et al.* Oxidative stress as common trait of endothelial dysfunction in chorionic arteries from fetuses with IUGR and LGA. *Placenta* **36,** 552–558 (2015).
9. Chiavaroli, V. *et al.* Progression of cardio-metabolic risk factors in subjects born small and large for gestational age. *PLoS One* **9,** e104278 (2014).
10. Perng, W., Gillman, M. W., Mantzoros, C. S. & Oken, E. A prospective study of maternal prenatal weight and offspring cardiometabolic health in midchildhood. *Ann. Epidemiol.* **24,** 793–800 (2014).
11. Curhan, G. C. *et al.* Birth weight and adult hypertension and obesity in women. *Circulation* **94,** 1310–1315 (1996).
12. Hayward, C. E. *et al.* Chorionic plate arterial function is altered in maternal obesity. *Placenta* **34,** 281–287 (2013).
13. Reynolds, R. M., Allan, K. M. & Edwin, A. Maternal obesity during pregnancy and premature mortality from cardiovascular event in adult offspring : *Br. Med. J.* **4539,** 1–10 (2013).
14. Furchgott, R. F. & Zawadzki, J. V. The obligatory role of endothelial cells in the relaxation of arterial smooth muscle by acetylcholine. *Nature* **288,** 373–6 (1980).
15. Borland, C. Endothelium in control. *Br. Heart J.* **66,** 405 (1991).
16. Ross, R. The pathogenesis of atherosclerosis: a perspective for the 1990s. *Nature* **362,** 801–809 (1993).
17. Panza, J. A., Quyyumi, A. A., Brush, J. E. & Epstein, S. E. Abnormal Endothelium-Dependent Vascular Relaxation in Patients with Essential Hypertension. *N. Engl. J. Med.* **323,** 22–27 (1990).
18. Hadi, H. A. R. & Suwaidi, J. Al. Endothelial dysfunction in diabetes mellitus. *Vasc. Health Risk Manag.* **3,** 853–76 (2007).
19. Deanfield, J. *et al.* Endothelial function and dysfunction. Part I. *J. Hypertens.* **23,** 7–17 (2005).
20. CHRISTENSEN, H. N. & COOPER, P. F. Glycine and alanine concentrations of body fluids; experimental modification. *J. Biol. Chem.* **168,** 191–196 (1947).
21. Panayiotidis, M. Reactive oxygen species (ROS) in multistage carcinogenesis. *Cancer Lett.* **266,** 3–5 (2008).
22. Halliwell, B. & Cross, C. E. Oxygen-derived species: their relation to human disease and environmental stress. *Environ. Health Perspect.* **102 Suppl 10,** 5–12 (1994).
23. Vásquez-Vivar, J. *et al.* Superoxide generation by endothelial nitric oxide synthase: The influence of cofactors. *Biochemistry* **95,** 9220–9225 (1998).
24. Fukai, T. & Ushio-Fukai, M. Superoxide Dismutases: Role in Redox Signaling, Vascular Function, and Diseases. *Antioxid. Redox Signal.* **15,** 1583–1606 (2011).
25. Dworakowski, R., Alom-Ruiz, S. P. & Shah, A. M. NADPH oxidase-derived reactive oxygen species in the regulation of endothelial phenotype. *Pharmacol. Rep.* **60,** 21–8 (2008).
26. Brand, M. D. *et al.* Mitochondrial superoxide: Production, biological effects, and activation of uncoupling proteins. *Free Radical Biology and Medicine* **37,** 755–767

(2004).
27. Huie, R. E. & Padmaja, S. The reaction of no with superoxide. *Free Radic. Res. Commun.* **18,** 195–9 (1993).
28. Radi, R. Nitric oxide, oxidants, and protein tyrosine nitration. *Proc. Natl. Acad. Sci. U. S. A.* **101,** 4003–8 (2004).
29. Niki, E., Yoshida, Y., Saito, Y. & Noguchi, N. Lipid peroxidation: Mechanisms, inhibition, and biological effects. *Biochem. Biophys. Res. Commun.* **338,** 668–676 (2005).
30. Poppek, D. & Grune, T. Proteasomal Defense of Oxidative Protein Modifications. *Antioxid. Redox Signal.* **8,** 173–184 (2006).
31. Hayakawa, H., Taketomi, A., Sakumi, K., Kuwano, M. & Sekiguchi, M. Generation and Elimination of 8-Oxo-7,8-dihydro-2'-deoxyguanosine 5'-Triphosphate, a Mutagenic Substrate for DNA Synthesis, in Human Cells. *Biochemistry* **34,** 89–95 (1995).
32. Birben, E. *et al.* Oxidative Stress and Antioxidant Defense. *WAO J.* **5,** 9–19 (2012).
33. Panda, S. K. Assay Guided Comparison for Enzymatic and Non-Enzymatic Antioxidant Activities with Special Reference to Medicinal Plants. *Intech* 381–400 (2012). doi:10.5772/50782
34. Ryu, H. *et al.* Sp1 and Sp3 are oxidative stress-inducible, antideath transcription factors in cortical neurons. *J Neurosci* **23,** 3597–3606 (2003).
35. Goettsch, C. *et al.* Arterial flow reduces oxidative stress via an antioxidant response element and Oct-1 binding site within the NADPH oxidase 4 promoter in endothelial cells. *Basic Res. Cardiol.* **106,** 551–561 (2011).
36. Hori, Y. S., Kuno, A., Hosoda, R. & Horio, Y. Regulation of FOXOs and p53 by SIRT1 modulators under oxidative stress. *PLoS One* **8,** e73875 (2013).
37. Polvani, S., Tarocchi, M. & Galli, A. PPARγ and Oxidative Stress: Con(β) Catenating NRF2 and FOXO. *PPAR Res.* **2012,** 641087 (2012).
38. Qutub, A. A. & Popel, A. S. Reactive Oxygen Species Regulate Hypoxia-Inducible Factor 1α Differentially in Cancer and Ischemia▿ †. *Mol. Cell. Biol.* **28,** 5106–5119 (2008).
39. Chen, X.-L. *et al.* Activation of Nrf2/ARE pathway protects endothelial cells from oxidant injury and inhibits inflammatory gene expression. *Am. J. Physiol. Heart Circ. Physiol.* **290,** H1862-70 (2006).
40. Bouanane, S. *et al.* Time course of changes in serum oxidant/antioxidant status in overfed obese rats and their offspring. *Clin. Sci.* **116,** 669–680 (2009).
41. Zhang, X., Strakovsky, R., Zhou, D., Zhang, Y. & Pan, Y.-X. A maternal high-fat diet represses the expression of antioxidant defense genes and induces the cellular senescence pathway in the liver of male offspring rats. *J. Nutr.* **141,** 1254–1259 (2011).
42. Malti, N. *et al.* Oxidative stress and maternal obesity: Feto-placental unit interaction. *Placenta* (2014). doi:10.1016/j.placenta.2014.03.010
43. Ma, Q. Role of nrf2 in oxidative stress and toxicity. *Annu. Rev. Pharmacol. Toxicol.* **53,** 401–26 (2013).
44. Kaspar, J. W., Niture, S. K. & Jaiswal, A. K. Nrf2:INrf2 (Keap1) signaling in oxidative stress. *Free Radic. Biol. Med.* **47,** 1304–9 (2009).
45. Nguyen, T., Sherratt, P. J., Huang, H.-C., Yang, C. S. & Pickett, C. B. Increased protein stability as a mechanism that enhances Nrf2-mediated transcriptional

activation of the antioxidant response element. Degradation of Nrf2 by the 26 S proteasome. *J. Biol. Chem.* **278,** 4536–41 (2003).
46. Stewart, D., Killeen, E., Naquin, R., Alam, S. & Alam, J. Degradation of transcription factor Nrf2 via the ubiquitin-proteasome pathway and stabilization by cadmium. *J. Biol. Chem.* **278,** 2396–402 (2003).
47. Nguyen, T., Nioi, P. & Pickett, C. B. The Nrf2-antioxidant response element signaling pathway and its activation by oxidative stress. *J. Biol. Chem.* **284,** 13291–5 (2009).
48. Niture, S. K., Kaspar, J. W., Shen, J. & Jaiswal, A. K. Nrf2 signaling and cell survival. *Toxicol. Appl. Pharmacol.* **244,** 37–42 (2010).
49. Jain, A. K., Bloom, D. a & Jaiswal, A. K. Nuclear import and export signals in control of Nrf2. *J. Biol. Chem.* **280,** 29158–68 (2005).
50. Itoh, K. *et al.* An Nrf2/small Maf heterodimer mediates the induction of phase II detoxifying enzyme genes through antioxidant response elements. *Biochem. Biophys. Res. Commun.* **236,** 313–22 (1997).
51. Erickson, A. M., Nevarea, Z., Gipp, J. J. & Timothy Mulcahy, R. Identification of a variant antioxidant response element in the promoter of the human glutamate-cysteine ligase modifier subunit gene: Revision of the are consensus sequence. *J. Biol. Chem.* **277,** 30730–30737 (2002).
52. Chorley, B. N. *et al.* Identification of novel NRF2-regulated genes by ChIP-Seq: influence on retinoid X receptor alpha. *Nucleic Acids Res.* **40,** 7416–29 (2012).
53. Gene, R., Favreau, L. V, Pickett, C. B. & Chern, C. B. J. B. Transcriptional Regulation of the Rat NAD (P) H : Quinone. **268,** 19875–19881 (1993).
54. Sun, Z., Chin, Y. E. & Zhang, D. D. Acetylation of Nrf2 by p300/CBP augments promoter-specific DNA binding of Nrf2 during the antioxidant response. *Mol. Cell. Biol.* **29,** 2658–72 (2009).
55. Kawai, Y., Garduño, L., Theodore, M., Yang, J. & Arinze, I. J. Acetylation-deacetylation of the transcription factor Nrf2 (nuclear factor erythroid 2-related factor 2) regulates its transcriptional activity and nucleocytoplasmic localization. *J. Biol. Chem.* **286,** 7629–40 (2011).
56. Sun, J. *et al.* Heme regulates the dynamic exchange of Bach1 and NF-E2-related factors in the Maf transcription factor network. *Proc. Natl. Acad. Sci. U. S. A.* **101,** 1461–6 (2004).
57. Li, Z. *et al.* The polycomb group protein EZH2 inhibits lung cancer cell growth by repressing the transcription factor Nrf2. *FEBS Lett.* **588,** 3000–3007 (2014).
58. Kang, K. A. *et al.* Epigenetic modification of Nrf2 in 5-fluorouracil-resistant colon cancer cells: involvement of TET-dependent DNA demethylation. *Cell Death Dis.* **5,** e1183 (2014).
59. Bird, A. Perceptions of epigenetics. *Nature* **447,** 396–398 (2007).
60. Luger, K., Mäder, A. W., Richmond, R. K., Sargent, D. F. & Richmond, T. J. Crystal structure of the nucleosome core particle at 2.8 A resolution. *Nature* **389,** 251–260 (1997).
61. Suzuki, T. & Yamamoto, M. Molecular basis of the Keap1-Nrf2 system. *Free Radical Biology and Medicine* **88,** 93–100 (2015).
62. Goll, M. G. & Bestor, T. H. EUKARYOTIC CYTOSINE METHYLTRANSFERASES. *Annu. Rev. Biochem.* **74,** 481–514 (2005).
63. Klose, R. J. & Bird, A. P. Genomic DNA methylation: the mark and its mediators. *Trends Biochem. Sci.* **31,** 89–97 (2006).

64. Berger, S. L. The complex language of chromatin regulation during transcription. *Nature* **447,** 407–412 (2007).
65. Fuks, F., Burgers, W. A., Brehm, A., Hughes-Davies, L. & Kouzarides, T. DNA methyltransferase Dnmt1 associates with histone deacetylase activity. *Nat. Genet.* **24,** 88–91 (2000).
66. Esteve, P.-O. *et al.* Direct interaction between DNMT1 and G9a coordinates DNA and histone methylation during replication. *Genes Dev.* **20,** 3089–3103 (2006).
67. Robertson, A. K., Geiman, T. M., Sankpal, U. T., Hager, G. L. & Robertson, K. D. Effects of chromatin structure on the enzymatic and DNA binding functions of DNA methyltransferases DNMT1 and Dnmt3a in vitro. *Biochem. Biophys. Res. Commun.* **322,** 110–118 (2004).
68. Viré, E. *et al.* The Polycomb group protein EZH2 directly controls DNA methylation. *Nature* **439,** 871–874 (2005).
69. Reik, W. Stability and flexibility of epigenetic gene regulation in mammalian development. *Nature* **447,** 425–432 (2007).
70. Wu, H. & Sun, Y. E. Epigenetic Regulation of Stem Cell Differentiation. *Pediatr. Res.* **59,** 21R–25R (2006).
71. Collas, P., Noer, A. & Timoskainen, S. Programming the genome in embryonic and somatic stem cells. *J. Cell. Mol. Med.* **11,** 602–20 (2007).
72. Tahiliani, M. *et al.* Conversion of 5-Methylcytosine to 5-Hydroxymethylcytosine in Mammalian DNA by MLL Partner TET1. *Science (80-.).* **324,** 930–935 (2009).
73. Kimura, A., Matsubara, K. & Horikoshi, M. A Decade of Histone Acetylation: Marking Eukaryotic Chromosomes with Specific Codes. *J. Biochem.* **138,** 647–662 (2005).
74. Kouzarides, T. Chromatin Modifications and Their Function. *Cell* **128,** 693–705 (2007).
75. Santos-Rosa, H. & Caldas, C. Chromatin modifier enzymes, the histone code and cancer. *Eur. J. Cancer* **41,** 2381–2402 (2005).
76. Cosgrove, M. S. & Wolberger, C. How does the histone code work? *Biochem. Cell Biol.* **83,** 468–476 (2005).
77. Wang, G. G., Allis, C. D. & Chi, P. Chromatin remodeling and cancer, part I: covalent histone modifications. *Trends Mol. Med.* **13,** 363–372 (2007).
78. Thiagalingam, S. *et al.* Histone deacetylases: unique players in shaping the epigenetic histone code. *Ann. N. Y. Acad. Sci.* **983,** 84–100 (2003).
79. Drewell, R. A., Goddard, C. J., Thomas, J. O. & Surani, M. A. Methylation-dependent silencing at the H19 imprinting control region by MeCP2. *Nucleic Acids Res.* **30,** 1139–44 (2002).
80. Kondo, E., Gu, Z., Horii, A. & Fukushige, S. The Thymine DNA Glycosylase MBD4 Represses Transcription and Is Associated with Methylated p16INK4a and hMLH1 Genes. *Mol. Cell. Biol.* **25,** 4388–4396 (2005).
81. Trewick, S. C., McLaughlin, P. J. & Allshire, R. C. Methylation: lost in hydroxylation? *EMBO Rep.* **6,** 315–320 (2005).
82. Henikoff, S. & Smith, M. M. Histone variants and epigenetics. *Cold Spring Harb. Perspect. Biol.* **7,** a019364 (2015).
83. Ahmad, K. & Henikoff, S. The histone variant H3.3 marks active chromatin by replication-independent nucleosome assembly. *Mol. Cell* **9,** 1191–200 (2002).
84. Mizuguchi, G. *et al.* ATP-Driven Exchange of Histone H2AZ Variant Catalyzed by

SWR1 Chromatin Remodeling Complex. *Science (80-.).* **303,** 343–348 (2004).
85. Kim, J. K., Samaranayake, M. & Pradhan, S. Epigenetic mechanisms in mammals. *Cellular and Molecular Life Sciences* **66,** 596–612 (2009).
86. Becker, P. B. & Hörz, W. ATP-Dependent Nucleosome Remodeling. *Annu. Rev. Biochem.* **71,** 247–273 (2002).
87. Pang, B. *et al.* Drug-induced histone eviction from open chromatin contributes to the chemotherapeutic effects of doxorubicin. *Nat. Commun.* **4,** 1908 (2013).
88. Tang, L., Nogales, E. & Ciferri, C. Structure and function of SWI/SNF chromatin remodeling complexes and mechanistic implications for transcription. *Prog. Biophys. Mol. Biol.* **102,** 122–8 (2010).
89. Deindl, S. *et al.* ISWI remodelers slide nucleosomes with coordinated multi-base-pair entry steps and single-base-pair exit steps. *Cell* **152,** 442–52 (2013).
90. Marfella, C. G. A. & Imbalzano, A. N. The Chd family of chromatin remodelers. *Mutat. Res.* **618,** 30–40 (2007).
91. Poli, J., Gasser, S. M. & Papamichos-Chronakis, M. The INO80 remodeller in transcription, replication and repair. *Philos. Trans. R. Soc. B Biol. Sci.* **372,** 20160290 (2017).
92. Pratt, A. J. & MacRae, I. J. The RNA-induced silencing complex: A versatile gene-silencing machine. *J. Biol. Chem.* **284,** 17897–17901 (2009).
93. Minajigi, A. *et al.* A comprehensive Xist interactome reveals cohesin repulsion and an RNA-directed chromosome conformation. *Science (80-.).* **349,** aab2276-aab2276 (2015).
94. Hacisuleyman, E. *et al.* Topological organization of multichromosomal regions by the long intergenic noncoding RNA Firre. *Nat. Struct. Mol. Biol.* **21,** 198–206 (2014).
95. Prasanth, K. V. *et al.* Regulating Gene Expression through RNA Nuclear Retention. *Cell* **123,** 249–263 (2005).
96. Tan, J. Y. *et al.* Extensive microRNA-mediated crosstalk between lncRNAs and mRNAs in mouse embryonic stem cells. *Genome Res.* **25,** 655–66 (2015).
97. Ng, S.-Y., Bogu, G. K., Soh, B. S. & Stanton, L. W. The Long Noncoding RNA RMST Interacts with SOX2 to Regulate Neurogenesis. *Mol. Cell* **51,** 349–359 (2013).
98. Heard, E. & Disteche, C. M. Dosage compensation in mammals: fine-tuning the expression of the X chromosome. *Genes Dev.* **20,** 1848–1867 (2006).
99. Kim, J., Bretz, C. L. & Lee, S. Epigenetic instability of imprinted genes in human cancers. *Nucleic Acids Res.* **43,** 10689–99 (2015).
100. Lavie, L., Kitova, M., Maldener, E., Meese, E. & Mayer, J. CpG Methylation Directly Regulates Transcriptional Activity of the Human Endogenous Retrovirus Family HERV-K(HML-2). *J. Virol.* **79,** 876–883 (2005).
101. Brickner, D. G. *et al.* H2A.Z-mediated localization of genes at the nuclear periphery confers epigenetic memory of previous transcriptional state. *PLoS Biol.* **5,** e81 (2007).
102. Tan-Wong, S. M., Wijayatilake, H. D. & Proudfoot, N. J. Gene loops function to maintain transcriptional memory through interaction with the nuclear pore complex. *Genes Dev.* **23,** 2610–24 (2009).
103. Gialitakis, M., Arampatzi, P., Makatounakis, T. & Papamatheakis, J. Gamma interferon-dependent transcriptional memory via relocalization of a gene locus to PML nuclear bodies. *Mol. Cell. Biol.* **30,** 2046–56 (2010).
104. Light, W. H., Brickner, D. G., Brand, V. R. & Brickner, J. H. Interaction of a DNA zip code with the nuclear pore complex promotes H2A.Z incorporation and INO1

transcriptional memory. *Mol. Cell* **40,** 112–25 (2010).
105. Guan, Q., Haroon, S., Bravo, D. G., Will, J. L. & Gasch, A. P. Cellular memory of acquired stress resistance in Saccharomyces cerevisiae. *Genetics* **192,** 495–505 (2012).
106. Light, W. H. *et al.* A conserved role for human Nup98 in altering chromatin structure and promoting epigenetic transcriptional memory. *PLoS Biol.* **11,** e1001524 (2013).
107. Wong, M. M. *et al.* Promoter-Bound p300 Complexes Facilitate Post-Mitotic Transmission of Transcriptional Memory. *PLoS One* **9,** e99989 (2014).
108. Hahn, S. Structure and mechanism of the RNA polymerase II transcription machinery. *Nat. Struct. Mol. Biol.* **11,** 394–403 (2004).
109. Svejstrup, J. Q. The RNA polymerase II transcription cycle: Cycling through chromatin. *Biochimica et Biophysica Acta - Gene Structure and Expression* **1677,** 64–73 (2004).
110. Li, B., Carey, M. & Workman, J. L. The Role of Chromatin during Transcription. *Cell* **128,** 707–719 (2007).
111. Cairns, B. R. The logic of chromatin architecture and remodelling at promoters. *Nature* **461,** 193–198 (2009).
112. Boeger, H. *et al.* Structural basis of eukaryotic gene transcription. in *FEBS Letters* **579,** 899–903 (No longer published by Elsevier, 2005).
113. Pan, G. & Greenblatt, J. Initiation of transcription by RNA polymerase II is limited by melting of the promoter DNA in the region immediately upstream of the initiation site. *J. Biol. Chem.* **269,** 30101–30104 (1994).
114. Pal, M., Ponticelli, A. S. & Luse, D. S. The role of the transcription bubble and TFIIB in promoter clearance by RNA polymerase II. *Mol. Cell* **19,** 101–110 (2005).
115. Armache, K. J., Mitterweger, S., Meinhart, A. & Cramer, P. Structures of complete RNA polymerase II and its subcomplex, Rpb4/7. *J. Biol. Chem.* **280,** 7131–7134 (2005).
116. Corden, J. L., Cadena, D. L., Ahearn, J. M. & Dahmus, M. E. A unique structure at the carboxyl terminus of the largest subunit of eukaryotic RNA polymerase II. *Proc. Natl. Acad. Sci. U. S. A.* **82,** 7934–8 (1985).
117. Buratowski, S. The CTD code. *Nat. Struct. Biol.* **10,** 679–680 (2003).
118. Komarnitsky, P., Cho, E. J. & Buratowski, S. Different phosphorylated forms of RNA polymerase II and associated mRNA processing factors during transcription. *Genes Dev.* **14,** 2452–2460 (2000).
119. Schroeder, S. C., Schwer, B., Shuman, S. & Bentley, D. Dynamic association of capping enzymes with transcribing RNA polymerase II. *Genes Dev.* **14,** 2435–2440 (2000).
120. Rodriguez, C. R. *et al.* Kin28, the TFIIH-Associated Carboxy-Terminal Domain Kinase, Facilitates the Recruitment of mRNA Processing Machinery to RNA Polymerase II. *Mol. Cell. Biol.* **20,** 104–112 (2000).
121. Qiu, H., Hu, C. & Hinnebusch, A. G. Phosphorylation of the Pol II CTD by KIN28 Enhances BUR1/BUR2 Recruitment and Ser2 CTD Phosphorylation Near Promoters. *Mol. Cell* **33,** 752–762 (2009).
122. Buratowski, S. Progression through the RNA Polymerase II CTD Cycle. *Molecular Cell* **36,** 541–546 (2009).
123. Cho, E. J., Kobor, M. S., Kim, M., Greenblatt, J. & Buratowski, S. Opposing effects of Ctk1 kinase and Fcp1 phosphatase at Ser 2 of the RNA polymerase II C-terminal

domain. *Genes Dev.* **15,** 3319–3329 (2001).
124. Tietjen, J. R. *et al.* Chemical-genomic dissection of the CTD code. *Nat. Struct. Mol. Biol.* **17,** 1154–1161 (2010).
125. Kwak, H. & Lis, J. T. Control of Transcriptional Elongation. *Annu. Rev. Genet.* **47,** 483–508 (2013).
126. Adelman, K. & Lis, J. T. Promoter-proximal pausing of RNA polymerase II: emerging roles in metazoans. *Nat. Rev. Genet.* **13,** 720–731 (2012).
127. Kwak, H., Fuda, N. J., Core, L. J. & Lis, J. T. Precise Maps of RNA Polymerase Reveal How Promoters Direct Initiation and Pausing. *Science (80-.).* **339,** 950–953 (2013).
128. Li, J. & Gilmour, D. S. Distinct mechanisms of transcriptional pausing orchestrated by GAGA factor and M1BP, a novel transcription factor. *EMBO J.* **32,** 1829–1841 (2013).
129. Peterlin, B. M. & Price, D. H. Controlling the Elongation Phase of Transcription with P-TEFb. *Molecular Cell* **23,** 297–305 (2006).
130. Banerji, J., Rusconi, S. & Schaffner, W. Expression of a ??-globin gene is enhanced by remote SV40 DNA sequences. *Cell* **27,** 299–308 (1981).
131. Ernst, J. & Kellis, M. Discovery and characterization of chromatin states for systematic annotation of the human genome. *Nat. Biotechnol.* **28,** 817–825 (2010).
132. Heintzman, N. D. *et al.* Distinct and predictive chromatin signatures of transcriptional promoters and enhancers in the human genome. *Nat. Genet.* **39,** 311–318 (2007).
133. Creyghton, M. P. *et al.* Histone H3K27ac separates active from poised enhancers and predicts developmental state. *Proc. Natl. Acad. Sci.* **107,** 21931–21936 (2010).
134. de Santa, F. *et al.* A large fraction of extragenic RNA Pol II transcription sites overlap enhancers. *PLoS Biol.* **8,** e1000384 (2010).
135. He, H. H. *et al.* Nucleosome dynamics define transcriptional enhancers. *Nat. Genet.* **42,** 343–347 (2010).
136. Thurman, R. E. *et al.* The accessible chromatin landscape of the human genome. *Nature* **489,** 75–82 (2012).
137. Bejarano-Jiménez, A., Escobar-Barrios, V. a., Kleijn, J. M., Ortíz-Ledón, C. a. & Cházaro-Ruiz, L. F. Supplementary Information. *J. Appl. Polym. Sci.* **c,** 1–10 (2014).
138. Schmidt, D. *et al.* A CTCF-independent role for cohesin in tissue-specific transcription. *Genome Res.* **20,** 578–588 (2010).
139. Wang, D. *et al.* Reprogramming transcription by distinct classes of enhancers functionally defined by eRNA. *Nature* **474,** 390–394 (2011).
140. Schaukowitch, K. *et al.* Enhancer RNA facilitates NELF release from immediate early genes. *Mol. Cell* **56,** 29–42 (2014).
141. D´Urso, A. & Brickner, J. H. Epigenetic transcriptional memory. *Curr. Genet.* 1–5 (2016). doi:10.1007/s00294-016-0661-8

CHAPTER 2

HUMAN UMBILICAL ARTERY ENDOTHELIAL CELLS FROM LARGE-FOR-GESTATIONAL-AGE NEWBORN HAVE INCREASED ANTIOXIDANT EFFICIENCY AND GENE EXPRESSION.

Manuscript accepted in J. Cell Physiology

DOI: 10.1002/jcp.28494

Human umbilical artery endothelial cells from Large-for-Gestational-Age newborn have increased antioxidant efficiency and gene expression.

Running title: Redox imbalance in large newborn´s endothelium

I. Carrasco-Wong[1§*], C. Hernández[2], C. Jara[3], O. Porras[4], P. Casanello[2,5*]

[1]Cell & Molecular Biology PhD Program, Faculty of Biological Sciences, Pontificia Universidad Católica de Chile, Santiago, Chile, [2]Department of Obstetrics, School of Medicine, Pontificia Universidad Católica de Chile, Santiago, Chile, [3]Centro de Investigaciones Biomédicas (CIB), Laboratorio de Estrés Oxidativo, Facultad de Medicina, Universidad de Valparaíso, Valparaíso, Chile, [4]Instituto de Nutrición y Tecnología de los Alimentos (INTA), Universidad de Chile, Santiago, Chile, [5]Department of Obstetrics and [5]Department of Neonatology, School of Medicine, Pontificia Universidad Católica de Chile, Santiago, Chile.

***Correspondence**: Dr. Paola Casanello
Department Obstetrics
Department of Neonatology
School of Medicine
Pontificia Universidad Católica de Chile
Marcoleta 391, Santiago, Chile.
Tel: 56-2-2354 8119
Fax: 56-2-632 1924
E-mail: pcasane@uc.cl

Ivo Carrasco MSc
PhD Program in Cell & Molecular Biology
Faculty of Biological Sciences

Pontificia Universidad Católica de Chile
Avda. Libertador Bernardo OHiggins 340, Santiago, Chile.
Tel: 56-2-2354 8119
Fax: 56-2-632 1924
E-mail: icarrasco@uc.cl

§ Current address: *Biomedical Research Center, School of Medicine, Universidad de Valparaíso, Valparaíso, Chile.*

ACKNOWLEDGEMENTS

This study was funded by the Chilean National Fund for Scientific and Technological Development, FONDECYT #1171406 and #1120201. We thank all the study participants for generously donating their samples for this research.

Total number of text figures & tables: 7 figures and 4 tables.

ASTRACT

Obesity is a public health problem worldwide, and especially in women in reproductive age where more than one in three are considered to have obesity. Maternal obesity is associated to an increased maternal, placental and newborn oxidative stress, which has been proposed as a central factor in vascular dysfunction in large-for-gestational-age (LGA) newborn. However, cellular and molecular mechanisms behind this effect have not been elucidated. Untreated human umbilical artery endothelial cells (HUAEC) from LGA (LGA-HUAEC) presented higher O_2^- levels, SOD activity and *HMOX1* mRNA levels, paralleled by reduced GSH:GSSG ratio and *NRF2* mRNA levels. In response to an oxidative challenge (H_2O_2), only HUAEC from LGA exhibited an enhanced *GPX1* expression, as well as a more efficient antioxidant machinery measured by the biosensor probe, HyPer. An open state of chromatin in the TSS region of *GPX1* in LGA-HUAEC was evidenced by DNase-HS assay. Altogether our data indicate that LGA-HUAEC have an altered cellular and molecular antioxidant system. We propose that a chronic pro-oxidant intrauterine milieu, as evidenced in pregestational obesity, could induce a more efficient antioxidant system in fetal vascular cells, which could be maintained by epigenetic mechanism during postnatal life.

Keywords: Oxidative stress; LGA; maternal obesity; endothelial cells; epigenetics

INTRODUCTION

Pre-gestational maternal obesity and excessive weight gain during pregnancy are associated with high blood pressure, altered lipid profile, insulin resistance, and obesity in the offspring (Adamo et al., 2012; Oken & Gillman, 2003). The cellular and molecular mechanisms underlying the alterations caused by these maternal conditions are not completely understood. Oxidative stress is one of the causes of obesity-related diseases (Marseglia et al., 2015), and elevated systemic markers of oxidative stress are reported in women with pregestational obesity and in the umbilical cord blood from large for gestational age (LGA) newborn from mothers with obesity (LGA-MO) (Malti et al., 2014)

Oxidative stress response involves the activation of the nuclear factor erythroid 2-related factor 2 (NFE2L2), whose gene product, NRF2, is a master transcription factor transactivating a plethora of antioxidant- and antixenobiotic-protein coding genes (Ma, 2013). NRF2 transactivates the antioxidant enzymes Glutathione Peroxidase 1 (GPX1), Heme Oxygenase 1 (HMOX1), and hydrogen peroxide (H_2O_2)-generating enzymes such as NADPH oxidase 4 (NOX4) and superoxide dismutases (SODs) (Ma, 2013). The genes coding for these pro- and anti-oxidant proteins are expressed in the human placenta and umbilical cord vascular cells (Barber et al., 2001; Schneider et al., 2015). However, the possible alteration in the expression of these genes, in umbilical artery endothelium of LGA newborn, has not been described so far.

Epigenetic mechanisms explain how diverse phenotypes are mitotically inherited without a change in DNA sequence and how cell differentiation occurs from a single cell during development (Bird, 2007). DNA methylation by methyltransferases in mammalian cells (Reik, 2007) associates with gene repression and is inherited through cell division (Klose &

Bird, 2006). Compaction and relaxation of chromatin structure requires the presence and activity of ATP-dependent chromatin remodeling complexes allowing access to specific histones or DNA regions by altering the nucleosome positions (Kim *et al.*, 2009). If chromatin structure is involved in the permanent effects that intrauterine oxidative stress-related adaptations in oxidative stress genes in LGA-derived endothelium has not been answered hitherto.

To answer these questions, we evaluated whether umbilical artery endothelial cells from LGA offspring from women with pregestational obesity show changes in their homeostatic redox capacity including the study of some of the most relevant genes and proteins expression as well as *in vitro* function.

MATERIALS AND METHODS

Samples

This research was conducted in accordance with the Declaration of Helsinki and Ethics Committee approval from the Faculty of Medicine at the Pontificia Universidad Católica de Chile. Patient informed consent was obtained at the moment of the maternity ward admission. Placentae were collected immediately after delivery from full-term offspring from normotensive, non-smoking, non-alcohol or drug consuming mothers, without any known medical or obstetrical complication. Maternal nutritional status, normal weight or obesity, was estimated calculating maternal BMI, corrected by gestational age (Rosso, 1985). Using a national standard curve (Milad *et al.*, 2010) newborn were classified in accordance to adequacy of weight for gestational age at birth. Neonates between percentile 10^{th} and 90^{th}

were considered adequate for gestational age and over percentile 90th as LGA. **Table 1** shows the maternal and neonatal general and anthropometric characteristics.

Cell isolation and culture

Human umbilical artery endothelial cells (HUAEC) were isolated as previously described (Krause *et al.*, 2013). Briefly, endothelial cells were isolated from umbilical arteries by collagenase digestion (0.2 mg/mL) and cultured (37°C, 5% CO_2) up to passage 3 in medium-131 containing microvascular growth supplement (MVGS), 3.2 mmol/L L-glutamine and 100 U/ mL penicillin–streptomycin. All the experiments were made at passage 3 of the primary cell cultures. Prior to protein or mRNA extraction, confluent cells were starved by reducing the MVGS supplement to 2% and then exposed overnight to 7% O_2 (oxygen partial pressure ~33.9 mmHg, normoxia for this cell type) using a gas mixture (5% CO_2-balanced N_2) in a hypoxia chamber connected to a PROOX 110 device (BioSpherix, NY, USA). On the next day the cells were exposed (or not) to H_2O_2 (100 μM) for 3 hours.

HUAEC infection with HyPer probe

Primary cultures of HUAEC, grown on 25 mm coverslips (5,000 cells/coverslip), were infected with 1:500 adenoviral dilution of HyPer. Two days after, cells were ready for HyPer imaging as previously published (Román *et al.*, 2017). HyPer probe was constructed as follows. Briefly, cDNAs of cyto-HyPer (Evrogen, Moscow, Russia) were sub-cloned into the commercial adenoviral vector pAdEasy-RFP with conventional molecular biology techniques, and homologous recombination was done by BJ5183 cells transformation. Recombinant adenoviral plasmids were digested with PacI and transfected in HEK-AD 293 (AdHek) cells with lipofectamine according to the manufacturer´s guidelines. Following observation of the cytopathic effects (CPE), usually after 14–21 days, cells were harvested

and subjected to three freeze–thaw cycles, followed by centrifugation to remove cellular debris, and the resulting supernatant (2 ml) used to infect a 10 cm dish of 90% confluent AdHek cells. After the observation of CPEs, normally after 2–3 days, viral particles were purified and expanded by infecting 10 plates of AdHek cells (Hernández et al., 2018).

Microscopy and imaging of HyPer biosensor

The experimental day, the HUAEC medium was replaced by Krebs-Ringer-HEPES-glucose-glutamine (KRH) buffer (in mM: 140 NaCl, 4.7 KCl, 20 Hepes, 1.25 MgSO4, 1.25 CaCl2, pH 7.4) supplemented with 5 mM glucose and each coverslip was mounted in an open recording chamber. Images of HUAEC were registered using a Nikon Ti inverted microscope equipped with 40X oil objective [numerical aperture, N.A. 1.3]. A Xenon lamp was coupled to the monochromator device (Cairn Research Ltd, Faversham, UK). Digital images were acquired by means of a cooled CCD camera (Hamamatsu ORCA 03, Japan). All devices were synchronized and operated by using a freeware micromanager software (Edelstein et al., 2014).

HyPer biosensor is composed by a circular permuted yellow fluorescent domain, suitable for dual excitation at 420 and 490 nm. Emitted light from these two excitation channels was collected with a long-pass filter over 520 nm. The biosensor signals from both excitation wavelengths were acquired each 20 seconds and converted in a ratio (490/420) making H_2O_2 measurements reliable and independent of the biosensor expression in the cells.

The biosensor responses were measured in HyPer-expressing C-HUAEC and LGA-HUAEC taking in consideration a baseline of at least 10 minutes to ensure a stable recording. Then, H_2O_2 pulses were applied (1, 5, 10, 25, 50, 100, 200 μM) to build a doses-response curve. All HyPer recordings ended with 1000 μM H_2O_2 pulse to obtain the maximal signal of the

biosensor. With this experimental approach, measurements at equilibrium (baseline and peak values) along with kinetic analysis (rising and recovery signals) of biosensor were possible.

Dihydroethidium (DHE) assay

In a black wall 96-well plate, previously coated with 1% of gelatin, $3x10^4$ C-HUAEC or LGA-HUAEC were seeded per well and incubated for 24 hrs. Prior to the DHE load, confluent cells were starved reducing to 2% the MVGS supplement and exposed overnight to 7% O_2. Cells were loaded with DHE (10 μM) and incubated for 30 minutes at 37°C in darkness. Cells were washed 2 times with 1x PBS (in mmol/L: 136 NaCl, 2.7 KCl, 7.8 Na2HPO4, 1.5 KH2PO4, pH 7.4), loaded with DAPI (300 nM) and incubated during 5 minutes at room temperature in darkness. Cells were washed 2 times with 1x PBS and maintained in KRH buffer (in mM: 140 NaCl, 4.7 KCl, 20 Hepes, 1.25 $MgSO_4$, 1.25 $CaCl_2$, pH 7.4) supplemented with 5 mM glucose. The fluorescence was measured immediately on a Synergy II microplate fluorescence reader (BioTek Instruments, VT), equipped with Gen5 software at excitation/emission wavelength 489/<580nm and 358/461 nm, for DHE and DAPI respectively. DHE fluorescence was normalized by DAPI fluorescence and presented as DHE/DAPI ratio.

GSH:GSSG assay

Endothelial cells were grown in 60 mm culture dishes until they reached 70–80% confluence. Later, they were washed twice with PBS and scrapped in presence of hypotonic buffer (in M: NaCl 0.15, Na_2HPO_4 0.01, NaH_2PO_4 0.01, pH 7.4). The cell suspension was transferred to a1.5 mL microtube and centrifuged at 1000g for 5 min at 4°C. After the supernatant was discarded, the pellet was resuspended in 1 mL of cold PBS. To ensure a complete cell lysis,

the cell homogenates were sonicated. The cell lysate (100 µL treated with 2 µL 2-vinylpyridine) were incubated at 37°C with 700 µL of potassium phosphate buffer with EDTA (KPE) (0.1 M potassium phosphate buffer with 5 mM EDTA disodium salt, pH 7.5), 60 µL of 280 µM NADPH and 60 µL 10 mM 5,5'-dithio-bis (2-nitrobenzoic acid) (DTNB) for 10 min at 30°C to oxidize all the GSH to GSSG. GSSG was then reduced by adding 60 µL GSH reductase. The rate of TNB formation was followed at 412 nm and was proportional to the sum of GSH and GSSG present. The rate was compared with a standard curve of GSH in buffer.

Determination of superoxide dismutase activity (SOD)

This analysis was performed as described by Fridovich (Fridovich, 1995). In an aliquot of cell lysate (as previously described), the reduction of cytochrome by the superoxide radical in the xanthine/xanthine oxidase system, was measured by spectrophotometry. Solution A was composed of 0.5 mM xanthine and 20 µM cytochrome c dissolved in PBS pH 7.8; Solution B contained xanthine oxidase and EDTA 0.1 mM (1:40). Enzymatic activity was detected at 550 nm after mixing 2.9 mL solution A, 50 µL solution B and 100 µL of sample, and expressed as units of enzyme/mg protein using the total protein determined with the Lowry method (Lowry et al., 1951), using bovine albumin (BSA) as standard.

Western blotting

Proteins from C-HUAEC or LGA-HUAEC (40 µg) were separated in polyacrylamide gel (12%) electrophoresis, including a lane with 7 µl of a prestained protein ladder (cat # 26619, ThermoFisher, USA), and transferred to 0.45 mm PVDF membranes (BioRad). Membranes were blocked with 5% BSA in Tris buffered saline (TBS) with 0.1% Tween (TBST) for 1

hour. The membranes were probed with anti-NRF2 antibody (Thermo Fisher Scientific Cat# PA5-27882, RRID:AB_2545358), rabbit monoclonal anti-NOX4 antibody (Abcam Cat# ab109225, RRID:AB_10861375), mouse monoclonal anti-β-Actin antibody (Sigma-Aldrich Cat# A5316, RRID:AB_476743), mouse monoclonal anti-HMOX1 antibody (BD Biosciences Cat# 610712, RRID:AB_398035), rabbit monoclonal GPX1 antibody (Abcam Cat# ab108427, RRID:AB_10890636) or mouse monoclonal SOD1 antibody (Abcam Cat# ab20926, RRID:AB_445919) for 1 hour at room temperature. Membranes were washed in TBST, and incubated (1 h, 22 °C) in TBST containing horseradish peroxidase-conjugated goat anti-rabbit or anti-mouse secondary antibodies. Proteins were detected by enhanced chemiluminescence and quantified by densitometry using ImageJ (https://imagej.net, RRID:SCR_003070) as described elsewhere.

Immunohistochemistry

Immunohistochemistry analysis of protein expression in umbilical arteries was done as previously reported (Schneider et al., 2015). Briefly, umbilical cords were washed with cold PBS, dissected in segments of 5 mm, treated overnight with paraformaldehyde (4% in PBS) and included in paraffin. Deparaffinized and rehydrated histological sections of 4 mm were subjected to heat-induced antigen retrieval using 100 mmol/L citrate buffer (pH 6.0) in a steam cooker for 15 min at 95°C. Samples were treated with 3% H_2O_2 in PBS for 30 min to quench endogenous peroxidase activity. After rinsing in PBS for 5 min, all slides were incubated for 1 h with protein block solution (Cas- Block, Zymed Laboratories, South San Francisco, CA, USA). Sections were incubated overnight at 4°C with primary anti-SOD1 (1:1000) (Abcam Cat# ab20926, RRID:AB_445919), NOX4 (1:500) (Abcam Cat# ab109225, RRID:AB_10861375) and GPX1 (1:500) (Abcam Cat# ab108427,

RRID:AB_10890636) antibodies. Immunostaining was performed using horseradish peroxidase (HRP)- conjugated secondary antibodies and binding was determined with NovaRED kit (Vector, Burlingame, CA, USA), treated for 4 min. Slides were counterstained with Harris hematoxylin and permanently mounted. Specificity of the staining was determined by incubation of sections in the absence of the primary antibody. Sections were examined under an IX81-Olympus microscope, and images were captured using a digital camera (Olympus DP-71) and software (Olympus DP-BSW). At least two slides of every sample were analyzed for each antibody probed in three samples from each group.

The analyzes of the images were made using ImageJ software (https://imagej.net, RRID:SCR_003070). Following the protocol previously described (Fuhrich, Lessey, & Savaris, 2013), the images were corrected subtracting the background, region of interest (ROI) containing 6 to 7 endothelial cells were selected using the drawing tool, H DAB deconvolution plugin was used to separate immunostaining color (i.e. brown) from hematoxilin color (i.e. blue), the intensity of immunostaining were measured into the previously generated ROIs, and the reciprocal intensity were calculated before statistical analyzes (D. Nguyen & Nguyen, 2013).

Isolation of total RNA and reverse transcription

Total RNA was isolated using Trizol (Invitrogen, USA) as described (Krause et al., 2016). RNA quality and integrity were ensured by gel visualization and spectrophotometric analysis (OD260/280) and quantified at 260 nm. Aliquots of 1 μg of total RNA were reversed transcribed using IMPROM II RT kit (Promega, USA).

Quantitative PCR

Polymerase chain reactions were performed as described (Krause et al., 2013), using oligonucleotide primers for human genes of interest (GOI) *NRF2*, *FOXO3A*, *HMOX1*, *GPX1*, *TXNDR*, *PRDX3*, *PRDX6*, *SOD1*, *SOD2*, *p66sch* and *NOX4*. Three different mRNAs, *RPLP0*, *RPLP2* and *ATP5F1*, were selected as reference genes for relative quantity (RQ) calculation, since they showed the lowest standard deviation of raw Cts in all the experimental groups (data not shown), as it was previously described (Mane, Heuer, Hillyer, Navarro, & Rabin, 2008) (**Table 2**). The PCR efficiency for each primer was calculated using a curve of cDNA made by five-fold serial dilutions (from 1x to 1/625x). All the amplifications were done using a 1/10 dilution of cDNA. Quantification was carried out using the algorithm proposed by Pfaffl (Pfaffl, 2001). The final RQ for each gene of interest (GOI) mRNA was calculated considering the geometrical mean of the three different reference genes.

DNase Hypersensitivity assay

DNase hypersensitivity assay was performed as described by Stewart et al. (1991). Control- and LGA-HUAEC were cultured in 6 well plates until confluence. After washing with PBS, partial DNA digestion was performed by adding 1 mL digestion buffer (in mM Tris-HCl 15 mM pH 7.5, KC1 60 mM, NaCl 15 mM, $MgCl_2$ 5 mM, EGTA 0.5 mM, sucrose 300 mM, β-mercaptoethanol 0.5 mM and NP40 0.5%) containing 0 U (Control) or 6.25 U of RQ1 DNase (Promega, USA). After incubation for 5 min at room temperature (22-25°C), the digestion buffer was aspirated and cells were lysed with 0.5 mL of 50 mM Tris-HCl pH 8.0, 20 mM EDTA, 1% SDS, Proteinase K (200 µg/mL) (ThermoFischer, USA) and RNase A (20 µg/mL) (Affymetrix, USA); and incubated for 1 h at 37°C. DNA was extracted by Phenol-chloroform method (Green & Sambrook, 2017). Twenty-five ng of DNA per reaction were

used to amplify the *NRF2* transcription start site (TSS), *HMOX1* TSS and *GPX1* TSS (GOI) and *PAX7* TSS as reference gene (Primer details in **Table 3**). The quantification was carried out using the algorithm proposed by Pfaffl (Pfaffl, 2001).

Statistical analysis.

The HyPer experiments were done in 21 and 57 single different C-HUAEC and LGA-HUAEC respectively, derived from 3 different subjects per group. Protein and mRNA assays were carried out in replicates using at least 4 independents primary HUAEC cultures obtained from different umbilical cords. For DNase accessibility assays cell cultures from 3 different subjects per group were performed. For the superoxide quantification (DHE), SODs activity, GSH and GSSG (GSH:GSSG ratio) the HUAEC from 5 subjects of each group were used. Values are mean ± S.E.M. or median ± interquartile range as indicated in each figure. Comparisons between two treatments or conditions were performed by Mann–Whitney U or t-test, accordingly. All the analyses were carried out with the statistical software Graphpad Prism v6.01 (https://www.graphpad.com, RRID:SCR_015807). A value of $p<0.05$ was considered the cut-off for statistical significance.

RESULTS

LGA-HUAEC have an altered redox status and an increased exogenous H_2O_2 buffering capacity

To evaluate if LGA-HUAEC present a modified redox status such as altered antioxidant machinery, we used HyPer, an oxidative stress biosensor, combined with H_2O_2 pulses. C- or LGA-HUAEC were infected with adenoviral particles containing HyPer and left proliferate for 48 h before H_2O_2 treatment. **Figure 1**, shows representative curves obtained in C-HUAEC

(**Figure 1A**) and LGA-HUAEC (**Figure 1B**), respectively. Before any treatment, baseline ratio values were recorded until evident stability was reached. Steady-state HyPer values from LGA-HUAEC were consistently higher than those observed in C-HUAEC (**Figure 1C**), suggesting a higher oxidant tone in LGA-HUAEC, possibly due to higher levels of endogenous H_2O_2 or a diminished disulfide reducing activity.

To assess the antioxidant machinery in LGA-HUAEC the EC_{50} of Hyper fluorescence was estimated by recording the biosensor responses to increasing exogenous H_2O_2 concentrations. These responses were later referred to a percentage of the value obtained to the maximal stressor tested (1 mM H_2O_2). The maximal value obtained for the cells from both groups was comparable, indicating that dynamic ranges of the biosensor were comparable between groups. The EC_{50} values were 44.9 μM and 104.9 μM for C-HUAEC and LGA-HUAEC, respectively (**Figure 1D**). The difference in the EC_{50} between groups indicates that LGA-HUAEC have an increased exogenous H_2O_2 buffering capacity compared to C-HUAEC. It is noteworthy to point that independent of the cell group tested, the biosensor responses were always transient upon removal of the oxidant pulse, indicating that an intrinsic property of the cytosolic environment acts on the biosensor redox status.

The kinetic of the biosensor was further analyzed to assess if the antioxidant performance of LGA-HUAEC differed from C-HUAEC. With this purpose in mind, the HyPer signal values obtained in the first 300 seconds after H_2O_2 treatment (100 μM) were used to compare the kinetics of increase in both groups (**Figure 1E**). The C-HUAEC curve reached an equilibrium between 200-300 seconds after the H_2O_2 pulse. On the other side, the HyPer signal from LGA-HUAEC showed a significant slower biosensor response (**Figure 1E and Table 4**). Several parameters related to HyPer fluorescence kinetic were calculated for each group. The

slope, taken from the linear phase of the curve (80 to 180 s), were 0.83 ± 0.16 percent/s for C-HUAEC; and 0.14 ± 0.02 percent/s for LGA-HUAEC. The half-time value was calculated resulting in 144.9 ± 10 seconds for C-HUAEC and 196 ± 7.6 seconds for LGA-HUAEC. Finally, the area under the curve (AUC) of HyPer fluorescence in LGA-HUAEC was smaller than C-HUAEC AUC (**Table 4**). All these data indicate that LGA-HUAEC present a delayed and diminished oxidation of the HyPer probe by H_2O_2, suggesting that these cells have a constitutional efficient intracellular antioxidant machinery.

Hyper signal recovery results, which indicate the reduction of disulfide bond on the biosensor, gives an idea of reductive capacity of cells. To check if LGA-HUAEC had an altered reductive system, we compared the decay of biosensor signal during first 260 seconds after H_2O_2 withdrawal. **Figure 1F** and **Table 4** show significant differences between the fluorescence level reached by C- and LGA-HUAEC in the recovery curves. The slope of the decreasing curve (80 to 180 s) was -0.23 ± 0.05 and -0.48 ± 0.04 for C-HUAEC and LGA-HUAEC, respectively. The fluorescence decay half-time was calculated in 123.4 ± 11.9 seconds for C-HUAEC whereas for LGA was 140 ± 4.1 seconds. On the other hand, AUC analysis confirms that recovery of the biosensor signal was significantly lower in LGA-HUAEC compared to control (**Table 4**). These results indicate a higher and faster rate of recovery of the probe, and therefore a higher capacity to reduce H_2O_2-oxidized cysteine residues in LGA-HUAEC.

The results obtained with this tool, that allows the monitoring of the peroxide neutralizing system and disulfide reducing activity *in vivo*, indicate that LGA-HUAEC seem to have a more robust antioxidant/reductive system compared to Control cells.

LGA-HUAEC have reduced superoxide anion level and increased SOD activity

To evaluate if increased basal level of H_2O_2 in LGA-HUAEC could be due to an increase in SOD activity, the levels of superoxide anion, using the DHE fluorescent probe and the SOD activity were measured in C- and LGA-HUAEC. **Figure 2A** shows that LGA-HUAEC present a significant reduction of DHE and an increased SOD activity (**Figure 2B**).

LGA-HUAEC have reduced GSH:GSSG ratio

Since increased levels of H_2O_2 in LGA-HUAEC suggest an intracellular pro-oxidant environment, the levels of reduced (GHS) and oxidized (GSSG) glutathione were measured, and the GHS:GSSG ratio calculated. As shown in **Figure 2C**, the GSH:GSSG ratio is reduced in LGA-HUAEC, associated to a diminished level of GSH (**Figure 2D**), without changes in the GSSG levels (**Figure 2D**), when compared to C-HUAEC.

LGA-HUAEC do not present changes in pro- or antioxidant proteins expression

We later quantified pro- and antioxidant protein levels in C- and LGA-HUAEC to verify if the results obtained with the HyPer probe could be explained with changes in the expression of some of the proteins involved in the intracellular oxidative status. **Figures 3A** and **3B** show representative Western blots of NRF2, NOX4, HMOX1 and GPX1, SOD1, respectively, using β-actin as an internal control. Although, NOX4 (**Figure 3C**) and GPX1 (**Figure 3G**) protein levels are elevated in LGA-HUAEC, the difference with C-HUAEC did not reach statistical significance, as well as HMOX1 (**Figure 3D**), NRF2 (**Figure 3E**), and SOD1 (**Figure 3F**). These data suggest that the protein levels in the HUAEC homogenates do not explain the functional results revealed by HyPer.

Umbilical arteries endothelium from LGA newborn form women with pregestational obesity (LGA-OM) show altered levels of pro- and anti-oxidant enzymes

To evaluate the *in situ* levels of pro- and antioxidant enzymes, histological sections from umbilical cords from Control and LGA-OM were immunoassayed for NOX4, GPX1 and SOD1 enzymes (**Figure 4A**). As shown in **Figure 4B**, the reciprocal intensity of NOX4 and SOD1 are increased in LGA-HUAEC; however, the GPX1 did not show any difference between the groups.

LGA-HUAEC have altered *NRF2* and *HMOX1* gene expression

To verify whether LGA-HUAEC´s augmented reducing capacity could be due to an altered antioxidant machinery, including transcriptional activation of genes, we determined the expression of several genes involved in the intracellular redox homeostasis. Using qPCR we calculated the relative quantity of *NRF2, FOXO3A, HMOX1, GPX1, TXNDR, PRDX3, PRDX6, SOD1*, *SOD2*, *p66sch* and *NOX4* mRNAs in both C- and LGA-HUAEC (**Figures 5A-5K**). However, the transcripts that could explain the biosensor data such as *GPX1*, *TXNDR, PRDX3, PRDX6, SOD1, SOD2, p66sch* and *NOX4* mRNAs showed no significant differences between groups. Conversely, a decrease in *NRF2* (**Figure 5A**) and an increase in *HMOX1* gene expression (**Figure 5C**), which is a target of Nrf2, was observed in LGA-HUAEC.

LGA-HUAEC overexpress the *GPX1* gene when exposed to a pro-oxidant stimulus

Following one of the premises of the "Developmental origins of health and disease (DOHaD)", where it has been proposed that the intrauterine oxidative stress milieu can reprogram the development and function of the offspring´s cardiovascular system, we decided to evaluate the response of LGA-derived HUAEC to an oxidative challenge. To test this, HUAEC where exposed to a moderate oxidative challenge (100 μM H_2O_2, 3 hours) after

which gene expression was evaluated. We detected a tenfold increase in *GPX1* mRNA levels in LGA-HUAEC, with no difference in C-HUAEC. Other transcripts such as *NRF2*, *PRDX3* and *SOD1* showed no differences between groups (**Figure 6A**). This result suggests that LGA-HUAEC could have some early programming of oxidative stress response during intrauterine life.

GPX1 gene transcription start site has an open state of chromatin in LGA-HUAEC

To evaluate if epigenetic mechanisms could be implicated in the increased gene expression of *GPX1* in H_2O_2-challenged LGA-HUAEC compared to C-HUAEC, we assessed the chromatin state of *GPX1*, *NRF2*, *HMOX1*, *PRDX3* and *SOD1* transcription start site (TSS). The magnitude of DNA digestion by DNase I depends directly on the chromatin state of the region evaluated. If chromatin has an open state (reduced nucleosome occupancy) DNase I can digest more DNA than in a closed state of the chromatin. In our approach, gDNA relative quantity after digestion was normalized by a constitutive closed chromatin region at *PAX7* TSS. Results show that there is no difference in the state of the chromatin at *NRF2*, *HMOX1*, *PRDX3* and *SOD1* TSS between LGA- and C-HUAEC. However, there was a higher DNA digestion in the *GPX1* TSS of LGA-HUAEC, indicating a more open state of chromatin in this proximal promoter site, compared to C-HUAEC (**Figure 6B**).

DISCUSSION

Among chronic diseases, cardiovascular conditions have become one of the most common causes of death worldwide. It is now very clear that intrauterine environment has a pivotal role in the risk of developing cardiovascular disease later in life. Large for Gestational Age

(LGA) newborn have an increased hazard risk of developing metabolic syndrome in their childhood (Boney *et al.*, 2005). LGA newborn from women with obesity present increased oxidative stress markers in the umbilical cord (Malti et al., 2014; Saker et al., 2008) associated with a decreased relaxation of chorionic arteries (Schneider et al., 2015). However, the cellular and molecular mechanisms by which this intrauterine environment can program the artery endothelial cell response to an oxidative challenge have not been clarified. The results shown in this work indicate that LGA-HUAEC presented a basal pro-oxidant status characterized by increased H_2O_2 levels and decreased GSH:GSSG ratio. The cells also have lower levels of superoxide anion associated to a high superoxide dismutase activity and elevated SOD1 and NOX4 protein levels in LGA-derived umbilical artery endothelium. A pro-oxidant challenge (peroxide) unveiled an increased H_2O_2 buffering capacity and an elevated disulfide reducing activity in LGA-HUAEC together with altered gene expression of critical antioxidant enzymes and changes in chromatin structure in the promotor of *GPX1*, strongly suggesting the participation of epigenetic mechanisms (summarized in **Figure 7**).

Earlier evidence have pointed out to oxidative stress as a common feature in the cardiovascular programming in LGA offspring (Malti et al., 2014; Schneider et al., 2015). However, to date no report has shown the mechanisms involved in this adaptation in artery endothelial cells isolated from LGA newborn exposed to maternal pregestational obesity.

The H_2O_2-biosensor HyPer, which has been useful to characterize redox homeostatic changes in living cells (Kallens et al., 2017; Román et al., 2017), evidenced that LGA-HUAEC elicited an increased oxidative tone at steady-state. The later could be explained by the elevated SODs activity together with the higher *in situ* SOD1 protein expression, which is supported by the reduced level of superoxide anion observed in LGA-HUAEC. The increased

expression of NOX4 in LGA-derived umbilical artery endothelium, could be participating in the altered redox status in this condition (Martyn et al., 2006). All these findings reflect the fine equilibrium between oxidative and reductive forces operating simultaneously in LGA-HUAEC.

Glutathione (GSH) is the major non-enzymatic cellular antioxidant (Dickinson & Forman, 2002). Glutathione peroxidases (GPX) uses GSH to reduce oxidized proteins generating the oxidized form of glutathione (GSSG) (Brigelius-Flohé & Maiorino, 2013). The intracellular GSH:GSSG ratio is broadly used to evaluate cell redox status (Locigno & Castronovo, 2001; Noctor & Foyer, 1998). The observation in our model that LGA-HUAEC had a lower GSH:GSSG ratio, due to lower levels of GSH, support the proposal that these cells exhibit a pro-oxidant status, as suggested by the results with the HyPer probe.

The analysis of the kinetics of the HyPer probe signals are useful to visualize the intrinsic components of the antioxidant machinery could be participating in the LGA-induced redox adaptations. The rate of the rising signal observed in the biosensor after the exogenous H_2O_2 pulses reflect the combination of two cellular aspects: the H_2O_2 permeability at plasma membrane defined mainly by aquaporins (Bienert & Chaumont, 2014; Miller et al., 2010) and the capacity of H_2O_2 to oxidize thiols on cytoplasmic proteins, since HyPer depends of peroxiredoxins (Stöcker e*t al.,* 2017). Our experiments indicate that after H_2O_2 exposure, LGA-HUAEC produce a slower increase in the biosensor signal compared to control cells, indicating that these cells better endure extracellular oxidant challenges. Moreover LGA-HUAEC showed to be more efficient to recover the HyPer signal than control cells, likely due to a better adapted machinery to reduce disulfide bonds on cytoplasmic proteins. Thus,

we propose that a chronic pro-oxidant fetal environment could modify the antioxidant machinery performance in LGA-HUAEC.

Then we decided to evaluate if there was an altered expression of antioxidant-related genes in LGA-HUAEC. Edlow et al. (2016) analyzed the cord blood transcriptome of the offspring from mothers with obesity, evidencing an altered segregation of mRNAs related to inflammatory signaling, glucose/lipid metabolism and ROS homeostasis, in comparison to newborn from lean mothers (Edlow *et al.*, 2016). In non-human primates, the mRNA of the reductive enzyme *Rdh12* was increased, among other candidate genes analyzed, in the liver of the offspring of dams fed a high-fat diet (Aagaard-Tillery *et al.*, 2008). Under basal conditions, we found that LGA-HUAEC have a down regulation of *NRF2* and an increase in *HMOX1* mRNA, both antioxidant proteins, indicating a possible programming of gene expression associated to a chronic pro-oxidant milieu secondary to maternal obesity.

The lack of induction of *NRF2* mRNA by oxidative stress could be explained by the fact that NRF2 actions depend mainly on its protein degradation/stabilization, and less on its gene transcription. It has been reported that NRF2 is constitutively degraded at the proteasome by a Keap1-dependent ubiquitination (McMahon *et al.*, 2003; Nguyen *et al.*, 2005). Oxidative stress induces the release of NRF2 from Keap-1, allowing its stabilization and nuclear translocation, where it binds to the gene promoter of target genes (Nguyen *et al.*, 2003). This action of NRF2 does not depend on its transcription rate but mainly on its protein stability and nuclear translocation (Nguyen *et al.*, 2009). In the Western blot experiments performed, the whole cell homogenates were analyzed, and no difference in the NRF2 protein was observed in LGA-HUAEC, compared to C-HUAEC. This result does not allow to differentiate between cytosolic and nuclear NRF2 protein location, which would have been

an interesting contribution to these data.

Remarkably, LGA-HUAEC showed an overexpression of *GPX1* mRNA in response to H_2O_2 treatment, compared to Control, resembling the Epigenetic Transcriptional Memory (ETM) described in immune cells exposed to inflammatory mediators (D´Urso & Brickner, 2016; Gialitakis et al., 2010). The ETM has been defined as an inducible gene overexpression when the same gene has been previously exposed to the same stimuli (Gialitakis *et al.*, 2010; Light *et al.*, 2013). ETM is explained by a first stimulus inducing regulatory proteins recruitment and an open state of the chromatin at the transcription start site (TSS) of inducible genes. The TSS of *GPX1* gene in LGA-HUAEC showed a higher DNase sensitivity, indicating an open state of the chromatin. This could be due to a previous regulatory protein recruitment that induced an enhanced response to the H_2O_2 challenge. If we consider the previously reported pro-oxidant environment in LGA fetuses from women with pregestational obesity (Malti et al., 2014; Catalano & Shankar, 2017), it is reasonable to ponder that oxidative response genes in LGA-derived HUAEC have been chronically stimulated during pregnancy, causing an epigenetic effect that can be mitotically inherited to cellular progeny. This mechanism could underlie the maintenance of an elevated risk of fast-onset endothelial dysfunction by future stressors in these subjects during their postnatal life (Gaillard, 2015).

The findings described here suggest the participation of oxidative stress, particularly H_2O_2, in the NO-dependent endothelial dysfunction observed in placental arteries from LGA newborn (Schneider *et al.*, 2015). After 10 minutes of H_2O_2 stimulation, a PI-3K/Akt-dependent endothelial Nitric Oxide Synthase (eNOS) activation is observed in bovine aortic endothelial cells (BAEC)(Cai *et al.*, 2003). However, BAEC treated for 24 h with H_2O_2 showed reduced levels of tetrahydrobiopterin (BH_4), a limiting cofactor for eNOS activity,

and its reducing enzyme dihydrofolate reductase (DHFR) (Chalupsky & Cai, 2005), leading to eNOS uncoupling and shifting to a superoxide producing enzyme (Förstermann & Münzel 2006). Thus, we propose that the previously described pro-oxidant intrauterine environment in pregnancies with LGA from women with obesity (Malti et al., 2014), leads LGA-HUAEC to shift to an adapted oxidative status. By the other hand, in genetic and chemical-induced oxidative cell models, a reduction of the GSH:GSSG ratio has been associated to endothelial dysfunction (Espinosa-Díez et al., 2018); characterized by eNOS uncoupling induced by elevated eNOS S-glutathionylation (Crabtree et al., 2013; Espinosa-Díez et al., 2018) and BH_4 oxidation to BH_2 (Crabtree *et al.*, 2013). Our group has previously shown evidence for eNOS inactivation in LGA-HUAEC (Muñoz-Muñoz *et al.*, 2018).

In order to survive, prokaryotic and eukaryotic cells have the ability of modify their cellular physiology in response to a pro-oxidant environment (Crawford & Davies, 1994; Lushchak, 2010). In the non-dividing human retinal pigmented epithelial cell line, chronic treatment with nonlethal H_2O_2 concentrations induced an increment of cell viability after lethal H_2O_2 treatment (3 mM, 1 h). The later was achieved due to high levels of catalase, CuZn-SOD and GPX1 activity (Jarrett and Boulton, 2005). A similar hormetic effect was found in mouse embryonic fibroblast (MEF) cells subjected to repeated treatments with low concentrations of H_2O_2 (Pickering *et al.*, 2013). Hence, we propose that LGA-derived HUAEC, which are chronically exposed to a pro-oxidant intrauterine environment, exhibit an oxidative adaptation characterized by an increased superoxide neutralizing system, higher SOD activity, SOD1 and NOX4 induced protein expression and an open chromatin status at the *GPX1* TSS.

Following the line of thought that support the early origins of chronic diseases (DOHaD), we propose that fetal endothelial cells from the offspring of women with pregestational obesity, exposed to oxidative stress during fetal development, can reprogram the redox system at a cellular and epigenetic level, to trigger a faster and more efficient response to subsequent oxidative-related insults.

CONCLUSIONS

This work evidences for the first time an increased antioxidant machinery performance in HUAEC isolated from LGA newborn from women with pregestational obesity, could impact the offspring´s endothelial function at birth. Based in the findings in gene expression and chromatin structure we propose that detrimental fetal environment could epigenetically modify gene expression and thus function in endothelial vascular cells (Block & El-Osta, 2017; Mcmillen, 2005). The long-term effects of these cellular adaptations need to be further studied in the postnatal life of LGA offspring, to confirm that these early findings induced by an altered maternal and fetal nutritional environment during pregnancy could lead to higher cardiovascular risk (Adamo et al., 2012; Oken & Gillman, 2003).

CONFLICT OF INTEREST.

Authors declare that they have no conflict of interest.

AUTHORS' CONTRIBUTION

ICW, OP, CJ and PC conceived and designed the experiments. ICW, OP, CH and CJ collected and analyzed the experimental data. ICW, OP, CJ and PC interpreted the experimental data. ICW, OP, CJ and PC drafted the article that was approved by all authors.

ORCID

Ivo Carrasco-Wong https://orcid.org/0000-0003-1020-734X

Omar Porras https://orcid.org/0000-0001-6314-9345

Paola Casanello http://orcid.org/0000-0002-2355-1476

REFERENCES

Aagaard-Tillery, K. M., Grove, K., Bishop, J., Ke, X., Fu, Q., McKnight, R., & Lane, R. H. (2008). Developmental origins of disease and determinants of chromatin structure: Maternal diet modifies the primate fetal epigenome. *Journal of Molecular Endocrinology*, *41*(1–2), 91–102. https://doi.org/10.1677/JME-08-0025

Adamo, K. B., Ferraro, Z. M., & Brett, K. E. (2012). Can we modify the intrauterine environment to halt the intergenerational cycle of obesity? *International Journal of Environmental Research and Public Health*, *9*(4), 1263–1307. https://doi.org/10.3390/ijerph9041263

Barber, a, Robson, S. C., Myatt, L., Bulmer, J. N., & Lyall, F. (2001). Heme oxygenase expression in human placenta and placental bed: reduced expression of placenta endothelial HO-2 in preeclampsia and fetal growth restriction. *The FASEB Journal : Official Publication of the Federation of American Societies for Experimental Biology*, *15*(7), 1158–1168. https://doi.org/10.1096/fj.00-0376com

Bienert, G. P., & Chaumont, F. (2014, May). Aquaporin-facilitated transmembrane diffusion of hydrogen peroxide. *Biochimica et Biophysica Acta - General Subjects*. https://doi.org/10.1016/j.bbagen.2013.09.017

Bird, A. (2007). Perceptions of epigenetics. *Nature*, *447*(7143), 396–398. https://doi.org/10.1038/nature05913

Block, T., & El-Osta, A. (2017). Epigenetic programming, early life nutrition and the risk of metabolic disease. *Atherosclerosis*, *266*, 31–40. https://doi.org/10.1016/j.atherosclerosis.2017.09.003

Boney, C. M., Verma, A., Tucker, R., & Vohr, B. R. (2005). Metabolic syndrome in childhood: association with birth weight, maternal obesity, and gestational diabetes mellitus. *Pediatrics*, *115*(3), e290-6. https://doi.org/10.1542/peds.2004-1808

Brigelius-Flohé, R., & Maiorino, M. (2013). Glutathione peroxidases ☆. *BBA - General Subjects*, *1830*, 3289–3303. https://doi.org/10.1016/j.bbagen.2012.11.020

Cai, H. U. A., Li, Z., Davis, M. E., Kanner, W., Harrison, D. G., & Jr, S. C. D. (2003). Akt-Dependent Phosphorylation of Serine 1179 and Mitogen- Activated Protein Kinase Kinase / Extracellular Signal-Regulated Kinase 1 / 2 Cooperatively Mediate Activation of the Endothelial Nitric-Oxide Synthase by Hydrogen Peroxide. *Molecular Pharmacology*, *63*(2), 325–331.

Catalano, P. M., & Shankar, K. (2017). Obesity and pregnancy: Mechanisms of short term and long term adverse consequences for mother and child. *BMJ (Online)*. https://doi.org/10.1136/bmj.j1

Chalupsky, K., & Cai, H. (2005). Endothelial dihydrofolate reductase: critical for nitric oxide bioavailability and role in angiotensin II uncoupling of endothelial nitric oxide synthase. *Proceedings of the National Academy of Sciences of the United States of America*, *102*(25), 9056–9061. https://doi.org/10.1073/pnas.0409594102

Crabtree, M. J., Brixey, R., Batchelor, H., Hale, A. B., & Channon, K. M. (2013). Integrated redox sensor and effector functions for tetrahydrobiopterin- and glutathionylation-dependent endothelial nitric-oxide synthase uncoupling. *Journal of Biological Chemistry*, *288*(1), 561–569. https://doi.org/10.1074/jbc.M112.415992

Crawford, D. R., & Davies, K. J. (1994). Adaptive response and oxidative stress.

Environmental Health Perspectives, *102 Suppl*, 25–28. https://doi.org/10.1289/ehp.94102s1025

D´Urso, A., & Brickner, J. H. (2016). Epigenetic transcriptional memory. *Current Genetics*, 1–5. https://doi.org/10.1007/s00294-016-0661-8

Dickinson, D. A., & Forman, H. J. (2002). Glutathione in defense and signaling: Lessons from a small thiol. In *Annals of the New York Academy of Sciences* (Vol. 973, pp. 488–504). John Wiley & Sons, Ltd (10.1111). https://doi.org/10.1111/j.1749-6632.2002.tb04690.x

Edelstein, A. D., Tsuchida, M. A., Amodaj, N., Pinkard, H., Vale, R. D., & Stuurman, N. (2014). Advanced methods of microscope control using μManager software. *Journal of Biological Methods*, *1*(2), 10. https://doi.org/10.14440/jbm.2014.36

Edlow, A. G., Hui, L., Wick, H. C., Fried, I., & Bianchi, D. W. (2016). Assessing the fetal effects of maternal obesity via transcriptomic analysis of cord blood: A prospective case-control study. *BJOG: An International Journal of Obstetrics and Gynaecology*, *123*(2), 180–189. https://doi.org/10.1111/1471-0528.13795

Espinosa-Díez, C., Miguel, V., Vallejo, S., Sánchez, F. J., Sandoval, E., Blanco, E., … Lamas, S. (2018). Role of glutathione biosynthesis in endothelial dysfunction and fibrosis. *Redox Biology*, *14*(August 2017), 88–99. https://doi.org/10.1016/j.redox.2017.08.019

Förstermann, U., & Münzel, T. (2006). Endothelial nitric oxide synthase in vascular disease: From marvel to menace. *Circulation*, *113*(13), 1708–1714. https://doi.org/10.1161/CIRCULATIONAHA.105.602532

Fridovich, I. (1995). Superoxide Radical and Superoxide Dismutases. *Annual Review of Biochemistry*, *64*(1), 97–112. https://doi.org/10.1146/annurev.bi.64.070195.000525

Fuhrich, D. G., Lessey, B. A., & Savaris, R. F. (2013). Comparison of HSCORE Assessment of Endometrial β3 Integrin Subunit Expression with Digital HSCORE Using Computerized Image Analysis (ImageJ). *Anal Quant Cytopathol Histpathol*, *35*(4), 210–216.

Gaillard, R. (2015). Maternal obesity during pregnancy and cardiovascular development and disease in the offspring. *European Journal of Epidemiology*, *30*(11), 1141–1152. https://doi.org/10.1007/s10654-015-0085-7

Gialitakis, M., Arampatzi, P., Makatounakis, T., & Papamatheakis, J. (2010). Gamma interferon-dependent transcriptional memory via relocalization of a gene locus to PML nuclear bodies. *Molecular and Cellular Biology*, *30*(8), 2046–2056. https://doi.org/10.1128/MCB.00906-09

Green, M. R., & Sambrook, J. (2017). Isolation of high-molecular-weight DNA using organic solvents. *Cold Spring Harbor Protocols*, *2017*(4), 356–359. https://doi.org/10.1101/pdb.prot093450

Hernández, H., Parra, A., Tobar, N., Molina, J., Kallens, V., Hidalgo, M., … Porras, O. (2018). Insights into the HyPer biosensor as molecular tool for monitoring cellular antioxidant capacity. *Redox Biology*, *16*, 199–208. https://doi.org/10.1016/j.redox.2018.02.023

Jarrett, S. G., & Boulton, M. E. (2005). Antioxidant up-regulation and increased nuclear DNA protection play key roles in adaptation to oxidative stress in epithelial cells. *Free*

Radical Biology and Medicine, *38*(10), 1382–1391. https://doi.org/10.1016/j.freeradbiomed.2005.02.003

Kallens, V., Tobar, N., Molina, J., Bidegain, A., Smith, P. C., Porras, O., & Martínez, J. (2017). Glucose Promotes a Pro-Oxidant and Pro-Inflammatory Stromal Microenvironment Which Favors Motile Properties in Breast Tumor Cells. *Journal of Cellular Biochemistry*, *118*(5), 994–1002. https://doi.org/10.1002/jcb.25650

Kim, J. K., Samaranayake, M., & Pradhan, S. (2009). Epigenetic mechanisms in mammals. *Cellular and Molecular Life Sciences*, *66*(4), 596–612. https://doi.org/10.1007/s00018-008-8432-4

Klose, R. J., & Bird, A. P. (2006). Genomic DNA methylation: the mark and its mediators. *Trends in Biochemical Sciences*, *31*(2), 89–97. https://doi.org/10.1016/j.tibs.2005.12.008

Krause, B. J., Costello, P. M., Muñoz-Urrutia, E., Lillycrop, K. A., Hanson, M. A., & Casanello, P. (2013). Role of DNA methyltransferase 1 on the altered eNOS expression in human umbilical endothelium from intrauterine growth restricted fetuses. *Epigenetics*, *8*(9), 944–952. https://doi.org/10.4161/epi.25579

Krause, B. J., Hernandez, C., Caniuguir, A., Vasquez-Devaud, P., Carrasco-Wong, I., Uauy, R., & Casanello, P. (2016). Arginase-2 is cooperatively up-regulated by nitric oxide and histone deacetylase inhibition in human umbilical artery endothelial cells. *Biochemical Pharmacology*, *99*, 53–59. https://doi.org/10.1016/j.bcp.2015.10.018

Light, W. H., Freaney, J., Sood, V., Thompson, A., D'Urso, A., Horvath, C. M., & Brickner, J. H. (2013). A conserved role for human Nup98 in altering chromatin

structure and promoting epigenetic transcriptional memory. *PLoS Biology*, *11*(3), e1001524. https://doi.org/10.1371/journal.pbio.1001524

Locigno, R., & Castronovo, V. (2001, August). Reduced glutathione system: role in cancer development, prevention and treatment. *International Journal of Oncology*. https://doi.org/10.3892/ijo.19.2.221

Lowry, O. H., Rosebrogh, N. J., Farr, A. L., & Randall, R. J. (1951). Protein measurement with the Folin phenol reagent. *The Journal of Biological Chemistry*, *193*(1), 265–275.

Lushchak, V. I. (2010). Adaptive response to oxidative stress: Bacteria, fungi, plants and animals. *Comparative Biochemistry and Physiology, Part C*, *153*, 175–190. https://doi.org/10.1016/j.cbpc.2010.10.004

Ma, Q. (2013). Role of nrf2 in oxidative stress and toxicity. *Annual Review of Pharmacology and Toxicology*, *53*, 401–426. https://doi.org/10.1146/annurev-pharmtox-011112-140320

Malti, N., Merzouk, H., Merzouk, S. A., Loukidi, B., Karaouzene, N., Malti, A., & Narce, M. (2014). Oxidative stress and maternal obesity: Feto-placental unit interaction. *Placenta*, *35*(6), 411–416. https://doi.org/10.1016/j.placenta.2014.03.010

Mane, V. P., Heuer, M. A., Hillyer, P., Navarro, M. B., & Rabin, R. L. (2008). Systematic method for determining an ideal housekeeping gene for real-time PCR analysis. *Journal of Biomolecular Techniques*, *19*(5), 342–347. https://doi.org/10.1111/j.1750-3841.2008.00880.x

Marseglia, L., Manti, S., D'Angelo, G., Nicotera, A., Parisi, E., Di Rosa, G., … Arrigo, T. (2015). Oxidative stress in obesity: A critical component in human diseases.

International Journal of Molecular Sciences, *16*(1), 378–400. https://doi.org/10.3390/ijms16010378

Martyn, K. D., Frederick, L. M., von Loehneysen, K., Dinauer, M. C., & Knaus, U. G. (2006). Functional analysis of Nox4 reveals unique characteristics compared to other NADPH oxidases. *Cellular Signalling*, *18*(1), 69–82. https://doi.org/10.1016/J.CELLSIG.2005.03.023

McMahon, M., Itoh, K., Yamamoto, M., & Hayes, J. D. (2003). Keap1-dependent Proteasomal Degradation of Transcription Factor Nrf2 Contributes to the Negative Regulation of Antioxidant Response Element-driven Gene Expression. *Journal of Biological Chemistry*, *278*(24), 21592–21600. https://doi.org/10.1074/jbc.M300931200

Mcmillen, I. C. (2005). Developmental Origins of the Metabolic Syndrome: Prediction, Plasticity, and Programming. *Physiological Reviews*, *85*(2), 571–633. https://doi.org/10.1152/physrev.00053.2003

Milad, M. A., Novoa P, J. M., Fabres, J. B., Margarita Samamé, M. M., Aspillaga, C. M., Rama de Neonatología, D., & Chilena de Pediatría, S. (2010). Recomendación sobre Curvas de Crecimiento Intrauterino. *Rev Chil Pediatr*, *81*(3), 264–274.

Miller, E. W., Dickinson, B. C., & Chang, C. J. (2010). Aquaporin-3 mediates hydrogen peroxide uptake to regulate downstream intracellular signaling. *Proceedings of the National Academy of Sciences*, *107*(36), 15681–15686. https://doi.org/10.1073/pnas.1005776107

Muñoz-Muñoz, E., Krause, B. J., Uauy, R., & Casanello, P. (2018). LGA-newborn from

patients with pregestational obesity present reduced adiponectin-mediated vascular relaxation and endothelial dysfunction in fetoplacental arteries. *Journal of Cellular Physiology*, *233*(10), 6723–6733. https://doi.org/10.1002/jcp.26499

Nguyen, D., & Nguyen, D. (2013). Quantifying chromogen intensity in immunohistochemistry via reciprocal intensity. *Protocol Exchange*. https://doi.org/10.1038/protex.2013.097

Nguyen, T., Nioi, P., & Pickett, C. B. (2009). The Nrf2-antioxidant response element signaling pathway and its activation by oxidative stress. *The Journal of Biological Chemistry*, *284*(20), 13291–13295. https://doi.org/10.1074/jbc.R900010200

Nguyen, T., Sherratt, P. J., Huang, H.-C., Yang, C. S., & Pickett, C. B. (2003). Increased protein stability as a mechanism that enhances Nrf2-mediated transcriptional activation of the antioxidant response element. Degradation of Nrf2 by the 26 S proteasome. *The Journal of Biological Chemistry*, *278*(7), 4536–4541. https://doi.org/10.1074/jbc.M207293200

Nguyen, T., Sherratt, P. J., Nioi, P., Yang, C. S., & Pickett, C. B. (2005). Nrf2 Controls Constitutive and Inducible Expression of ARE-driven Genes through a Dynamic Pathway Involving Nucleocytoplasmic Shuttling by Keap1. *Journal of Biological Chemistry*, *280*(37), 32485–32492. https://doi.org/10.1074/jbc.M503074200

Noctor, G., & Foyer, C. H. (1998). ASCORBATE AND GLUTATHIONE: Keeping Active Oxygen Under Control. *Annual Review of Plant Physiology and Plant Molecular Biology*, *49*(1), 249–279. https://doi.org/10.1146/annurev.arplant.49.1.249

Oken, E., & Gillman, M. W. (2003). Fetal origins of obesity. *Obesity Research*, *11*(4), 496–

506. https://doi.org/10.1038/oby.2003.69

Pfaffl, M. W. (2001). A new mathematical model for relative quantification in real-time RT-PCR. *Nucleic Acids Research*, *29*(9), e45.

Pickering, A. M., Vojtovich, L., Tower, J., & A Davies, K. J. (2013). Oxidative stress adaptation with acute, chronic, and repeated stress. *Free Radical Biology & Medicine*, *55*, 109–118. https://doi.org/10.1016/j.freeradbiomed.2012.11.001

Reik, W. (2007). Stability and flexibility of epigenetic gene regulation in mammalian development. *Nature*, *447*(7143), 425–432. https://doi.org/10.1038/nature05918

Román, F., Urra, C., Porras, O., Pino, A. M., Rosen, C. J., & Rodríguez, J. P. (2017). Real-Time H2 O2 Measurements in Bone Marrow Mesenchymal Stem Cells (MSCs) Show Increased Antioxidant Capacity in Cells From Osteoporotic Women. *Journal of Cellular Biochemistry*, *118*(3), 585–593. https://doi.org/10.1002/jcb.25739

Rosso, P. (1985). A new chart to monitor weight gain during pregnancy. *American Journal of Clinical Nutrition*, *41*(3), 644–652.

Saker, M., Soulimane Mokhtari, N., Merzouk, S. A., Merzouk, H., Belarbi, B., & Narce, M. (2008). Oxidant and antioxidant status in mothers and their newborns according to birthweight. *European Journal of Obstetrics Gynecology and Reproductive Biology*, *141*(2), 95–99. https://doi.org/10.1016/j.ejogrb.2008.07.013

Schneider, D., Hernández, C., Farías, M., Uauy, R., Krause, B. J., & Casanello, P. (2015). Oxidative stress as common trait of endothelial dysfunction in chorionic arteries from fetuses with IUGR and LGA. *Placenta*, *36*(5). https://doi.org/10.1016/j.placenta.2015.02.003

Stewart, A. F., Reik, A., & Schütz, G. (1991). A simpler and better method to cleave chromatin with DNase1 for hypersensitive site analyses. *Nucleic Acids Research*, *19*(11), 3157. https://doi.org/10.1093/nar/19.11.3157

Stöcker, S., Maurer, M., Ruppert, T., & Dick, T. P. (2017). A role for 2-Cys peroxiredoxins in facilitating cytosolic protein thiol oxidation. *Nature Chemical Biology*, *14*(2), 148–155. https://doi.org/10.1038/nchembio.2536

TABLES

Table 1. Baseline characteristics of the study population.

	Control group n = 20	LGA group n = 21
Gestational age (weeks)	38.5 ± 0.53	38.6 ± 0.19
Newborn Birth weight (g)	3464± 75.44	4168 ± 39.31****
Height (cm)	50.8 ± 0.60	52.2 ± 0.23**
Ponderal index	2.7 ± 0.07	2.9 ± 0.04**
Gender F/M	8/12	8/13
Maternal weight (g)	70.5 ± 1.20	88.2 ± 2.39****
Maternal height (m)	1.6 ± 0.01	1.6 ± 0.02
Maternal BMI	27.7 ± 0.18	34.0 ± 0.91****

Ponderal index expressed as birth weight x 100 x height^{-3} (g x cm^{-3}), and maternal body mass index (BMI) expressed as kg x m^{-2}. F and M indicate total number of female or male neonates. Values are mean ± S.E.M. or frequency. ***p < 0.001 ****p < 0.0001 determined by Mann-Whitney test or Chi^2, accordingly.

Table 2. Primers sequences and amplification conditions for mRNA RT-qPCR

mRNA Target	Forward Sequence 5¨--- 3¨	Reverse Sequence 5¨--- 3¨	Annealing T°	Efficiency (%)
NRF2	caactactcccaggttgccc	agtgactgaaacgtagccga	58°	109,5
HMOX1	caaagtgcaagattctgcccc	caactgtcgccaccagaaag	58°	96
FOXO3A	acaaacggctcactctgtcc	ggatggagttcttccagccg	60°	105
GPX1	agtgcgaggtgaacggtgcg	ggggtcggtcataagcgcgg	58°	94
PRDX3	tgccattccttggggcatt	catgaggaactggtgctgaat	58°	102,9
PRDX6	ctcgggactttaccccagtg	tgatatccttgctccaggca	58°	92,2
TXNDR1	gcatttgcagcagagcgaaa	tgccctcctgataagcaagaa	58°	97
SOD1	ggtgtggccgatgtgtctat	cctttgcccaagtcatctgc	58°	90,6
SOD2	tggggttggcttggtttcaa	tagtaagcgtgctcccacac	58°	97,9
NOX4	tccagtccttccgttggtttgc	cctttgcccaagtcatctgc	58°	99,4
p66sch	gaacaaatcacacctctgggc	cattgaagaattcaggggtcca	60°	99,5
ATP5F1	gccctgacagattctcctatcg	caataccctggacctaggaag	58°	103
RPLP0	aatctccaggggcaccattg	gaacacctgctggatgacca	58°	93
RPLP2	gcgccaaggacatcaagaag	ccagcaggtacactggcaa	56°	96

Table 3. Primers sequences and amplification conditions for gDNA qPCR

gDNA Target	Forward Sequence 5¨--- 3¨	Reverse Sequence 5¨--- 3¨	Annealing T°	Efficiency (%)
NRF2 TSS	ctggagttcggacgctttga	ttctcgggcggtaaagtgag	58	98
HMOX1 TSS	tggccagactttgtttccca	tgaggacgctcgagaggag	58	97
GPX1 TSS	ggacgcgtgctcctcctaag	cccacatcctaactcaggaacc	64	103
PAX7 TSS	taaaagaaaagtccgaacctatc	gtttcagggctggacgga	60	90

Table 4. Parameters of HyPer fluorescence kinetics in C-HUAEC and LGA-HUAEC.

		C-HUAEC	LGA-HUAEC
Increment	Maximum reached (%)	115.7 ± 53.5	41.29 ± 23.4****
	Slope (percent/s)	0.83 ± 0.16	0.14 ± 0.02****
	Half-time (s)	144.9 ± 10	196 ± 7.6****
	AUC	18089 ± 11749	4480 ± 2683***
Recovery	Minimum reached (%)	58.94 ± 38.2	11.42 ± 27.1****
	Slope (percent/s)	-0.23 ± 0.05	-0.48 ± 0.04****
	Half-time (s)	123.4 ± 11.9	140 ± 4.1****
	AUC	18644 ± 3619	13441 ± 3969****

Maximum and minimum reached are the last data collected in increment and recovery curves, respectively. The slope of each curve was calculated between 80 and 180 seconds, which matches a clear increase and reduction of fluorescence in the increment and recovery curves, respectively. AUC= Area under the curve. Values are mean ± SEM. *** $p < 0,001$, ****$p < 0,0001$ determined by t-test with Welch´s correction (C-HUAEC n= 3, 21 experimental replicates and LGA-HUAEC n=3, 57 experimental replicates).

FIGURE LEGENDS

Figure 1. Indirect H_2O_2 measurement in C-HUAEC and LGA-HUAEC by HyPer under basal and oxidative stress conditions. (A) and (B) Representative data obtained by HyPer in Control- and LGA-HUAEC, respectively. After transduction of HUAEC with HyPer, cells were washed and placed with Krebs buffer to achieve resting conditions. Under an epifluorescence microscope, excitation was performed at 420 and 490 nm and fluorescence was acquired at 530 nm every 20 sec for resting conditions and after a curve of H_2O_2 concentration (1 to 200 µM) for each experiment, ending with a 1000 µM dose for calibration purposes. (C) Basal fluorescence of HyPer-probe in C- and LGA-HUAEC. Fluorescence at the end stabilizing stage were compared between C-HUAEC and LGA-HUAEC. In the box plots, the mean, the interquartile range are indicated. The end of whiskers indicate the minimal and maximal values, respectively. **** $p<0.0001$, Mann-Whitney test. (D) The H_2O_2 concentration-response curve. The highest fluorescence reached with every H_2O_2 concentration were used to calculate and to compare EC50, in C- and LGA-HUAEC, in a normalized percentage of response *vs* log H_2O_2 concentration curve. EC50 were 44.89 and 104.9 µM for C-HUAEC and LGA-HUAEC, respectively. Values are mean ± S.E.M. (C-HUAEC n= 3, 21 replicates and LGA-HUAEC n=3, 57 replicates). (E) HyPer signal increment following H_2O_2 challenge. A normalized percentage of response *vs* time (seconds) was made with fluorescence collected during the first 300 seconds of 100 µM H_2O_2 treatment. C-HUAEC data fitted in a Non-Linear Boltzman sigmoidal curve. Lineal regression was used to calculate LGA-HUAEC fluorescence kinetic data. Values are Mean ± S.E.M. **** $p< 0.0001$, Two-way ANOVA, Bonferroni's multiple comparisons test. (C-

HUAEC n= 3, 14 replicates and LGA-HUAEC n=3, 49 replicates) (F) HyPer signal reduction following H_2O_2 withdraw. A normalized percentage of response *vs* time (seconds) was made with fluorescence collected during the first 260 seconds after H_2O_2 withdraw. Linear regression was used to calculate both C- and LGA-HUAEC fluorescence kinetic data. Values are Mean ± S.E.M. *** p< 0.001, Two-way ANOVA, Bonferroni's multiple comparisons test (C-HUAEC n=3, 21 replicates and LGA-HUAEC n=3, 57 replicates).

Figure 2. Basal superoxide anion level, SODs activity and quantitative measurement of GSH and GSSG in C-HUAEC and LGA-HUAEC. (A) Superoxide anion determination. C- and LGA-HUAEC were incubated with DHE 10 mM for 30 min at 37°C in darkness, washed 3 times with PBS previous incubation with DAPI 300 nM for 5 min in darkness at room temperature. Excesses of fluorescent molecules were rinsed 3 times. Cells were maintained Krebs buffer in darkness and immediately measured in a multiplate reader. DHE and DAPI fluorescence were acquired at (excitation/emission) 490/580 nm and 358/461 nm, respectively. ** p<0.01, Mann-Whitney test, (C-HUAEC n= 5, LGA-HUAEC n=5). (B) For SODs activity, C- and LGA-HUAEC lysate (50 µL) were used to determine the reduction of cytochrome c by the superoxide radical in the xanthine/xanthine oxidase system. The activity was measured by 2 min at 37°C in spectrophotometer at 550 nm. * p<0.05, Mann-Whitney test (C-HUAEC n= 5, LGA-HUAEC n=5). (C, D and E) For the GSH/GSH assay, the C- and LGA-HUAEC lysate (100 µL) were incubated to 37°C and mixed with of KPE buffer, NADPH and DTNB to oxidize all GSH to GSSG and produce the TNB chromophore. The rate of TNB formation was followed by 2 min at 412 nm. The rate was compared with a standard curve of GSH and GSSG in buffer. ** p<0.01, **** p<0.0001, Mann-Whitney test.

(C-HUAEC n= 5, LGA-HUAEC n=5). In the box plots, the mean, the interquartile range are indicated. The end of whiskers below and above the box indicate the minimal and maximal values, respectively. **** $p<0.0001$, Mann-Whitney test.

Figure 3. Basal Protein level of antioxidant and pro-oxidant enzymes in C-HUAEC and LGA-HUAEC. (A) and (B) are representative Western blots for the proteins analyzed. The relative amount of NRF2 (C), HMOX1 (D), GPX1 (E), SOD1 (F) and NOX4 (G) between C- and LGA-HUAEC is presented. In the box plots, the mean, the interquartile range are indicated. The end of whiskers below and above the box indicate the minimal and maximal values, respectively. **** $p<0.0001$, Mann-Whitney test (C-HUAEC n= 8, LGA-HUAEC n=11).

Figure 4. Umbilical artery endothelium *in situ* levels of H_2O_2 producing and reducing enzymes in Control and LGA-MO umbilical cords. (A) Representative microphotography from histological sections of umbilical cords stained for NOX4, SOD1 and GPX1. The intensity of DAB, in endothelial cells, was measured using HDAB color deconvolution plug-in of Fiji version of ImageJ software. Scale bar = 200 μm. (B) Statistical analyses of reciprocal intensity from NOX4, SOD1 and GPX1 in Control and LGA-MO umbilical cords. In the box plots, the mean, the interquartile range are indicated. The end of whiskers below and above the box indicate the minimal and maximal values, respectively. ** $p<0.01$, **** $p<0.0001$, Mann-Whitney test (C-HUAEC n=5 and LGA-HUAEC n=5), where 40 groups of 6 cells (C-HUAEC) and 57 groups of 6 cells (LGA-HUAEC) were analyzed.

Figure 5. Basal mRNA level of genes involved in the antioxidant and pro-oxidant response in C-HUAEC and LGA-HUAEC. Total RNA was extracted with Trizol® and quantified. The cDNA was obtained from 500 ng of RNA by reverse transcription. Relative quantities of mRNA for *NRF2* (A), *FOXO3A* (B), *HMOX1* (C), *GPX1* (D), *TXNDR* (E), *PRDX3* (F), *PRDX6* (G), *SOD1* (H), *SOD2* (I), *p66sch* (J) and *NOX4* (K) comparing between C-HUAEC and LGA-HUAEC was performed by qPCR. In the box plots, the mean, the interquartile range are indicated. The end of whiskers below and above the box indicate the minimal and maximal values, respectively. * $p< 0.05$ **$p< 0.01$, Mann-Whitney test (C-HUAEC n= 4, LGA-HUAEC n=7).

Figure 6. Transcript levels of antioxidant and pro-oxidant genes after H_2O_2 treatment and its chromatin accessibility in C-HUAEC and LGA-HUAEC. (A) Transcript levels of NRF2, HMOX1, GPX1, PRDX3 and SOD1 genes in C-HUAEC and LGA-HUAEC after H_2O_2 treatment. Cells were challenged with 100 μM of H_2O_2 for 3 h. Then, total RNA was extracted with Trizol® and quantified, 500 ng of RNA were reverse transcribed, and qPCR was performed. Values are mean ± S.E.M. * $p< 0.05$ vs C-HUAEC, Mann-Whitney test (C-HUAEC n= 3, LGA-HUAEC n=3). (B) DNase hypersensitivity assay for antioxidant gene promoters. Primary C-HUAEC and LGA-HUAEC were lysed and the DNA obtained was digested with zero or 6,25 U of DNase I for 5 minutes at 22°C. The Genomic DNA (gDNA) was extracted by phenol-chloroform method and quantified. Using 25 ng of gDNA, relative quantities of *NRF2*, *HMOX1* and *GPX1* gDNA were calculated using *PAX7* as endogenous control. Values are mean ± S.E.M. * $p< 0.05$ vs C-HUAEC, Mann-Whitney test (C-HUAEC n= 3, LGA-HUAEC n=3).

Figure 7. HUAEC from LGA-MO newborn show a pro-oxidant status and a higher antioxidant performance. The altered redox status of LGA-HUAEC is characterized by increased H_2O_2 level and decreased GSH:GSSG ratio. The cells also showed a diminished level of superoxide anion associated to a high activity superoxide dismutases; associated to elevated protein levels of SOD1 and NOX4, both H_2O_2 producer enzymes. A pro-oxidant challenge revealed in LGA-HUAEC an increased H_2O_2 buffering capacity and an elevated reductive activity. In front of an oxidative stimulus, in LGA-HUAEC *GPX1* gene was overexpressed associated with an open chromatin structure at basal level, strongly suggesting the participation of epigenetic mechanisms.

FIGURES

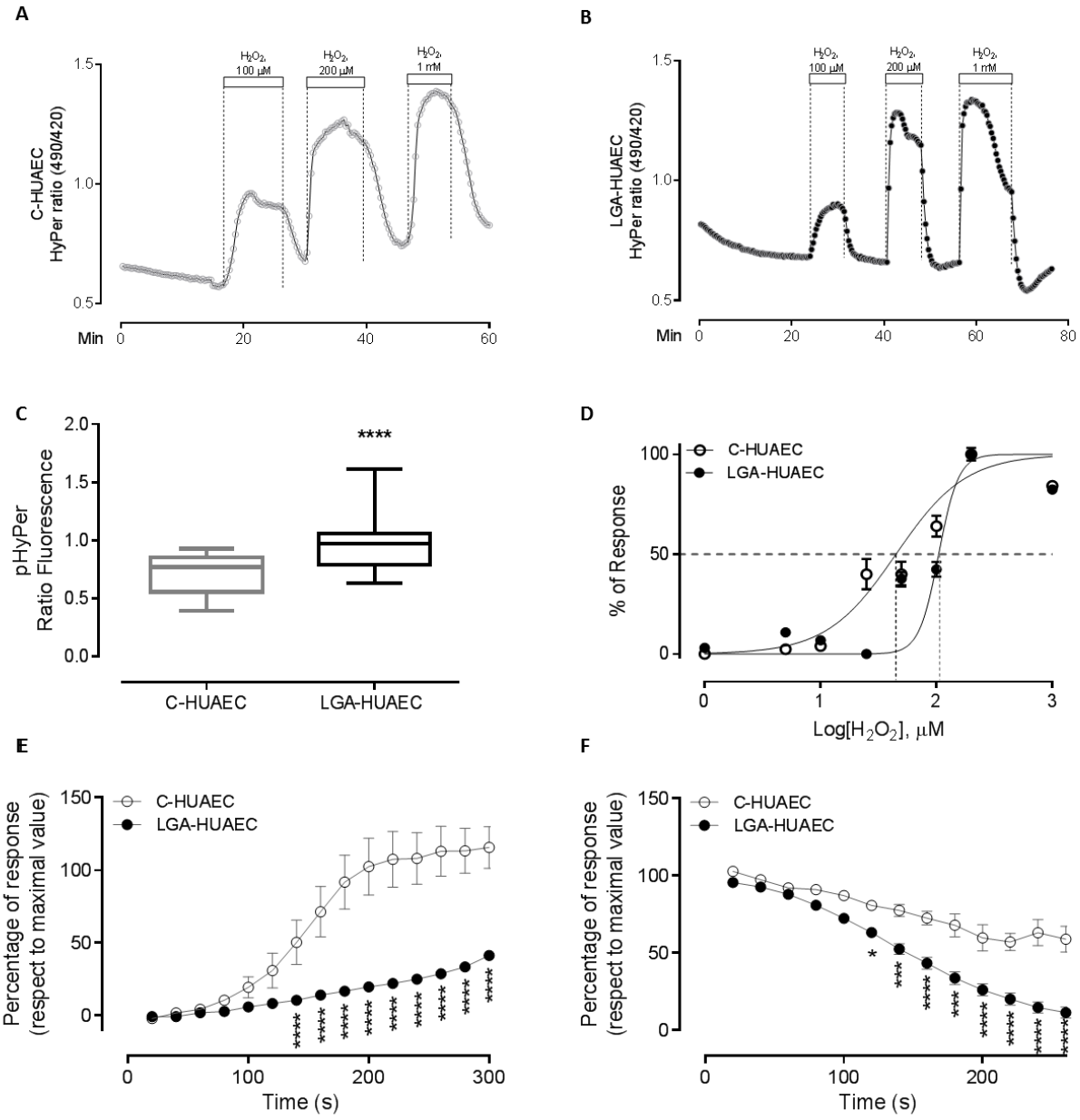

Figure 1. Indirect H_2O_2 measurement in C-HUAEC and LGA-HUAEC by HyPer under basal and oxidative stress conditions

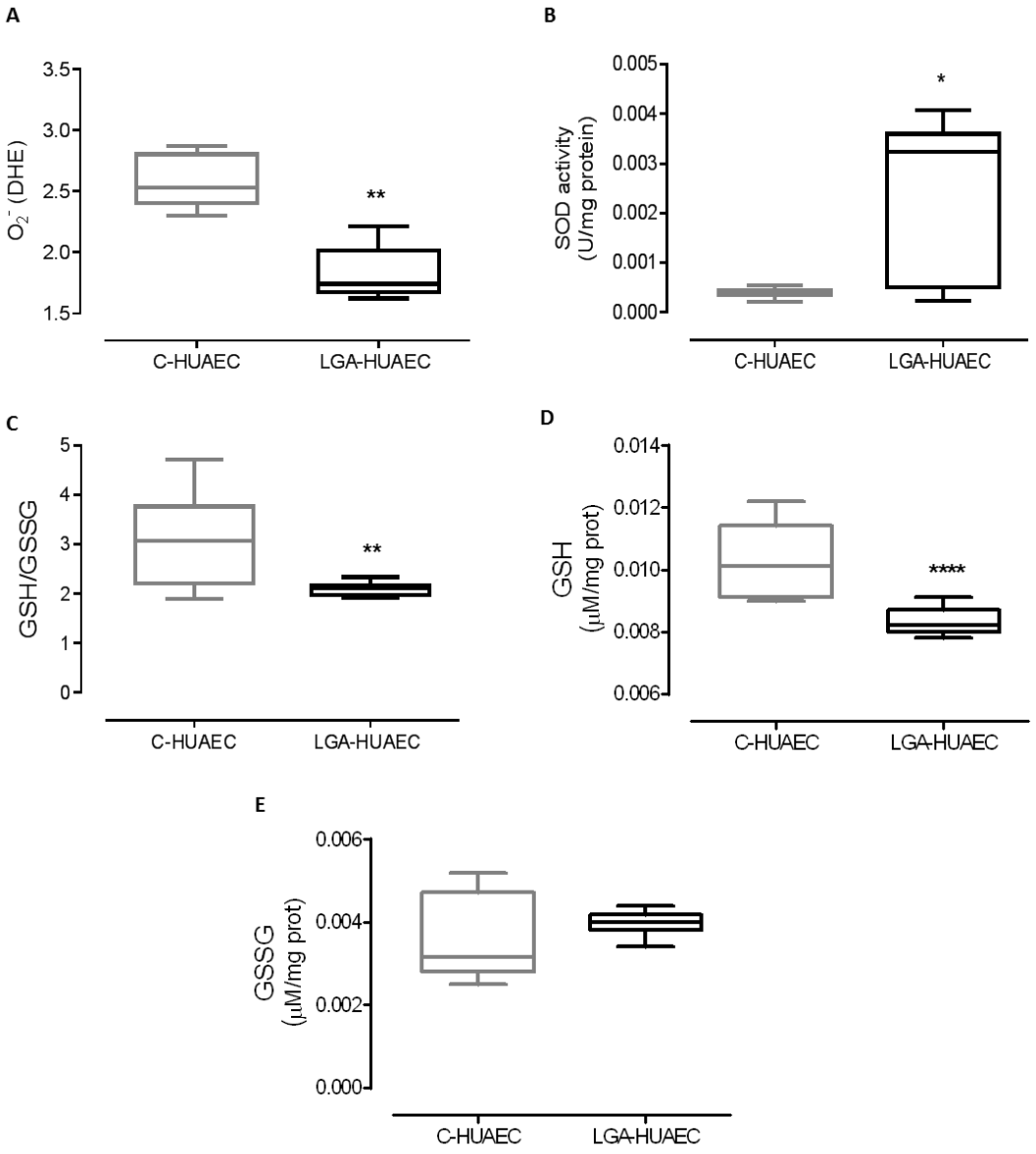

Figure 2. Basal superoxide anion level, SODs activity and quantitative measurement of GSH and GSSG in C-HUAEC and LGA-HUAEC.

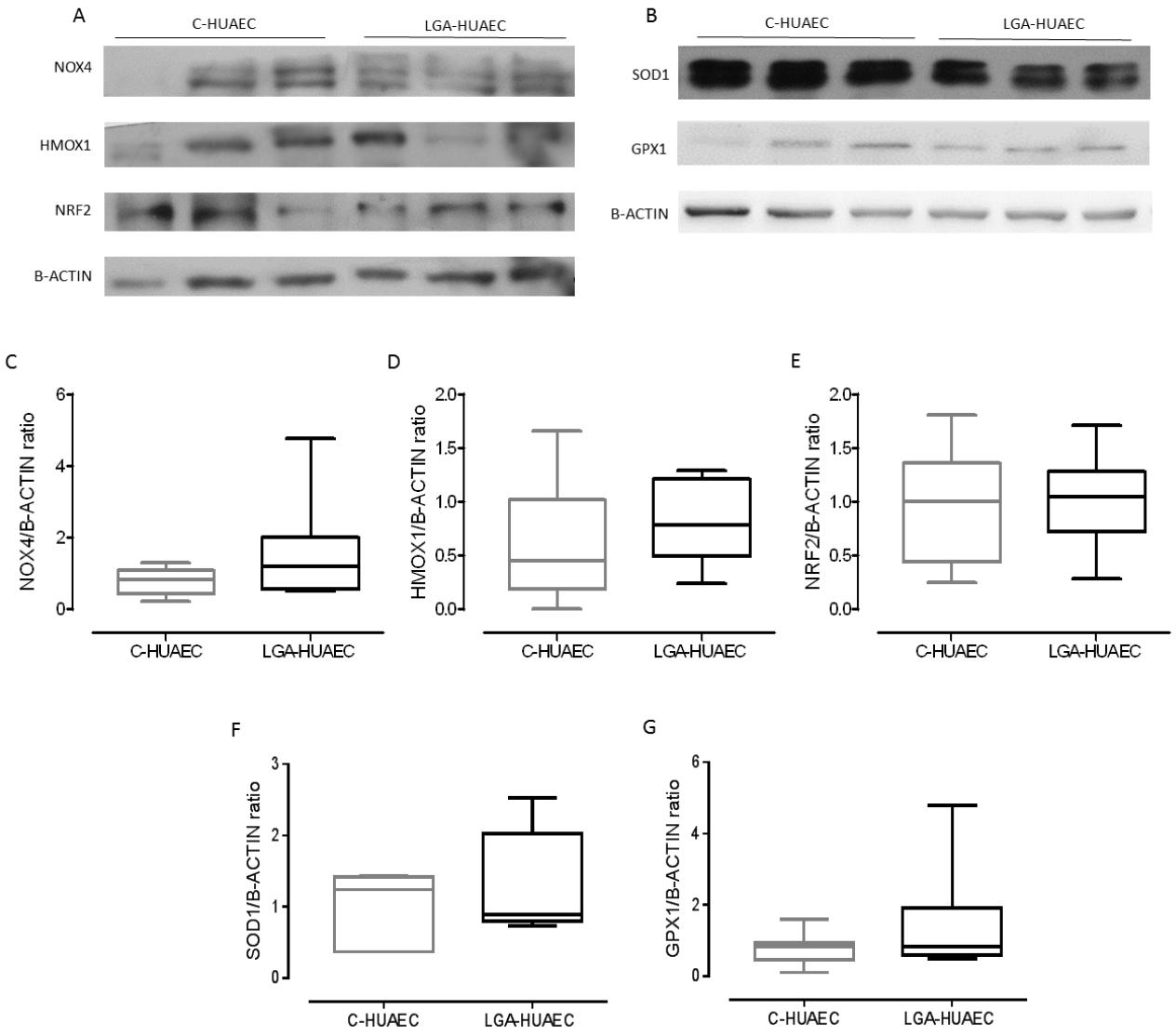

Figure 3. Basal Protein level of antioxidant and pro-oxidant enzymes in C-HUAEC and LGA-HUAEC.

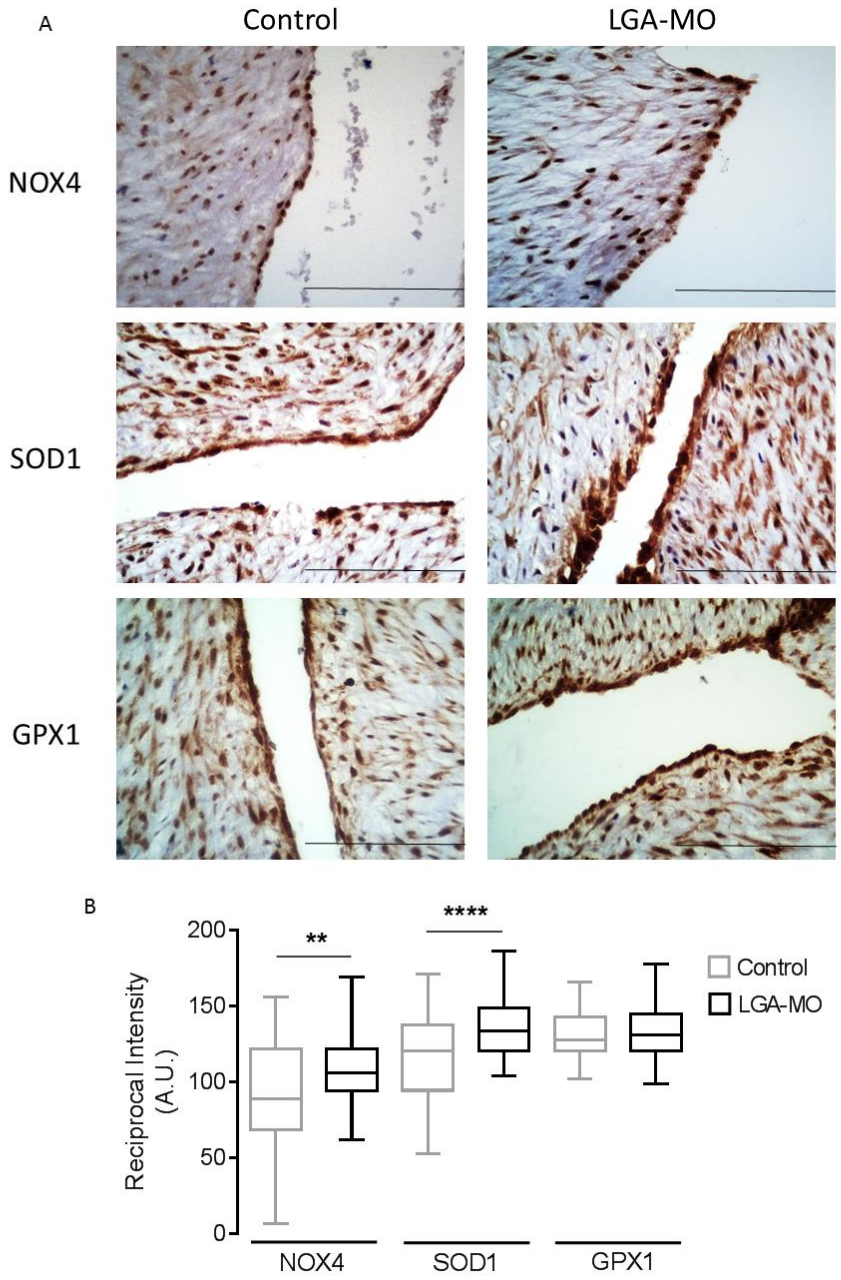

Figure 4. Umbilical artery endothelium *in situ* levels of H_2O_2 producing and reducing enzymes in Control and LGA-MO umbilical cords.

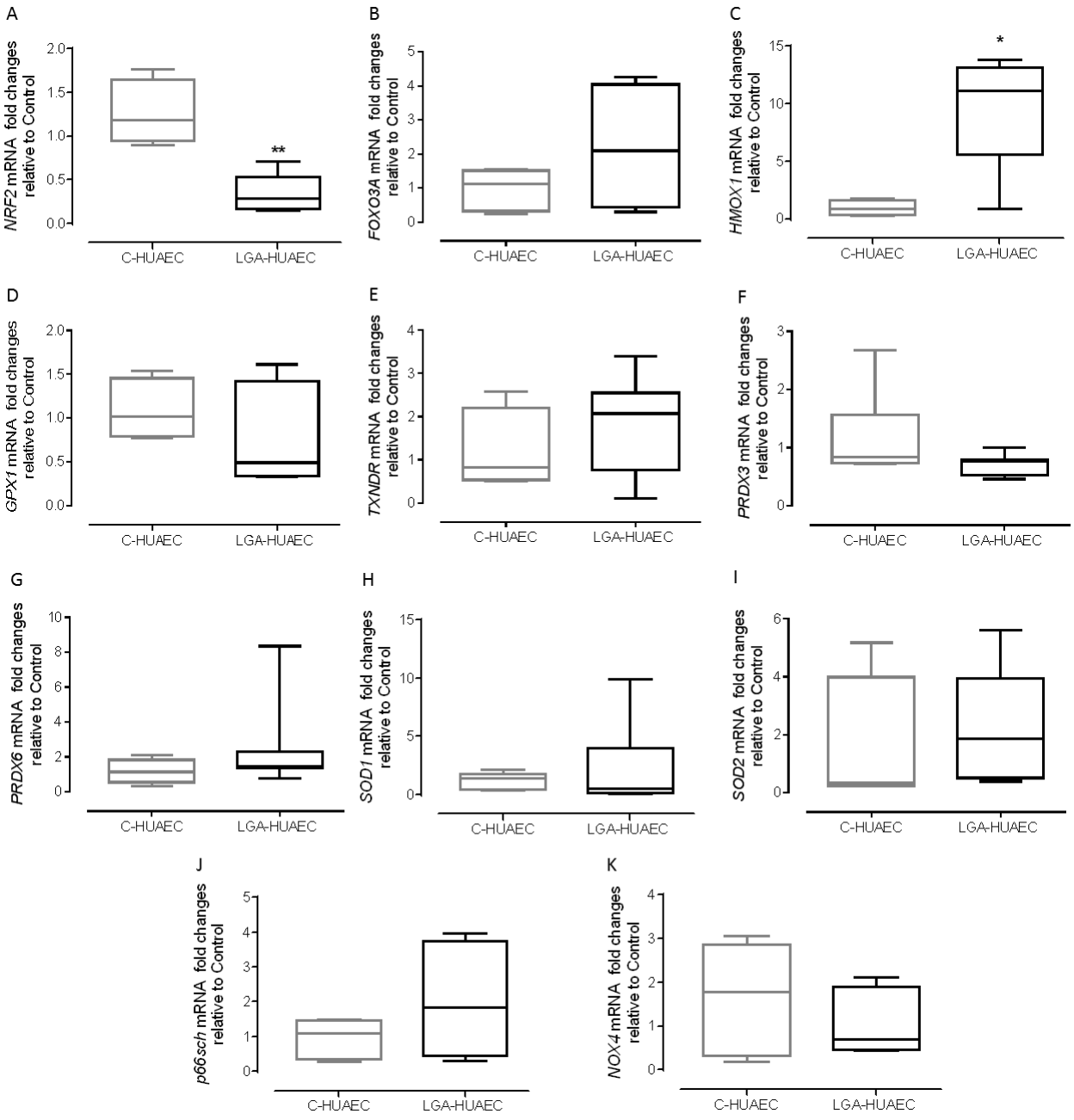

Figure 5. Basal mRNA level of genes involved in the antioxidant and pro-oxidant response in C-HUAEC and LGA-HUAEC.

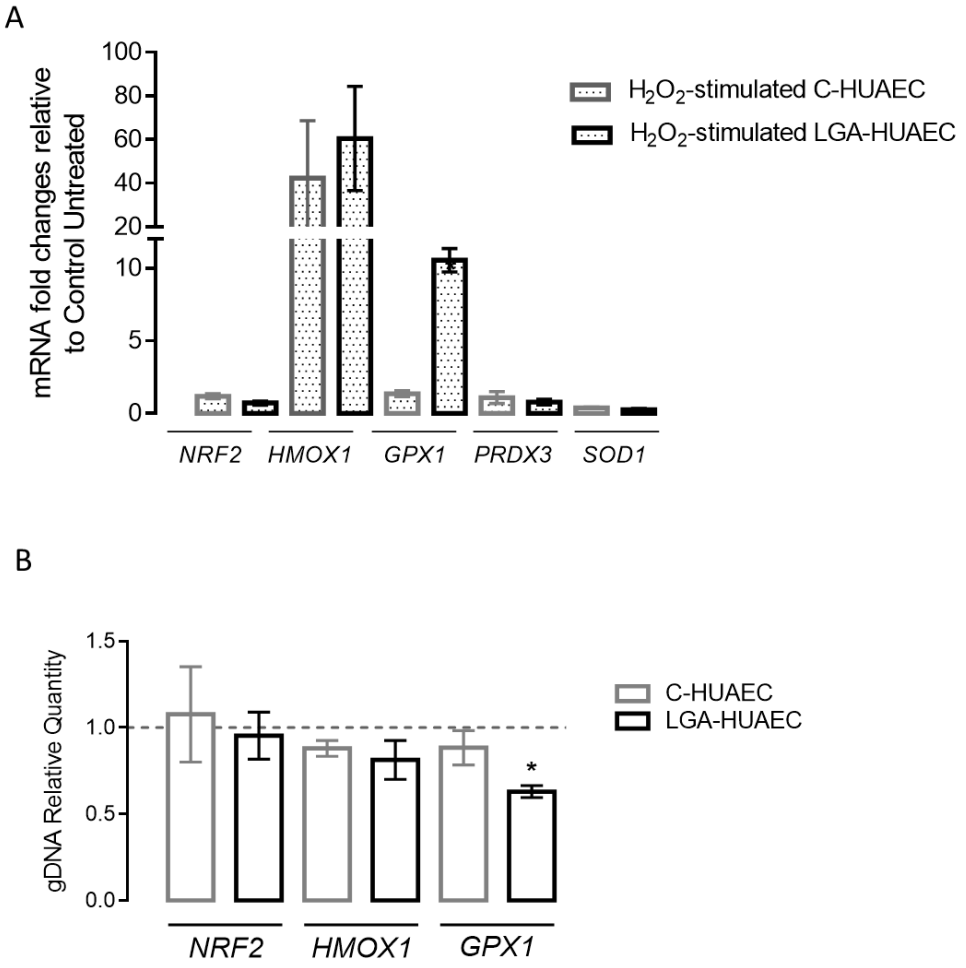

Figure 6. Transcript levels of antioxidant and pro-oxidant genes after H_2O_2 treatment and its chromatin accessibility in C-HUAEC and LGA-HUAEC.

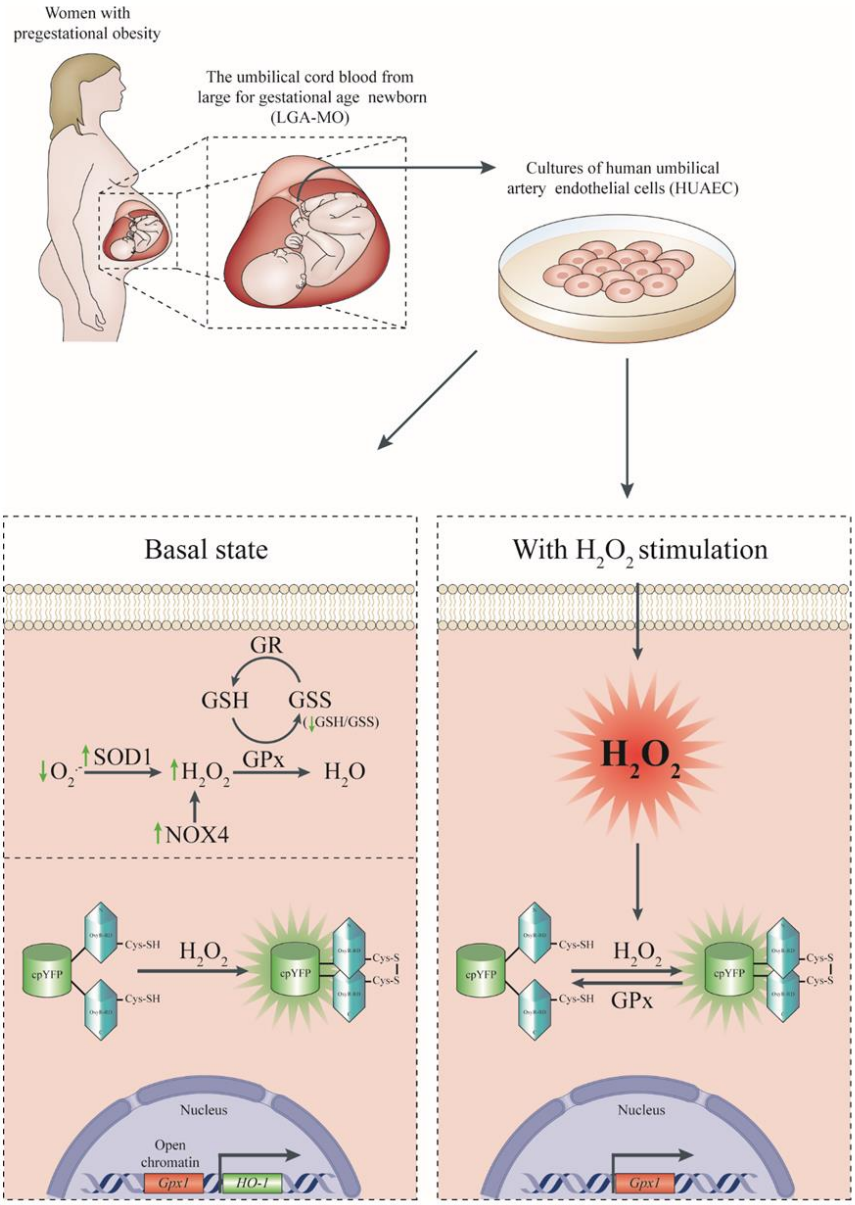

Figure 7. HUAEC from LGA-MO newborn show a pro-oxidant status and a higher antioxidant performance.

CHAPTER III

NRF2 PRE-RECRUITMENT AT ENHANCER2 IS A HALLMARK OF H_2O_2-INDUCED EPIGENETIC TRANSCRIPTIONAL MEMORY IN *HMOX1* IN HUMAN ENDOTHELIAL CELLS.

(Unsubmitted draft)

NRF2 PRE-RECRUITMENT AT ENHANCER2 IS A HALLMARK OF H_2O_2-INDUCED EPIGENETIC TRANSCRIPTIONAL MEMORY IN *HMOX1* IN HUMAN ENDOTHELIAL CELLS.

Ivo Carrasco-Wong[1], Gernot Längst[2], Paola Casanello[3,4]

[1]Cell & Molecular Biology PhD Program, Faculty of Biological Sciences, Pontificia Universidad Católica de Chile, Santiago, Chile, [2]Biochemistry III; Biochemistry Centre Regensburg (BCR), University of Regensburg, Regensburg, Germany, [3]Department of Obstetrics and [4]Department of Neonatology, School of Medicine, Pontificia Universidad Católica de Chile, Santiago, Chile.

***Correspondence**: Dr Paola Casanello
Department of Obstetrics
Department of Pediatrics
School of Medicine
Pontificia Universidad Católica de Chile
Marcoleta 391, Santiago, Chile.
Tel: 56-2-2354 8119
Fax: 56-2-632 1924
E-mail: pcasane@uc.cl

Ivo Carrasco MSc
PhD Program in Cell & Molecular Biology
Faculty of Biological Sciences
Pontificia Universidad Católica de Chile
Avda. Libertador Bernardo OHiggins 340, Santiago, Chile.
Tel: 56-2-2354 8119
Fax: 56-2-632 1924
E-mail: icarrasco@uc.cl

§ Current address: *Biomedical Research Center, School of Medicine, Universidad de Valparaíso, Valparaíso, Chile.*

ABSTRACT

Maternal obesity is a major cause of increased cardiometabolic risk in the offspring. Large for gestational age newborns from obese mothers, present endothelial dysfunction in chorionic and umbilical arteries. Alterations in physiologic and cellular redox status are strongly associated with altered gene regulation in arteries from large for gestational age newborn. However, specific mechanisms by which the pro-oxidant fetal environment could modulate gene expression during the offspring lifespan are still elusive. Here, we evidence that oxidative-stress can reprogram the stimulus-response of antioxidant coding-genes, by epigenetic transcriptional memory mechanism. Using an H_2O_2 double-hit-protocol we found that *HMOX1* gene presents an ETM-like response, associated with chromatin structure changes at the *HMOX1* gene regulatory regions. The ETM-like response was characterized by a paused-RNAPII and NRF2 enrichment at transcription start site and enhncer2 of *HMOX1* gene, respectively. Here we show that ETM can be induced by an oxidative challenge, suggesting that ETM could be one of the epigenetic mechanisms involved in fetal programming.

Keywords: Epigenetic transcriptional memory, oxidative stress, *HMOX1*, NRF2, endothelium.

INTRODUCTION

Obesity is a global epidemic(1). Maternal obesity has been related to increased cardiometabolic risk in the offspring during lifespan(2,3). Endothelial dysfunction has been found in chorionic arteries isolated from large for gestational age (LGA) newborn from obese mothers (OM), associated with an anomalous response to oxidative stress(4). Previous reports evidence an increase in oxidative stress markers in the umbilical cord and peripheral blood from LGA newborn and OM, respectively(5). Suggesting that oxidative stress possibly plays a pivotal role in the detrimental fetal programming of vascular function.

In the vasculature, the main source of ROS are NADPH oxidases (NOX), Xanthine oxidoreductase (XOR), uncoupled endothelial nitric oxide synthase (eNOS) and mitochondrial respiration complexes(6,7). By the other hand, there are several antioxidant systems such as the thioredoxin, peroxiredoxin or glutathione systems that protect or repair the damage caused by reactive oxygen species (ROS) or reactive nitrogen species (RNS)(8,9). The implication of oxidative stress in anomalous vascular function is clear since exogenous antioxidants as N-acetylcysteine (NAC)(4) and sulforaphane(10) decrease endothelial dysfunction.

Notably, the relationship between a pro-oxidant milieu and metabolic diseases has been clearly established. Male mice that overexpress Glutathione peroxidase 1 (GPX1) developed higher body weight and insulin resistance(11). The phenomenon of hyperglycemia-induced metabolic memory in antioxidant-coding genes is due to epigenetic mechanisms (12). The later, as well as other reports, have evidenced that detrimental metabolic states can induce permanent changes in antioxidant cellular systems(13–15).

In previous unpublished results, our group found that in human umbilical artery endothelial cell (HUAEC) isolated from LGA newborn *NRF2* and *HMOX1* mRNA basal level was downregulated and overexpressed, respectively. Interestingly, after H_2O_2 treatment *GPX1* gene expression was tenfold higher in LGA-HUAEC than Control-HUAEC, suggesting to epigenetic transcriptional memory (ETM) as a possible underlying mechanism.

ETM is the mechanism, in which genic response to a first induction is "remembered", inducing an over-expression of the same gene by a second stimulus (Reviewed in (16)). The memory can be maintained by four or five cell divisions, without any re-stimulation in the meantime(17–19). The events and mechanisms that control ETM have been studied mainly in eukaryotic cells, in both yeast and human cells. The features that characterize ETM can be summarized as follows: 1) The second gene induction is faster and stronger compared to the first induction(20); 2) the "memory" is maintained up to five cell divisions(18); 3)the locus of genes that acquire ETM are recruited to nuclear boundary during gene transcription and they stay there for 4 to 12 hours after gene expression(20); 4) the proximal-promoter of primed genes have an open state of chromatin(17); 5) it could there be a long-range interaction between gene regulatory regions (*e.g.*, proximal promoter and enhancers), forming a chromatin loop, sustained by cohesins(21); 6) also, incorporation of histone variants H2A.Z to proximal-promoter chromatin region(20),(22); and, 7) an enrichment of H3K4me2 histone modification and poised-RNAPII during "resting period" (after the first activation)(19,23). In general, *in vitro* ETM experimental design includes a double-hit-protocol, where two stimuli are separated by several cellular divisions(17,19).

Here, we propose here that oxidative-stress can induce, by itself, an ETM-like response in antioxidant coding-genes. To evaluate our hypothesis we tested oxidant stressors in a double-

hit-protocol on Control-HUAEC and endothelial cell line EA.hy926. The models allowed to evaluate chromatin-related features associated with ETM, increasing the knowledge about the gene regulation by oxidative stress.

RESULTS

H_2O_2-priming induces an epigenetic transcriptional memory-like response in primary HUAEC

To evaluate the hypothesis proposed, a double-hit-protocol using classical oxidative stressors was applied. As a first attempt, a double-hit-protocol with 40 μM tBHQ in quiescence-induced HUAEC was implemented, mimicking post-mitotic state of endothelial cells *in vivo* (**Supplementary Figure 1A**). Several mRNA levels of candidate genes were determined by qPCR. There were no differences between cells treated once or twice (**Supplementary Figure 1B).** Since it has been described that mRNA transcription and translation are stopped during mitosis(24), we decided to introduce a cellular proliferative step between the first and second stress, including cell splitting. Using the experimental design described in **Figure 1A** it was possible to get four different experimental conditions i) cells that were Unprimed/Untreated (UP/UT), ii) Primed/Untreated (P/UT), iii) Unprimed/Treated (UP/T) and iv) Primed/Treated (P/T). Using 100 μM H_2O_2 as a stressor in priming and treatment, we found that *HMOX1* mRNA accumulation was increased in P/T cells in comparison to UP/T cells (**Figure 1C**). The mRNA levels of as *NRF2* (**Figure 1B**) or *GCLM* (**Figure 1D**) did not show any difference. Using tBHQ as the stressor, neither *NRF2, HMOX1* nor *GCLM* expressed differential mRNA levels between UP/T and P/T cells, (**Figures 1E**, **1F**, and **1G**, respectively).

These data show that an ETM-like response can be induced by H_2O_2 in primary HUAEC.

H_2O_2-priming induces an epigenetic transcriptional memory-like response in EA.hy926 cells.

. Using the experimental design described in **Figure 2A**, only *HMOX1* mRNA showed an ETM-like response in P/T cells when H_2O_2 was used as a stressor. On the other hand, tBHP or tBHQ showed no difference in mRNA expression between UP/T and P/T cells (**Figure 2C** and **2D**, respectively). *NRF2*, *GPX1*, *GCLM* or *NQO1* mRNA levels, also were analyzed, showing no difference in gene expression (**Supplementary Figure 2**).

To evaluate whether the H_2O_2-induced ETM-like response in the *HMOX1* gene is specific to endothelial cells or it could be a general cellular response, we try double-hit-protocol in HeLa cells. As in EA.hy926 cells, *HMOX1* gene showed an ETM-like response, but in this case, using tBHP as a stressor (**Supplementary Figure 3C**).

Interestingly, H_2O_2-priming induced a diminishing of proliferation rate in EA.hy926 and HeLa cells (**Supplemental figure 5A and 5C**, respectively). However, H_2O_2 priming in EA.hy926 cells did not change cellular sensitivity to a high concentration of H_2O_2 (**Supplemental figure 5B**).

Summarizing, *HMOX1* showed a consistent ability to respond to oxidative stress in an ETM-like manner in both human endothelial and carcinogenic cell lines.

mRNA accumulation in P/T cells is not caused by an alteration in mRNA decay

The increment of *HMOX1* mRNA level in P/T cells could be an effect of an alteration in mRNA decay. To evaluate this option, *HMOX1* mRNA half-life was calculated in the four experimental conditions generated by H_2O_2 double-hit-protocol in EA-hy926. After inducing

an ETM-like response, using 100 μM of H_2O_2 for 3h (**Figure 3A**), general transcription was stopped by treatment with Actinomycin-D (10 μM for 0, 2, 4, 6 or 8 h) and the mRNA levels were measured by qPCR. *HMOX1* mRNA level at each time-point was calculated relative to untreated cells. Using the curves shown in **Figure 3B**, *HMOX1* mRNA half-life was calculated: UP/UT= 4.7 h, P/UT= 5.7 h, UP/T= 2.8 h and P/T= 2.9 h.

The results indicate that treated cells have a shorter mRNA half-life than untreated. However, there is no difference between mRNA half-life UP/T and P/T, indicating that ETM-like response is not related to an altered mRNA decay.

H_2O_2-primed cells have an open state of chromatin in the *HMOX1* regulatory regions

Previously, ETM has been related to chromatin structure modification at the core promoter of the *HLA-DRA* gene(17). Thus, we decided to evaluate DNase I accessibility to regulatory regions of the *HMOX1* gene, including the transcription start site (TSS), Enhancer 1 at about -4kb (E1) and Enhancer 2 at -9 kb from TSS (E2). To evaluate the priming effect on chromatin accessibility, we only included the UP/UT and P/UT conditions at the end of the double-hit-protocol, in EA.hy926. Following the DNase I HS protocol(25), chromatin was partially digested by 0, 6.25, 12.5 and 25 U of DNase I. After DNA extraction, regions of interest were amplified by qPCR. The *PAX7* TSS region was used as an endogenous control to calculate the relative quantity of gDNA. Using this experimental approach, we found that in P/UT cells, E2 and TSS region of *HMOX1* were more digested than UP/UT cells (**Figures 4B** and **4D**, respectively), evidencing that H_2O_2 priming in those regions induces an open state of the chromatin, suggesting the participation of epigenetic mechanisms in this condition.

Phospho-S5-RNAPII at TSS and NRF2 at E2 are enriched in H_2O_2-primed cells

In previous models of ETM, the open state of the chromatin observed in primed cells has been related with an enrichment of RNAPII protein complex(17,19). To determine if H_2O_2-induced ETM had similar features the enrichment of RNAPII-CTD, RNAPII phosphorylated at serine 5 (pS5-RNAP) of CTD and NRF2 at regulatory regions of the *HMOX1* gene were evaluated, using ChIP-qPCR. the The data obtained showed that the TSS region of *HMOX1* had a significant enrichment of RNAPII and pS5-RNAP in P/UT cells, compared to UP/UT cells (**Figures 5A** and **5C**, respectively). Also in P/UT cells, E2 showed a significant enrichment of NRF2 (**Figure 5E**). These results indicate that chromatin structure modifications, induced by the H_2O_2-priming, were related to an enrichment of crucial transcription-related proteins in the core promoter of *HMOX1*.

pS5-RNAPII and NRF2 enrichment is not different between UP/T and P/T cells

To evaluate if priming was related to an enrichment of RNAP-CTD, pS5-RNA and NRF2, at *HMOX1* gene regulatory regions, in UP/T and P/T cells, was calculated. As is showed in **Figures 5B**, **5D** and **5F**, there was no difference in the enrichment levels of these proteins, indicating that after 3 h of H_2O_2 treatment, at least in the evaluated proteins, the transcriptional behavior is the same in both experimental conditions.

DISCUSSION

Intrauterine life impacts cardiometabolic performance during lifespan (Reviewed in(26)); a phenomenon identified as fetal programming(27). Epigenetic has been the most logic mechanism that can explain the phenomenon (Reviewed in (28–30)). However, specific mechanisms are still elusive. Previously, our group demonstrated that fetal chorionic arteries

from LGA newborn from OM have endothelial-dysfunction associated to an altered antioxidant defence (4). Unpublished data indicated that, in LGA-HUAEC, *GPX1* gene has an increased response to an H_2O_2 challenge. We then proposed that the pro-oxidant fetal environment, observed in maternal obesity(31), could act as a chronic stress to endothelial cells, inducing ETM in antioxidant coding-genes. To evaluate if oxidative stress by itself can induce ETM in antioxidant-coding genes, a previously reported double-hit-protocol(17,19) was used. In order to mimic the *in vivo* cellular state, we tried the double-hit-protocol in quiescent cells, induced by serum starvation. Using that approach there were no differences between cells treated once or twice. These results were interpreted as in quiescent cells, the first stress increased antioxidant proteins levels; then, buffering the second challenge and normalizing the gene activation. Then, we introduced a proliferative step in the double-hit-protocol. The results, from that approach, indicated that the *HMOX1* gene showed an ETM-like response in Control-HUAEC, EA.hy926 and HeLa cells, and this was not related to an alteration of mRNA stability. Changes in chromatin structure in *HMOX1* gene regulatory regions were associated to an enrichment of total RNAPII, RNAPII phosphorylated at serine 5 (pS5-RNAPII), a mark of the paused RNAPII, and NRF2 enrichment at the TSS and Enhancer 2, respectively.

Here, we show that H_2O_2 can induce ETM in endothelial cells, characterized by an NRF2 pre-recruitment in Enhancer 2, suggesting ETM as a possible mechanism involved in the programming of endothelial dysfunction.

It is known that oxidative stress induces an adaptive response in prokaryotic and eukaryotic cells(32). However, in several publications using double-hit protocols, both challenges were done in the same cell cycle(33,34). The latter suggests an adaptive response due to the

overexpression of antioxidant enzymes/scaffolds induced by the first challenge, which allows the cell to survive to a second oxidative challenge. A similar effect could ensue in the first experimental design, in which two challenges were made in serum-starved culture media, which induces cell quiescence(35).

In order to evaluate the effect of oxidative-stress on gene expression, a turning-off of the transcriptional machinery was attempted. Gottesfeld(24), indicated that during cellular division general gene expression is silenced. Then, in the experimental protocol, a proliferative step between two challenges was introduced, reinforced by cellular trypsinization and reseeding. Using the new approach it was obtained an ETM-like response at *HMOX1* gene; which not only occurred in HUAEC and EA.hy926 cells, by H_2O_2 treatment but also in HeLa cells, using tBHP as a stressor. These results indicated that oxidative stress is able to induce an ETM-like response, by itself; which it is not a cell-type dependent effect.

In stimuli-responsive genes, ETM is associated to epigenetic modifications made by a first stimulus, also called gene priming; which favors an over-expression of the gene when cells are stimulated again (mechanisms are reviewed by D´Urso and Brickner(36)). ETM has been induced in chicken *Hsp70* gene by heat(37), in *IL2* gene among others in Jurkat cells by phorbol 12-myristate 13-acetate (PMA) combined with calcium ionophore (PMA/I)(38); and in *HLA-DRA* gene among others using INF-γ in HeLa cells(17,19). However, the ETM-like response by oxidative stress in primary human cells or human cell lines has not been reported.

Previous unpublished data suggested that *GPX1* gene in LGA-HUAEC could have acquired ETM due to the pro-oxidant environment developed in obese pregnant. Contrary to the expected, the gene did not show any over-induction after second stimuli with stressors,

suggesting that oxidative-stress, *per se,* it is not sufficient to alter gene expression of *GPX1*. Further experiment must be made to find the possible mechanism.

Several publications indicated that *HMOX1* mRNA half-life increased when gene expression is induced by hypoxia(39), shear-stress/atorvastatin(40) or nitric oxide(41). We evaluated if H_2O_2 induced ETM-like response is related with an altered *HMOX1* mRNA decay, pointing to possible post-transcriptional mechanisms. Contrary to published data, in our model mRNA half-life were longer in non-treated cells than treated cells. We think that, in EA.hy926 cells, the high amount of *HMOX1* mRNA could be detrimental for the cell. Then, it is necessary to reduce elevated mRNA level quickly. However, there was no difference in the *HMOX1* half-life between unprimed or primed conditions, indicating that mRNA decay mechanisms are not altered in ETM-like response.

An open state of chromatin at gene promoters also is associated with ETM(17). If the region of interest in the genome has a small nucleosome occupancy (open state chromatin), endonucleases (in this case DNase I) are able to digest gDNA easier than a region with high nucleosome occupancy (closed state of chromatin). Using a modified protocol of DNase HS assay, we found that, in primed cells, the regulatory regions Enhancer2 and TSS, of the *HMOX1* gene, have an increased accessibility to the endonuclease. Suggesting that, in our model, epigenetic mechanisms could be involved. Since RNAPII enrichment at gene promoter of primed genes has been also described in ETM(21), we decided to evaluate RNAPII enrichment at *HMOX1* gene regulatory regions. H_2O_2-primed EAhy926 showed a significant enrichment of RNAPII at *HMOX1* TSS. Contrary to data reported by Light et al.(19), we found also an enrichment of pS5-RNAPII modification, evidencing an paused-RNAPII recruitment (Reviewed in (43,44)). Compared to untreated state, when both

unprimed and primed cells were stimulated, the enrichment of RNAPII and its serine-5 phosphorylation level decreased. A possible explanation is that during productive elongation phase, RNAPII goes into gene-body(44), decreasing its presence at gene promoter.

After oxidative or electrophilic stress, NRF2-sMAFG/K heterodimer binds at Enhancer1 (-4kb) and Enhancer2 (-9kb) of *HMOX1* gene(45) inducing its transactivation(46). In the H_2O_2-primed cell, we found a clear enrichment of NRF2 in Enhancer 2. As a similar phenomenon, Tu et al. described ETM of *TNFSF10* gene, induced by PMA/I, associated with chromatin structure changes and the enrichment of transcription factor ETS-1 at the gene enhancer(38). Although it has been reported that NRF2 can be retained at nucleus by heterodimerization with sMAFG(47), the mechanism of inheritance through cell cycle are not reported yet. Possibly an alteration in NRF2 nuclear exportation after gene transactivation(48) maintains to NRF2 bound. An interesting finding was reported in NF-E2p45, another member of the family of transcription factors(49) which NRF2 belongs(50). Xin et al. evidenced an enrichment of NF-E2p45 at β-globin enhancer/promoter gene during mitosis, acting as a bookmark of previously activated genes(51).

Further studies must be done to fully depict the epigenetic mechanisms that underlie H_2O_2-induced ETM. Since BACH1 has been evidenced as a MAFK-dependent *HMOX1* repressor(52,53), to evaluate its enrichment at *HMOX1* enhancers in H_2O_2-primed cells becomes relevant. However, other ETM general mechanism could be found in our model. Specific histones modifications, as H3K4me2 at core-promoter(17,19) of *HLA-DRA* gen or H3ace and H4ace at core-promoter/enhancers of *FOS* gene(21), has been associated respectively to INF-γ-induced and PMA/I-induced ETM. Changes in DNA methylation have previously been described. After the first stimulus, demethylation at specific CpG of *IL2*

enhancer induced Oct-1 transcription factor recruitment conducting to an increased response to a second stimulus (54). Interestingly, the *HMOX1* gene has a CpG island at TSS region (from -97 to +163) with 37 CpG; Enhancer 2 also has a high amount of CpGs (**Supplementary Figure 2**). Contrarily to the TSS region, that does not possess an ARE motif, Enhancer 2 has CG dinucleotide in three of its five non-canonical ARE motifs, enabling that changes in the methylation of these CpGs could underlie NRF2 enrichment in H_2O_2-primed cells.

Summarizing, we have evidenced that oxidative stress can induce ETM as a general cellular mechanism. We propose that this phenomenon could be one of the epigenetic mechanisms that programs endothelial dysfunction in offspring of women with pregestational obesity. Further studies are necessary to depict hormonal or stress associated cellular signaling, epigenetic remodelling of chromatin and their possible impact on the cardiovascular physiology.

MATERIAL AND METHODS

Samples

This research was conducted in accordance with the Declaration of Helsinki and Ethics Committee approval from the Faculty of Medicine at the Pontificia Universidad Católica de Chile and by the FONDECYT, as well as patient informed consent were obtained. Placentae were collected immediately after delivery from full-term pregnancies from normotensive, non-smoking, non-alcohol or drug consuming mothers, without intrauterine infection or any other medical or obstetrical complication. Maternal nutritional status was calculated by maternal BMI at delivery corrected by the gestational age (55). Using the National standard

curve(56) newborn where classified according to birth weight and gestational age at birth in adequate (AGE) or large for gestational age (LGA) if their percentile was between 10^{th} and 90^{th} (control group) or > 90^{th} percentile respectively.

Cell isolation and culture

Human umbilical artery (HUAEC) were isolated as described(57). Briefly, endothelial cells were isolated from umbilical arteries by collagenase digestion (0.2 mg/mL) and cultured (37 °C, 5% CO2) up to passage 4 in medium 199 (M199) containing 5 mmol/L D-glucose, 10% newborn calf serum, 10% fetal calf serum, 3.2 mmol/L L-glutamine and 100 U/ mL penicillin-streptomycin. The medium was fully replaced every 2 days until confluence. Prior to extraction confluent cells were exposed to normoxia using a gas mixture (5% CO2-balanced N_2) to obtain 5% O2 [oxygen partial pressure (PO_2) ~33.9 mmHg, normoxia for these endothelial cells] in a hypoxia chamber connected to a PROOX 110 device (BioSpherix, NY, USA), deprived of growth factor (overnight) and then exposed to double-hit-protocol.

EA.hy926 cells were kindly donated by Dr. Simone Mörtl (AG Klinische Strahlenbiologie, Helmholtz Zentrum, München). EAhy926 and HeLa Cells were grown in Iscove's Modified Dulbecco's Medium (Thermo Fisher Scientific) supplemented with sodium bicarbonate (3.024 g/L) and 10% Fetal bovine serum (GIBCO), under standard conditions (37 °C, 5% CO2). Cells were split every 2 days and cultured in fresh media.

Treatments

The double-hit-protocols were performed with H_2O_2 (100 µM), (Merck, USA); *tert*-Butyl Hydroquinone, (tBHQ, 10, 20 or 30 µM) (Sigma,Germany); or *tert*-Butyl Hydroperoxide, (tBHP, 20 or 40 µM) (Sigma, Germany). Actinomycin-D (10 µM) (GIBCO, USA) was used for the mRNA decay assay. DNase HS assay was made using DNase I, RQ1, endonuclease (Promega, USA).

Isolation of total RNA and reverse transcription

Total RNA was isolated using Trizol (Invitrogen, USA) as described(58). RNA quality and integrity was ensured by gel visualization and spectrophotometric analysis (OD260/280) and quantified at 260 nm. Aliquots of 500 ng of total RNA was reversed transcribed using IMPROM II RT kit (Promega, USA).

Relative Quantitative of mRNA

Polymerase chain reactions were performed as described(57), using oligonucleotide primers for human genes of interest (GOI) *GCLM, GPX1*, *HMOX1*, *NRF2* or *NQO1*. Three different mRNAs, *RPLP0, RPLP2* and *ATP5F1*, were used as reference genes for quantification (for primers specification see **supplemental table 1**). Quantification was carried out using the algorithm proposed by Pfaffl(59). GOI mRNA level was relative to the three different reference genes.

mRNA decay assay

Assay was conducted as described(60). At the end of double-hit-protocol, cells were treated with 10 µM of Actinomycin-D for 0, 2, 4, 6 and 8 hrs. At each time point, RNA was extracted

with Trizol and retrotranscribed. *HMOX1* mRNA relative level was determined by qPCR. Using *PAX7* TSS region as endogenous control.

DNAse Hypersensitivity assay

The original protocol by Stewart et al.(25) was used, with some modifications. Briefly C-HUAEC and LGA-HUAEC were cultured in 6 well plates until confluence. After washing with PBS (2X), *in vivo* partial DNA digestion was reached by adding 1 mL of digestion buffer (15 mM Tris-HCl pH 7.5, 60 mM KC1, 15 mM NaCl, 5 mM $MgCl_2$, 0.5 mM EGTA, 300 mM sucrose, 0.5 mM 2-mercaptoethanol, 0.5% NP40 and freshly added 0 U (Control) or 6.25 U of RQ1 DNase (Promega)). After incubation for 5 min at room temperature (22-25°C), the digestion buffer was aspirated and cells were lysed with 0.5 mL of lysis buffer (50 mM Tris-HCl pH 8.0, 20 mM EDTA, 1% SDS, 200 µg/mL Proteinase K (Thermo Scientific) and 20 µg/mL RNase A(Affymetrix, USA) and incubated for 1 h at 37°C. DNA was extracted by the phenol-chloroform method(61). Twenty five ng of DNA per reaction were used for amplifying *NRF2* transcription start site (TSS), *HMOX1* TSS and *GPX1* TSS (GOI). The *PAX7* TSS was used as the reference gene (Primer details in **Supplementary Table 1**). Quantification of DNA was carried out using the algorithm proposed by Pfaffl (59).

Chromatin immune precipitation (ChIP) assay

The ChIP assays was performed as previously described(62). Briefly, chromatin was crosslinked with 1% of formaldehyde in PBS and incubated for 15 min at room temperature. Cells were lysed and sonicated to shear chromatin. Immunoprecipitation was made with the following antibodies: RNAPII-CDT (1 ug; clone 8WG16, #ab817, Abcam), RNAPII-CDT phosphorylated at serine 5 (1 ug; #ab513, Abcam) and NRF2 (5 ug, D1Z9C, Cell signaling).

Crosslinking was reverted and bound DNA was extracted using the phenol:chloroform method(61). Quantitaive PCR was made with 2 uL of sample per reaction for *HMOX1* TSS, Enhancer 1 and Enhancer 2 regions (Primer sequences are described in **Supplementary Table 1**). The amount of immunoprecipitated DNA in each sample was calculated using % of input analysis.

Statistical analysis.

The experiments were done in 3 different control-HUAEC and LGA-HUAEC. In EA.hy926 and HeLa cells the replicates were three or more, as indicated in the figure legend. Values shown are mean ± S.E.M. Comparisons between different experimental conditions were analyzed using Two-way ANOVA, Bonferroni's multiple test, considering $p< 0.05$ as the statistical significance threshold. All the analyses were carried out with the statistical software GraphPad Prism 6.01 (GraphPad Software Inc., San Diego, CA, USA).

Disclosure of Potential Conflicts of Interest

Authors declare that they have no conflict of interest.

Acknowledgements

We thank all the participants in this study for generously helping us in this research. Especially to Dr. Simone Mörtl (AG Klinische Strahlenbiologie, Helmholtz Zentrum, München) for kindly donating the EA.hy926 cells.

Funding

This study was funded by the Chilean National Fund for Scientific and Technological Development, FONDECYT #1171406 and #1120201.

REFERENCES

1. Hamann A. Aktuelles zur Adipositas (mit und ohne Diabetes). Diabetologe 2017:331–41. Doi: 10.1007/s11428-017-0241-7.
2. Gaillard R., Steegers EAP., Duijts L., et al. Childhood cardiometabolic outcomes of maternal obesity during pregnancy: The generation r study. Hypertension 2014;63(4):683–91. Doi: 10.1161/HYPERTENSIONAHA.113.02671.
3. Gaillard R., Steegers EAP., Franco OH., Hofman A., Jaddoe VW V. Maternal weight gain in different periods of pregnancy and childhood cardio-metabolic outcomes. The Generation R Study. Int J Obes 2015;39(4):677–85. Doi: 10.1038/ijo.2014.175.
4. Schneider D., Hernández C., Farías M., Uauy R., Krause BJ., Casanello P. Oxidative stress as common trait of endothelial dysfunction in chorionic arteries from fetuses with IUGR and LGA. Placenta 2015;36(5):552–8. Doi: 10.1016/j.placenta.2015.02.003.
5. Malti N., Merzouk H., Merzouk SA., et al. Oxidative stress and maternal obesity: Feto-placental unit interaction. Placenta 2014;35(6):411–6. Doi: 10.1016/j.placenta.2014.03.010.
6. Li J-M. Endothelial cell superoxide generation: regulation and relevance for cardiovascular pathophysiology. AJP Regul Integr Comp Physiol 2004;287(5):R1014–30. Doi: 10.1152/ajpregu.00124.2004.
7. Cai H., Harrison DG. Endothelial dysfunction in cardiovascular diseases: The role of oxidant stress. Circ Res 2000;87(10):840–4. Doi: 10.1161/01.RES.87.10.840.
8. Young D., Pedre B., Ezeri D., et al. Protein promiscuity in H 2 O 2 signaling 2017:1–115. Doi: 10.1089/ars.2017.7013.
9. Xiong Y., Uys JD., Tew KD., Townsend DM. S-Glutathionylation: From Molecular Mechanisms to Health Outcomes. Antioxid Redox Signal 2011;15(1):233–70. Doi: 10.1089/ars.2010.3540.
10. Pereira A., Fernandes R., Crisóstomo J., Seiça RM., Sena CM. The Sulforaphane and pyridoxamine supplementation normalize endothelial dysfunction associated with type 2 diabetes 2017;(October):13–5. Doi: 10.1038/s41598-017-14733-x.
11. Mcclung JP., Roneker CA., Mu W., et al. Development of insulin resistance and obesity in mice overexpressing cellular glutathione peroxidase. PNAS 2004;101(24):8852–7.
12. El-Osta A. Redox mediating epigenetic changes confer metabolic memories. Circ Res 2012:262–4. Doi: 10.1161/CIRCRESAHA.112.274936.
13. Oo Khor T., Fuentes F., Shu L., et al. Epigenetic DNA Methylation of Anti-oxidative Stress Regulator NRF2 in Human Prostate Cancer. Cancer Prev Res 2014;7(12):1186–97. Doi: 10.1158/1940-6207.CAPR-14-0127.
14. Nguyen A., Duquette N., Mamarbachi M., Thorin E. Epigenetic regulatory effect of exercise on glutathione peroxidase 1 expression in the skeletal muscle of severely dyslipidemic mice. PLoS One 2016;11(3):1–17. Doi: 10.1371/journal.pone.0151526.
15. Sung HY., Choi BO., Jeong JH., Kong KA., Hwang J., Ahn JH. Amyloid beta-mediated hypomethylation of heme oxygenase 1 correlates with cognitive impairment in Alzheimer's disease. PLoS One 2016;11(4):1–20. Doi: 10.1371/journal.pone.0153156.
16. D´Urso A., Brickner JH. Epigenetic transcriptional memory. Curr Genet 2016:1–5. Doi: 10.1007/s00294-016-0661-8.

17. Gialitakis M., Arampatzi P., Makatounakis T., Papamatheakis J. Gamma interferon-dependent transcriptional memory via relocalization of a gene locus to PML nuclear bodies. Mol Cell Biol 2010;30(8):2046–56. Doi: 10.1128/MCB.00906-09.
18. Guan Q., Haroon S., Bravo DG., Will JL., Gasch AP. Cellular memory of acquired stress resistance in Saccharomyces cerevisiae. Genetics 2012;192(2):495–505. Doi: 10.1534/genetics.112.143016.
19. Light WH., Freaney J., Sood V., et al. A conserved role for human Nup98 in altering chromatin structure and promoting epigenetic transcriptional memory. PLoS Biol 2013;11(3):e1001524. Doi: 10.1371/journal.pbio.1001524.
20. Brickner DG., Cajigas I., Fondufe-Mittendorf Y., et al. H2A.Z-mediated localization of genes at the nuclear periphery confers epigenetic memory of previous transcriptional state. PLoS Biol 2007;5(4):e81. Doi: 10.1371/journal.pbio.0050081.
21. Wong MM., Byun JS., Sacta M., Jin Q., Baek S., Gardner K. Promoter-Bound p300 Complexes Facilitate Post-Mitotic Transmission of Transcriptional Memory. PLoS One 2014;9(6):e99989. Doi: 10.1371/journal.pone.0099989.
22. Light WH., Brickner DG., Brand VR., Brickner JH. Interaction of a DNA zip code with the nuclear pore complex promotes H2A.Z incorporation and INO1 transcriptional memory. Mol Cell 2010;40(1):112–25. Doi: 10.1016/j.molcel.2010.09.007.
23. Tan-Wong SM., Wijayatilake HD., Proudfoot NJ. Gene loops function to maintain transcriptional memory through interaction with the nuclear pore complex. Genes Dev 2009;23(22):2610–24. Doi: 10.1101/gad.1823209.
24. Gottesfeld JM., Forbes DJ. Mitotic repression of the transcriptional machinery. Trends Biochem Sci 1997;22(6):197–202. Doi: 10.1016/S0968-0004(97)01045-1.
25. Stewart AF., Reik A., Schütz G. A simpler and better method to cleave chromatin with DNase1 for hypersensitive site analyses. Nucleic Acids Res 1991;19(11):3157. Doi: 10.1093/nar/19.11.3157.
26. Poston L. Influence of maternal nutritional status on vascular function in the offspring. Microcirculation 2011;18(4):256–62. Doi: 10.1111/j.1549-8719.2011.00086.x.
27. de Boo H a., Harding JE. The developmental origins of adult disease (Barker) hypothesis. Aust N Z J Obstet Gynaecol 2006;46(1):4–14. Doi: 10.1111/j.1479-828X.2006.00506.x.
28. Wang G., Walker SO., Hong X., Bartell TR., Wang X. Epigenetics and early life origins of chronic noncommunicable diseases. J Adolesc Heal 2013;52(2 SUPPL.2):S14–21. Doi: 10.1016/j.jadohealth.2012.04.019.
29. Laker RC., Wlodek ME., Connelly JJ., Yan Z. Epigenetic origins of metabolic disease: The impact of the maternal condition to the offspring epigenome and later health consequences. Food Sci Hum Wellness 2013;2(1):1–11. Doi: 10.1016/j.fshw.2013.03.002.
30. Kirchner H., Osler ME., Krook A., Zierath JR. Epigenetic flexibility in metabolic regulation: Disease cause and prevention? Trends Cell Biol 2013;23(5):203–9. Doi: 10.1016/j.tcb.2012.11.008.
31. Malti N., Merzouk H., Merzouk S a., et al. Oxidative stress and maternal obesity: Feto-placental unit interaction. Placenta 2014. Doi: 10.1016/j.placenta.2014.03.010.
32. Lushchak VI. Adaptive response to oxidative stress: Bacteria, fungi, plants and animals. Comp Biochem Physiol Part C 2010;153:175–90. Doi: 10.1016/j.cbpc.2010.10.004.

33. Pickering AM., Vojtovich L., Tower J., A Davies KJ. Oxidative stress adaptation with acute, chronic, and repeated stress. Free Radic Biol Med 2013;55:109–18. Doi: 10.1016/j.freeradbiomed.2012.11.001.
34. Jarrett SG., Boulton ME. Antioxidant up-regulation and increased nuclear DNA protection play key roles in adaptation to oxidative stress in epithelial cells 2005. Doi: 10.1016/j.freeradbiomed.2005.02.003.
35. Deshpande NN., Sorescu D., Seshiah P., et al. Mechanism of hydrogen peroxide-induced cell cycle arrest in vascular smooth muscle. AntioxidRedoxSignal 2002;4(5):845–54.
36. D'Urso A., Brickner JH. Mechanisms of epigenetic memory. Trends Genet 2014:1–7. Doi: 10.1016/j.tig.2014.04.004.
37. Kisliouk T., Cramer T., Meiri N. Methyl CpG level at distal part of heat-shock protein promoter HSP70 exhibits epigenetic memory for heat stress by modulating recruitment of POU2F1-associated nucleosome-remodeling deacetylase (NuRD) complex. J Neurochem 2017;141(3):358–72. Doi: 10.1111/jnc.14014.
38. Tu WJ., Hardy K., Sutton CR., et al. Priming of transcriptional memory responses via the chromatin accessibility landscape in T cells. Sci Rep 2017;7:44825. Doi: 10.1038/srep44825.
39. Panchenko M V., Farber HW., Korn JH. Induction of heme oxygenase-1 by hypoxia and free radicals in human dermal fibroblasts. Am J Physiol Cell Physiol 2000;278(1):C92–101. Doi: http://www.ncbi.nlm.nih.gov/pubmed/10644516.
40. Ali F., Zakkar M., Karu K., et al. Induction of the cytoprotective enzyme heme oxygenase-1 by statins is enhanced in vascular endothelium exposed to laminar shear stress and impaired by disturbed flow. J Biol Chem 2009;284(28):18882–92. Doi: 10.1074/jbc.M109.009886.
41. Kuwano Y., Rabinovic A., Srikantan S., Gorospe M., Demple B., No H. Analysis of nitric oxide-stabilized mRNAs in human fibroblasts reveals HuR-dependent heme oxygenase 1 upregulation. Mol Cell Biol 2009;29(10):2622–35. Doi: 10.1128/MCB.01495-08.
42. Singer S., Zhao R., Barsotti AM., et al. Nuclear pore component Nup98 is a potential tumor suppressor and regulates posttranscriptional expression of select p53 target genes. Mol Cell 2012;48(5):799–810. Doi: 10.1016/j.molcel.2012.09.020.
43. Liu X., Kraus WL., Bai X. Ready, pause, go: Regulation of RNA polymerase II pausing and release by cellular signaling pathways. Trends Biochem Sci 2015;40(9):516–25. Doi: 10.1016/j.tibs.2015.07.003.
44. Adelman K., Lis JT. Promoter-proximal pausing of RNA polymerase II: emerging roles in metazoans. Nat Rev Genet 2012;13(10):720–31. Doi: 10.1038/nrg3293.
45. Chorley BN., Campbell MR., Wang X., et al. Identification of novel NRF2-regulated genes by ChIP-Seq: influence on retinoid X receptor alpha. Nucleic Acids Res 2012;40(15):7416–29. Doi: 10.1093/nar/gks409.
46. Reichard JF., Motz GT., Puga A. Heme oxygenase-1 induction by NRF2 requires inactivation of the transcriptional repressor BACH1. Nucleic Acids Res 2007;35(21):7074–86. Doi: 10.1093/nar/gkm638.
47. Li W., Yu S., Liu T., et al. Heterodimerization with Small Maf Proteins Enhances Nuclear Retention of Nrf2 via Masking the NESzip Motif. Biochim Biophys Acta 2009;1783(10):1847–56. Doi: 10.1016/j.bbamcr.2008.05.024.Heterodimerization.
48. Sun Z., Zhang S., Chan JY., Zhang DD. Keap1 Controls Postinduction Repression of

the Nrf2-Mediated Antioxidant Response by Escorting Nuclear Export of Nrf2. Mol Cell Biol 2007;27(18):6334–49. Doi: 10.1128/MCB.00630-07.
49. Andrews NC., Erdjument-Bromage H., Davidson MB., Tempst P., Orkin SH. Erythroid transcription factor NF-E2 is a haematopoietic-specific basic?leucine zipper protein. Nature 1993;362(6422):722–8. Doi: 10.1038/362722a0.
50. Moi P., Chant K., Asunis I., Cao A., Kant YW., Kan YW. Isolation of NF-E2-related factor 2 (Nrf2), a NF-E2-like basic leucine zipper transcriptional activator that binds to the tandem NF-E2/AP1 repeat of the f-globin locus control region. Genetics 1994;91:9926–30.
51. Xin L., Zhou G-L., Song W., et al. Exploring cellular memory molecules marking competent and active transcriptions. BMC Mol Biol 2007;8:31. Doi: 10.1186/1471-2199-8-31.
52. Sun J., Hoshino H., Takaku K., et al. Hemoprotein Bach1 regulates enhancer availability of heme oxygenase-1 gene. EMBO J 2002;21(19):5216–24. Doi: 10.1093/emboj/cdf516.
53. Reichard JF., Motz GT., Puga A. Heme oxygenase-1 induction by NRF2 requires inactivation of the transcriptional repressor BACH1. Nucleic Acids Res 2007;35(21):7074–86. Doi: 10.1093/nar/gkm638.
54. Murayama A., Sakura K., Nakama M., et al. A specific CpG site demethylation in the human interleukin 2 gene promoter is an epigenetic memory. EMBO J 2006;25(5):1081–92. Doi: 10.1038/sj.emboj.7601012.
55. Rosso P. A new chart to monitor weight gain during pregnancy. Am J Clin Nutr 1985;41(3):644–52. 3976565.
56. González P R., Gómez M R., Castro S R., et al. Curva nacional de distribución de peso al nacer según edad gestacional. Chile, 1993 a 2000. Rev Med Chil 2004;132(10):1155–65. Doi: 10.4067/S0034-98872004001000001.
57. Krause BJ., Costello PM., Muñoz-Urrutia E., Lillycrop KA., Hanson MA., Casanello P. Role of DNA methyltransferase 1 on the altered eNOS expression in human umbilical endothelium from intrauterine growth restricted fetuses. Epigenetics 2013;8(9):944–52. Doi: 10.4161/epi.25579.
58. Krause BJ., Hernandez C., Caniuguir A., et al. Arginase-2 is cooperatively up-regulated by nitric oxide and histone deacetylase inhibition in human umbilical artery endothelial cells. Biochem Pharmacol 2016;99:53–9. Doi: 10.1016/j.bcp.2015.10.018.
59. Pfaffl MW. A new mathematical model for relative quantification in real-time RT-PCR. Nucleic Acids Res 2001;29(9):e45. 11328886.
60. Sambasivarao S V. Messenger RNA Half-Life Measurements in Mammalian Cells Chyi-Ying. Methods Enzymol 2013;18(9):1199–216. Doi: 10.1016/S0076-6879(08)02617-7.Messenger.
61. Green MR., Sambrook J. Isolation of high-molecular-weight DNA using organic solvents. Cold Spring Harb Protoc 2017;2017(4):356–9. Doi: 10.1101/pdb.prot093450.
62. Gómez A V., Galleguillos D., Maass JC., Battaglioli E., Kukuljan M., Andrés ME. CoREST Represses the Heat Shock Response Mediated by HSF1. Mol Cell 2008;31(2):222–31. Doi: 10.1016/j.molcel.2008.06.015.

FIGURES

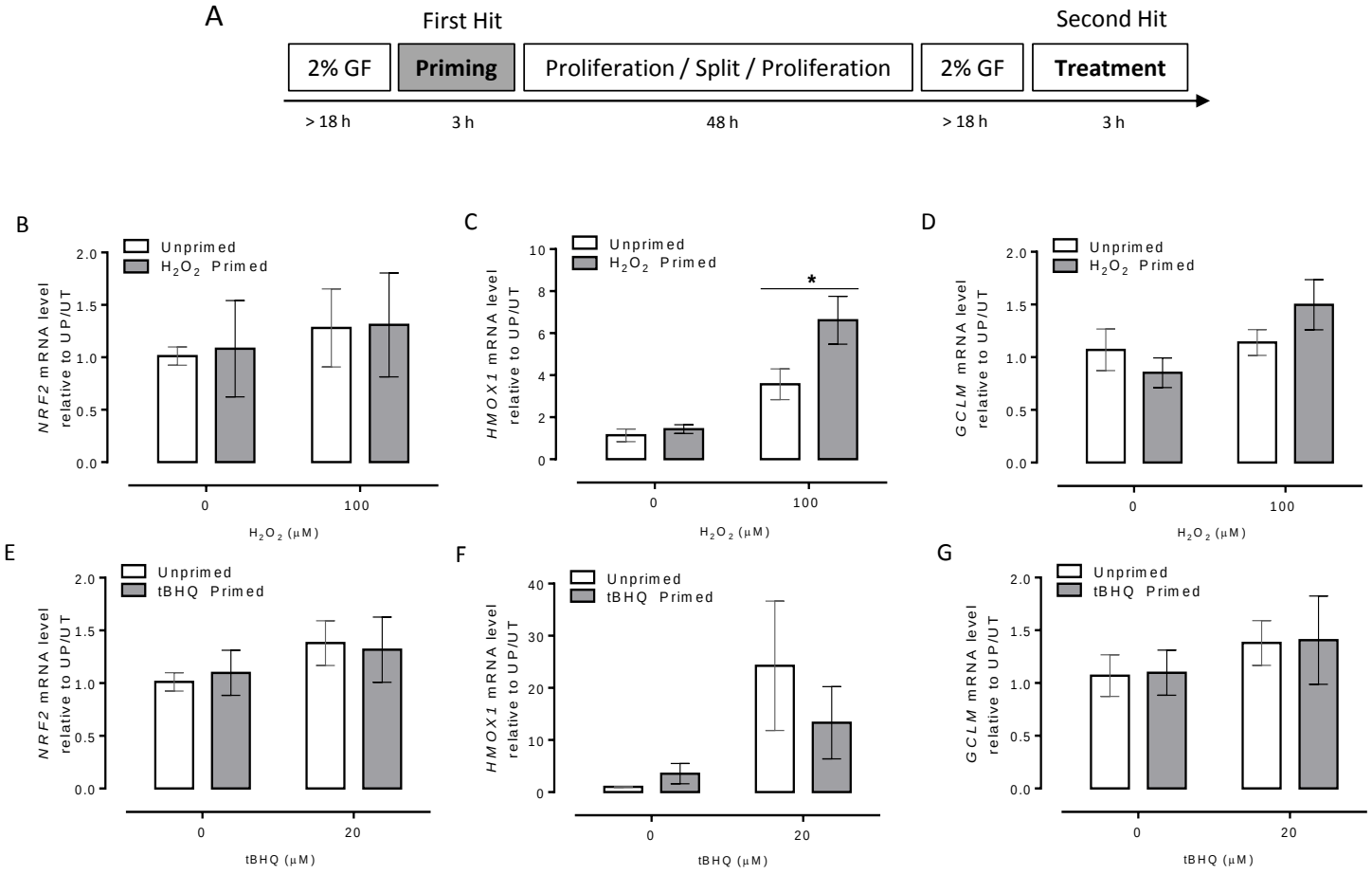

Figure 1. *NRF2, HMOX1* and *GCLM* mRNA level induced by double-hit-protocol in Control-HUAEC. (**A**) The double-hit-protocol scheme in primary Control-HUAEC. Before priming and treatment, cellular quiescence was induced by reduction of MVGF to 2% and atmospheric O_2 to 8%, at least for 18 h. Priming and treatment were made with H_2O_2 (100 µM) or tBHQ (40 µM) for 3 h. After priming, cells were left proliferate in normal culture conditions (21 h, 20% MVGF) and later trypsinized, split and seeded in new plates. Another 21 h of incubation in normal conditions occurred before quiescence induction and treatment (as described previously). The mRNA levels of (**B**) *NRF2*, (**C**) *HMOX1* and (**D**) *GCLM*, induced by the H_2O_2 double-hit-protocol. The mRNA levels of (**E**) *NRF2*, (**F**) *HMOX1* and and (**G**) *GCLM* induced by the tBHQ double-hit-protocol. Values are mean ± S.E.M. * p< 0.05, Unprimed *vs* Primed conditions. Two-way ANOVA, Bonferroni's multiple comparisons test. n=3.

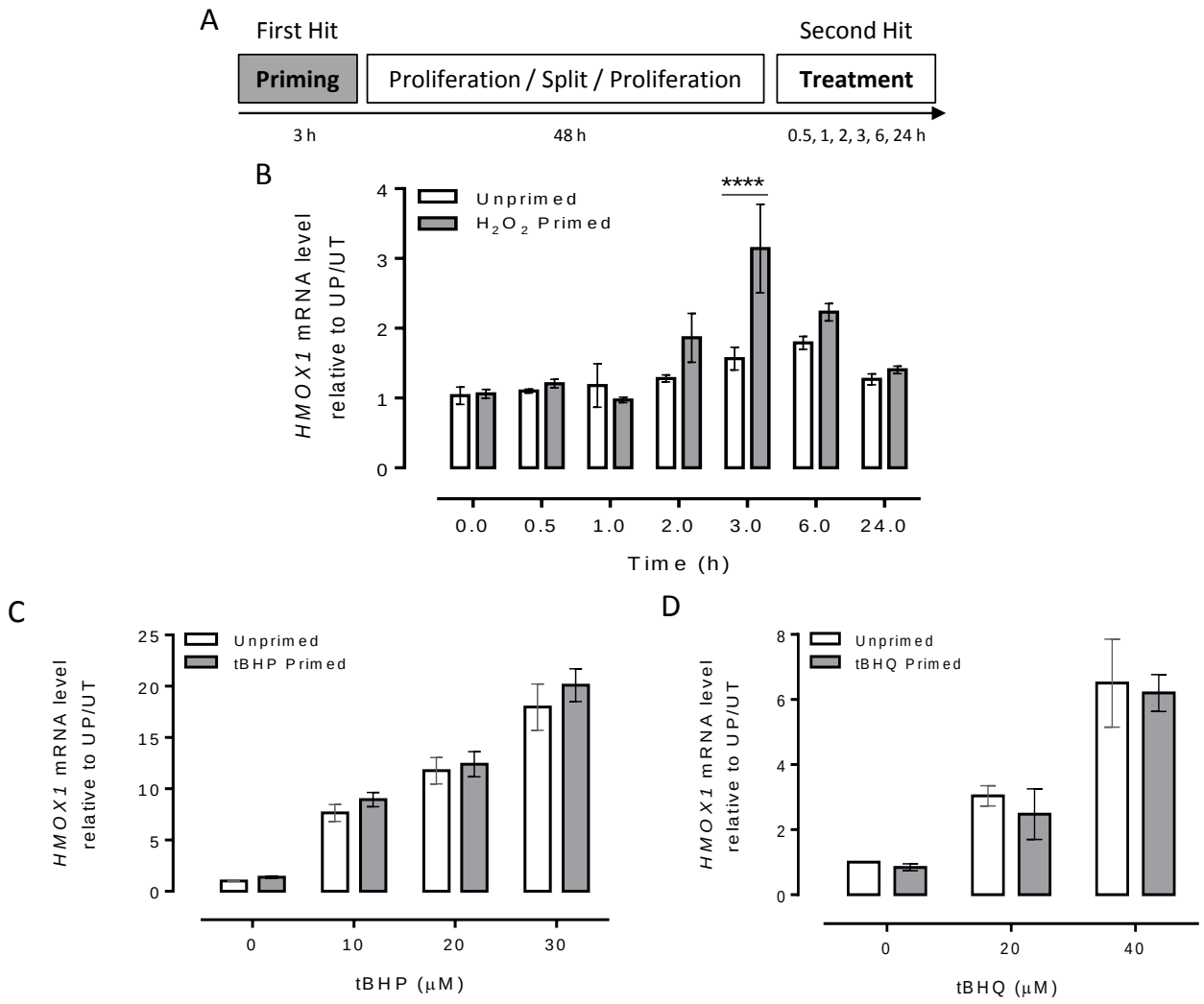

Figure 2. HMOX1 mRNA level induced by the double-hit-protocol in EA.hy926. (**A**) H_2O_2 Double-hit-protocol scheme for EA.hy926 cells. Priming and treatment were made using H_2O_2, tBHP or tBHQ. After priming, cells were left to proliferate (21 h) before trypsinization, splitting and re-seeding in new plates. (**B**) *HMOX1* mRNA level in a time-curve of H_2O_2 treatment, in Unprimed and Primed cells with H_2O_2 (100 µM, 3 h). One cycle of proliferation-split-proliferation during 48 h occurred before the second treatment with the same stressor and concentration, for 0.5, 1, 2, 3, 6 and 24 h. (**C**) Priming with tBHP (10 µM) and a second treatment with 0, 10, 20 or 30 µM of tBHP (3 h) (**D**) Priming with tBHQ (20 µM) and second treatment with 0, 20 or 40 µM of tBHQ (3h). Values are mean ± S.E.M. **** $p < 0.0001$, Unprimed *vs* Primed condition. Two-way ANOVA, Bonferroni's multiple comparisons test. n=3.

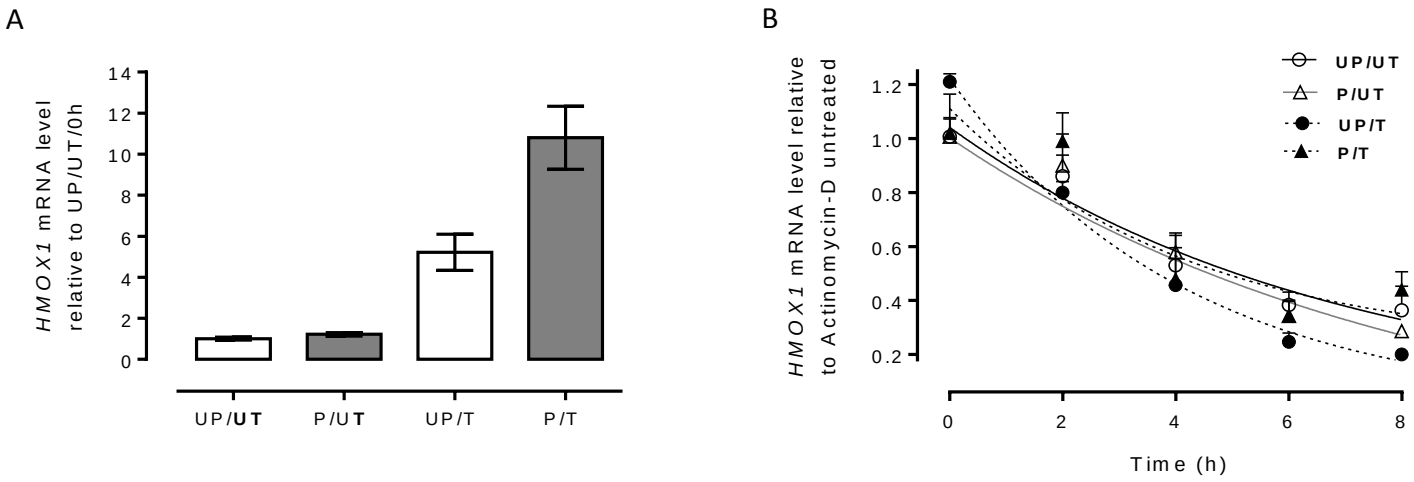

Figure 3. *HMOX1* mRNA half-life after double-hit-protocol in EA.hy926 cells. (**A**) Using H_2O_2 as a stressor (100 µM), the double-hit-protocol was applied to EA.hy926, and *HMOX1* mRNA level was quantified. (**B**) At the end of the protocol, the four experimental conditions were treated with Actinomycin-D (10 µM for 0, 2, 4, 6 and 8 h). For each experimental condition, *HMOX1* mRNA level was calculated (relative to 0 h of treatment). The data obtained were fitted to an exponential function and mRNA half-life calculated. Values for the different conditions were UP/UT= 4.7 h; P/UT= 5.7 h; UP/T= 2.8 h; P/T= 2.9 h. Values are mean ± S.E.M. n=3.

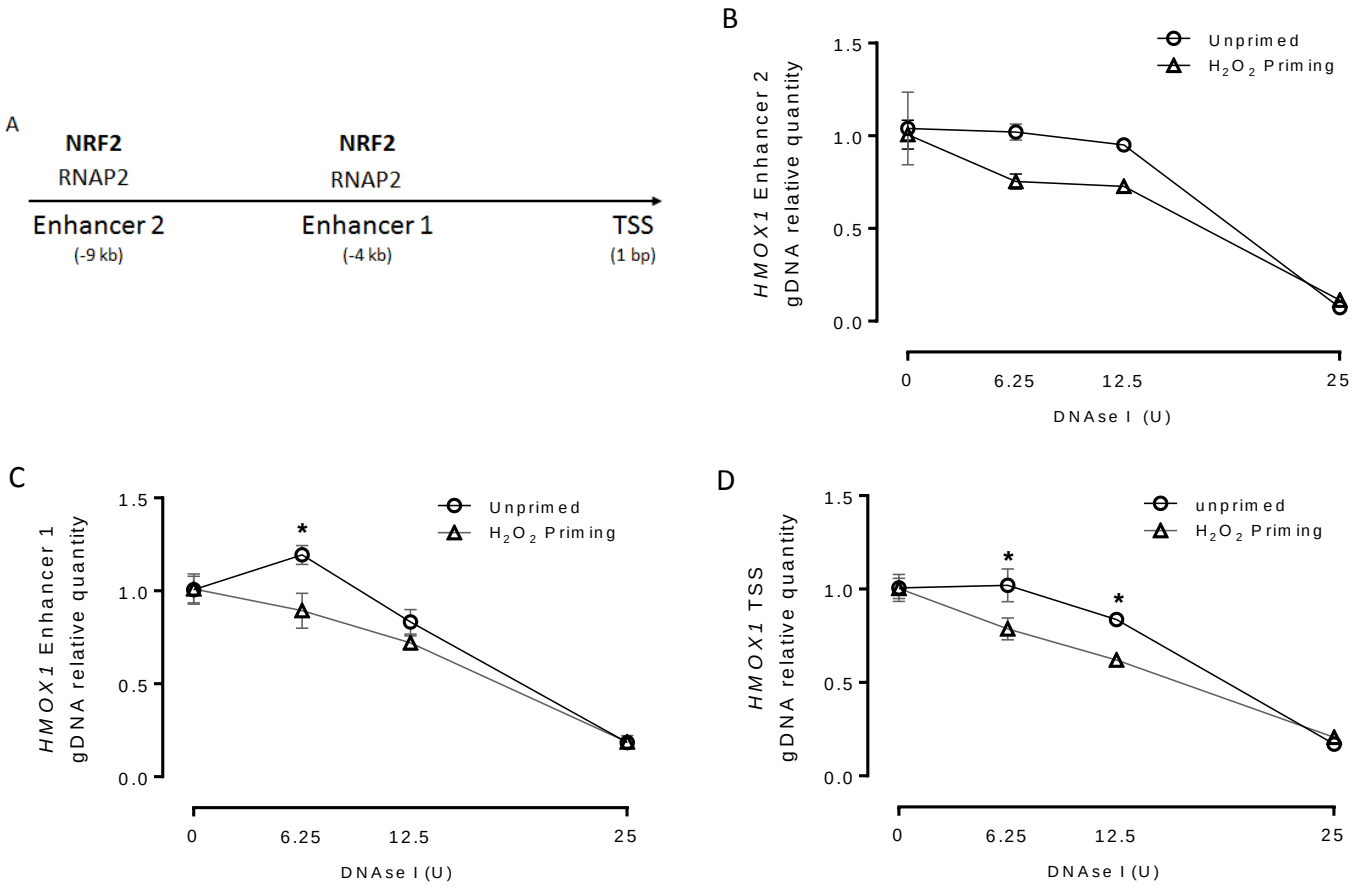

Figure 4. DNase I chromatin accessibility at HMOX1 gene regulatory regions in Unprimed and Primed EA.hy926. (**A**) *HMOX1* gene regulatory regions scheme, indicating sites of RNAPII and NRF2 enrichment described in the literature. EA.hy926 cells were primed or not with 100 µM H_2O_2 for 3 h. Then, the protocol described in **Figure 2A** was followed, but without any second treatment. *in vivo* gDNA digestion was made with 0, 6.25, 12.5 and 25 units of DNase I for 5 minutes at room temperature before cellular lysis and DNA extraction. gDNA relative quantity was calculated for *HMOX1* Enhancer 2 (**B**), Enhancer 1(**C**) and TSS (**D**). *PAX7* TSS was used as an endogenous control gene. Values are mean ± S.E.M. * p< 0.05, Unprimed Vs Primed condition. Two-way ANOVA, Bonferroni's multiple comparisons test. n=3.

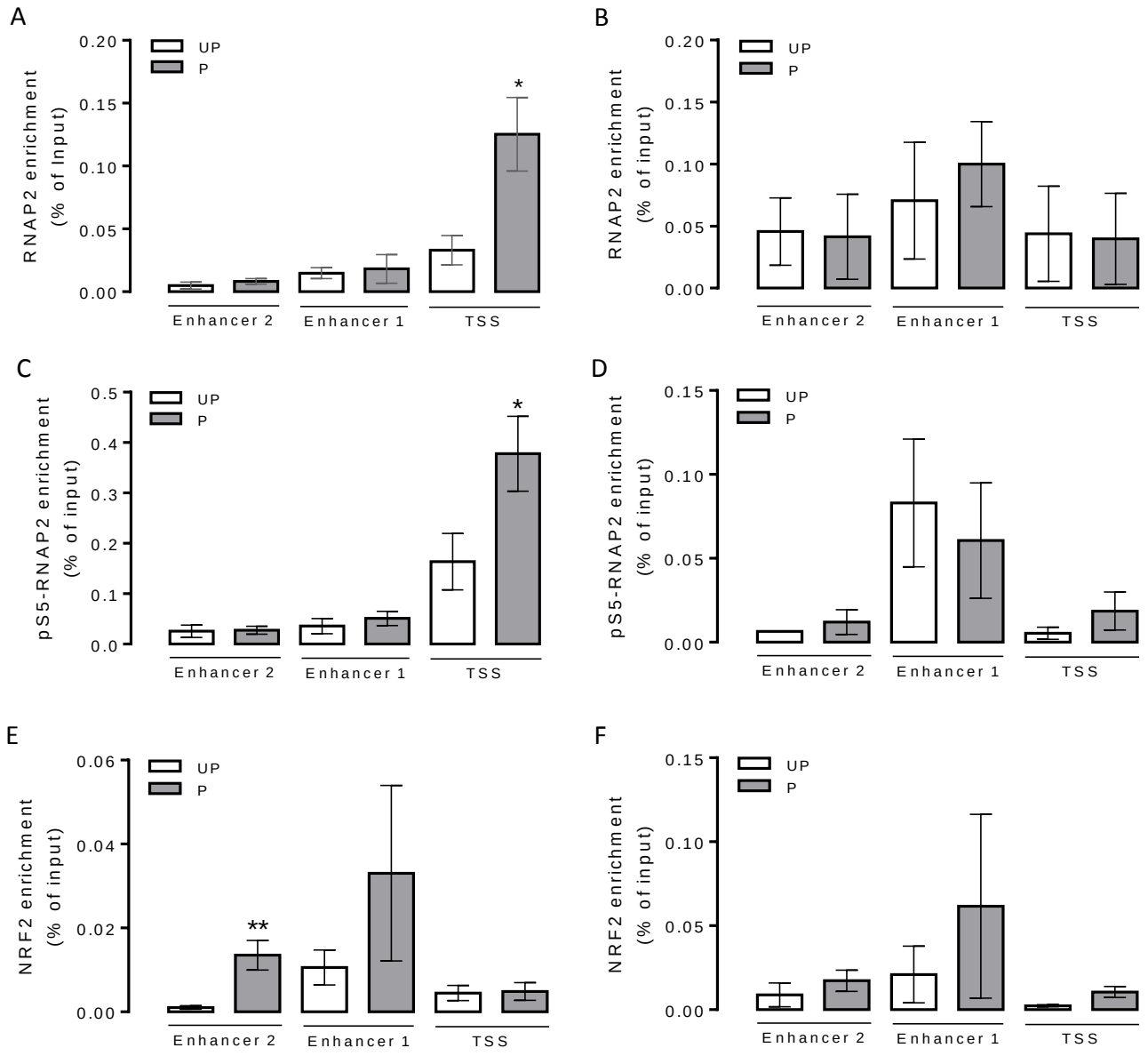

Figure 5. Enrichment of total RNAPII, pS5-RNAPII and NRF2 at *HMOX1* regulatory regions of unprimed or primed EA.hy926 cells in basal or induced transcriptional state. To analyze the basal transcriptional state, EA.hy926 cells were treated with H_2O_2 (100 µM, 3 h). Then, the protocol described in **Figure 2A** was followed, without the second treatment. Finally, ChIP assays were performed (see Methods) for (**A**) RNAPII, (**C**) pS5-RNAPII and (**E**) NRF2 and the *HMOX1* TSS, Enhancer 1 and Enhancer 2 were amplified. Values are mean ± S.E.M. *p< 0.05 **p< 0.01 for Unprimed *vs* Primed condition. Mann-Whitney test. n=6. For induced transcriptional level, double hit protocol was followed, including the second treatment with H_2O_2 (100 µM, 3 h). (**B**) RNAPII-total, (**D**) pS5-RNAPII and (**F**) NRF2 were immunoprecipitated and *HMOX1* TSS, Enhancer 1 and Enhancer 2 were amplified. Values are mean ± S.E.M. n=3.

Supplementary Table 1. Primers specifications.

Target gene	Ref. number ID	Sense	Antisense	Annealing °C	Efficiency %
mRNA					
NRF2	NM_001145412.2	AGGTTGCCCACATTCCCAAA	ACGTAGCCGAAGAAACCTCA	58°	109
HMOX1	NM_002133.2	AAGACTGCGTTCCTGCTCAA	GGGGGCAGAATCTTGCACTT	58°	96
GPX1	NM_000581.2	AGTGCGAGGTGAACGGTGCG	GGGGTCGGTCATAAGCGCGG	58°	94
GCLM	NM_002061.3	GCACAGGTAAAACCAAATAG	GGATCATTGTGAGTCAAC	60	91
NQO1	NM_000903.2	CCAGATATTGTGGCTGAA	CTCTCCTATGAACACTCG	60	107
RPLP0	NM_001002.3	AATCTCCAGGGGCACCATTG	GAACACCTGCTGGATGACCA	58°	93
RPLP2	NM_001004.3	AGCGCCAAGGACATCAAGAA	TAACCTTGTTGAGCCGGTCG	56°	96
ATP5F1	NM_001688.4	GCCCTGACAGATTCTCCTATCG	CAATACCCCTGGACCTAGGAAG	58°	103
gDNA					
PAX7 TSS	NC_000001.11	TAAAAGAAAAGTCCGAACCTATC	GTTCAGGGCTGGACGGA	60°	90
HMOX1 TSS	NC_000022.11	TGGCCAGACTTTGTTTCCCA	TGAGGACGCTCGAGAGGAG	58°	97
HMOX1 E1	NC_000022.11	AGTCGCGATTTCCTCATCCC	GAGAAGCTGAGGAGGCACTG	60°	93
HMOX1 E2	NC_000022.11	CTGCTGAGTAATCCTTTCCCGA	GGGGATTAAACCTGGAGCAGC	60°	109

Supplementary Table 2. Predicted NRF2-binding sites. *HMOX1* gene regulatory regions were inspected for NRF2 binding sites (ARE motif) using TBIND online-tool (http://tfbind.hgc.jp/; Bioinformatics, Vol.15, No.7/8, pp.622-630, 1999.)

Regulatory Region	Strand	Canonical motif	Predicted motif	Similarity (1 =100%)
Enhancer 2	(+)	TGCTGASTCAY	TGCTGAGTAAT	0.91
	(+)	TGCTGASTCAY	TGCTGAGTCAC	1.00
	(+)	TGCTGASTCAY	CGCTAAGTCAC	0.89
	(+)	TGCTGASTCAY	CGCTGAGTCAC	0.98
	(+)	TGCTGASTCAY	CGCTGAGTCAC	0.98
Enhancer 1	(+)	TGCTGASTCAY	TGGCGAGTCAC	0.81
	(+)	TGCTGASTCAY	TGCTGAGTCGC	0.91
	(+)	TGCTGASTCAY	TGCTGCGTCAT	0.90
	(+)	TGCTGASTCAY	TGCTGAGTCAC	1.00
	(+)	TGCTGASTCAY	TGCTGGGTCCC	0.86
Core promoter	(-)	TGCTGASTCAY	GGGCATCAGCT	0.81

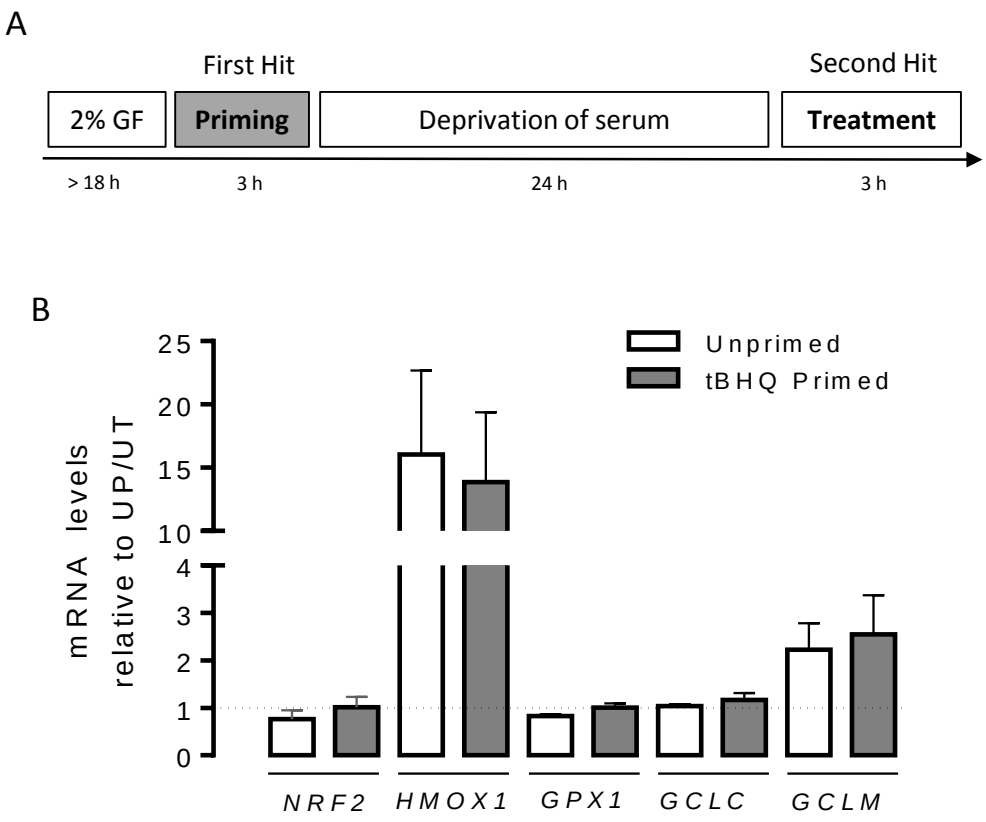

Supplementary Figure 1. Effect of tBHQ double-hit-protocol in antioxidant proteins mRNA level in Control-HUAEC. (**A**) The double-hit-protocol scheme in quiescent primary Control-HUAEC. Before priming cellular quiescence was induced by reduction of MVGF to 2% and atmospheric O_2 to 8%, at least for 18 h. The cells were primed or not with 40 µM tBHQ for 3 h. After priming, the fresh-deprivation medium was renewed and cells were incubated for another 21 h. To both unprimed and primed cells a treatment of 40 µM tBHQ for 3 h was applied. (**B**) Levels of *NRF2*, *HMOX1*, *GPX1*, *GCLC* and *GCLM* mRNAs induced by double-hit-protocol.

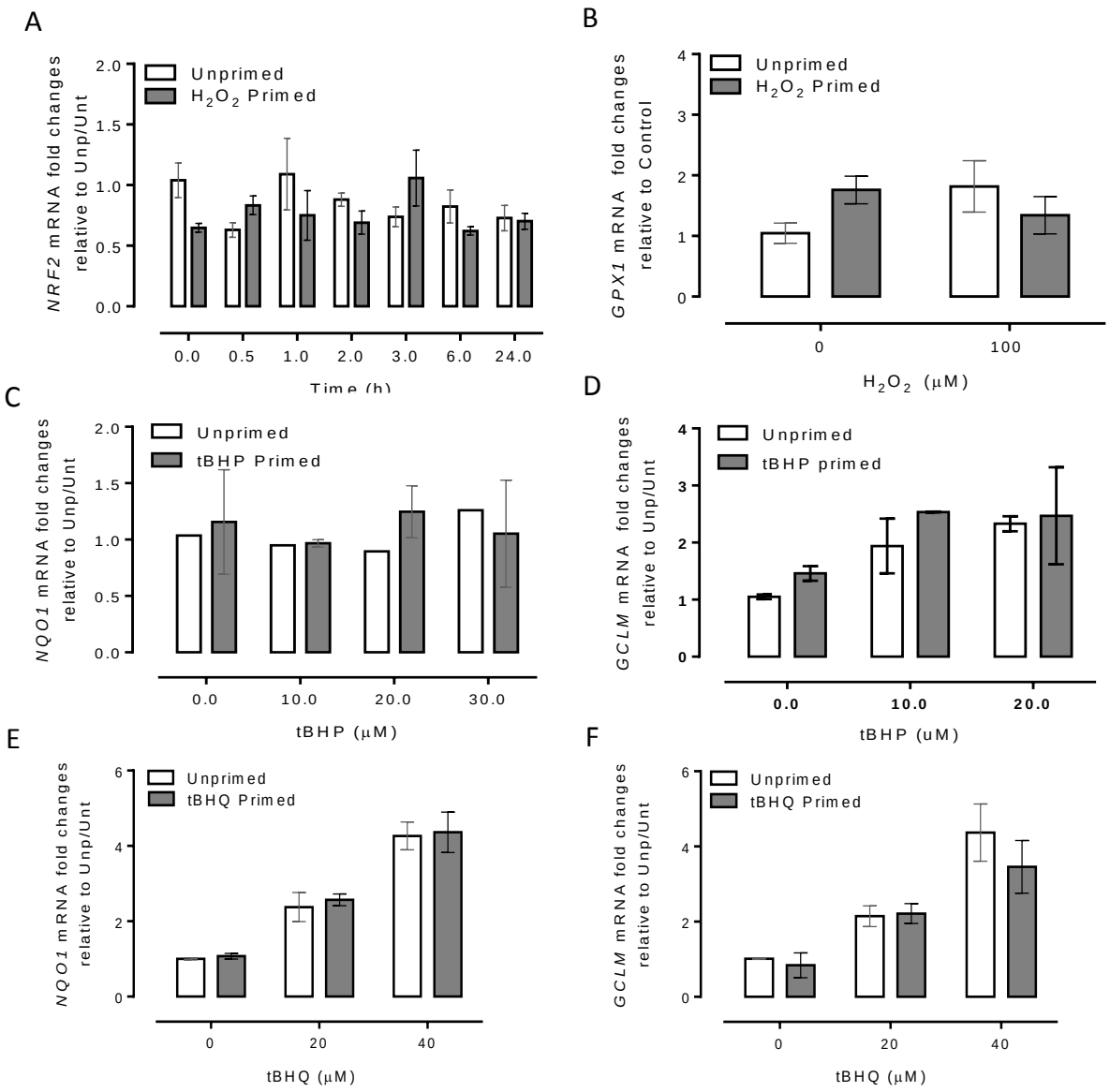

Supplementary Figure 2. *NRF2, GPX1 and GCLM* mRNA level induced by double-hit-protocol in EA.hy926. Double-hit-protocol was applied to EA.hy296 cells using H_2O_2, tBHQ or tBHP as stressors. (**A**) In the same experiment shown in **Fig.2 B** *NRF2* mRNA level was calculated. (**B**) 3 h of H_2O_2 treatment was selected to evaluate *GPX1* mRNA level in unprimed and H_2O_2-Primed cells. In the same experiment shown in **Fig. 2C** also was analyzed of *NQO1* (**C**) and *GCLM* (**D**) mRNA level. In the same experiment shown in **Fig. 2D** also was analyzed of *NQO1* (**E**) and *GCLM* (**F**) mRNA level. Values are mean ± S.E.M. n=3.

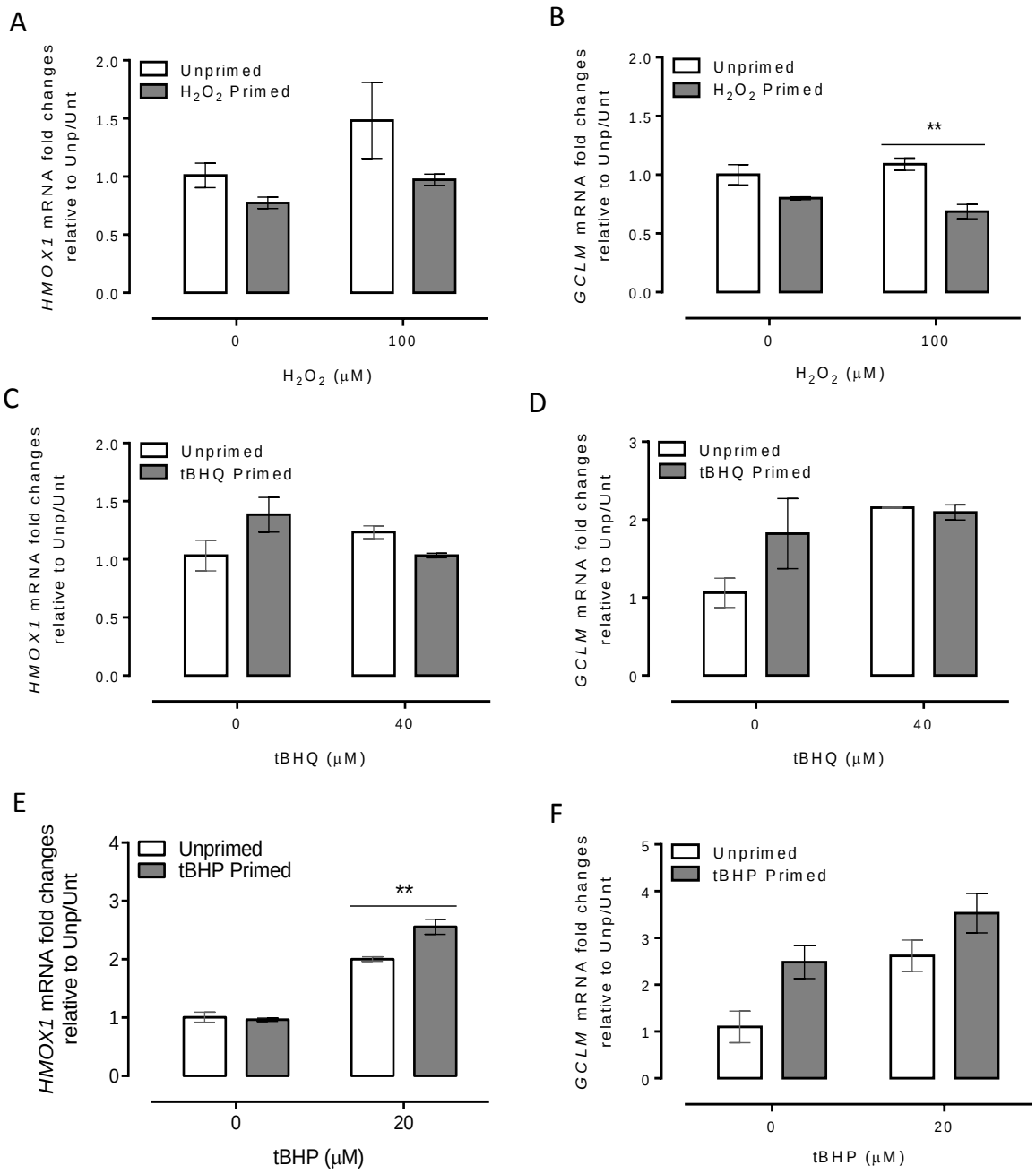

Supplementary Figure 3. *HMOX1 and GCLM* mRNA level induced by double-hit-protocol in HeLa cell. Double-hit-protocol was applied to HeLa cells using H_2O_2, tBHQ or tBHP as stressors. (**A**) *HMOX1* and (**B**) *GCLM* mRNA level were calculated using 100 µM H_2O_2 as stressor. (**C**) *HMOX1* and (**D**) *GCLM* mRNA level were calculated using 40 µM tBHQ as stressor. (**E**) *HMOX1* and (**F**) *GCLM* mRNA level were calculated using 20 µM tBHP as stressor. Values are mean ± S.E.M. * $p< 0.05$, Unprimed Vs Primed condition. Two-way ANOVA, Bonferroni's multiple comparisons test. n=3.

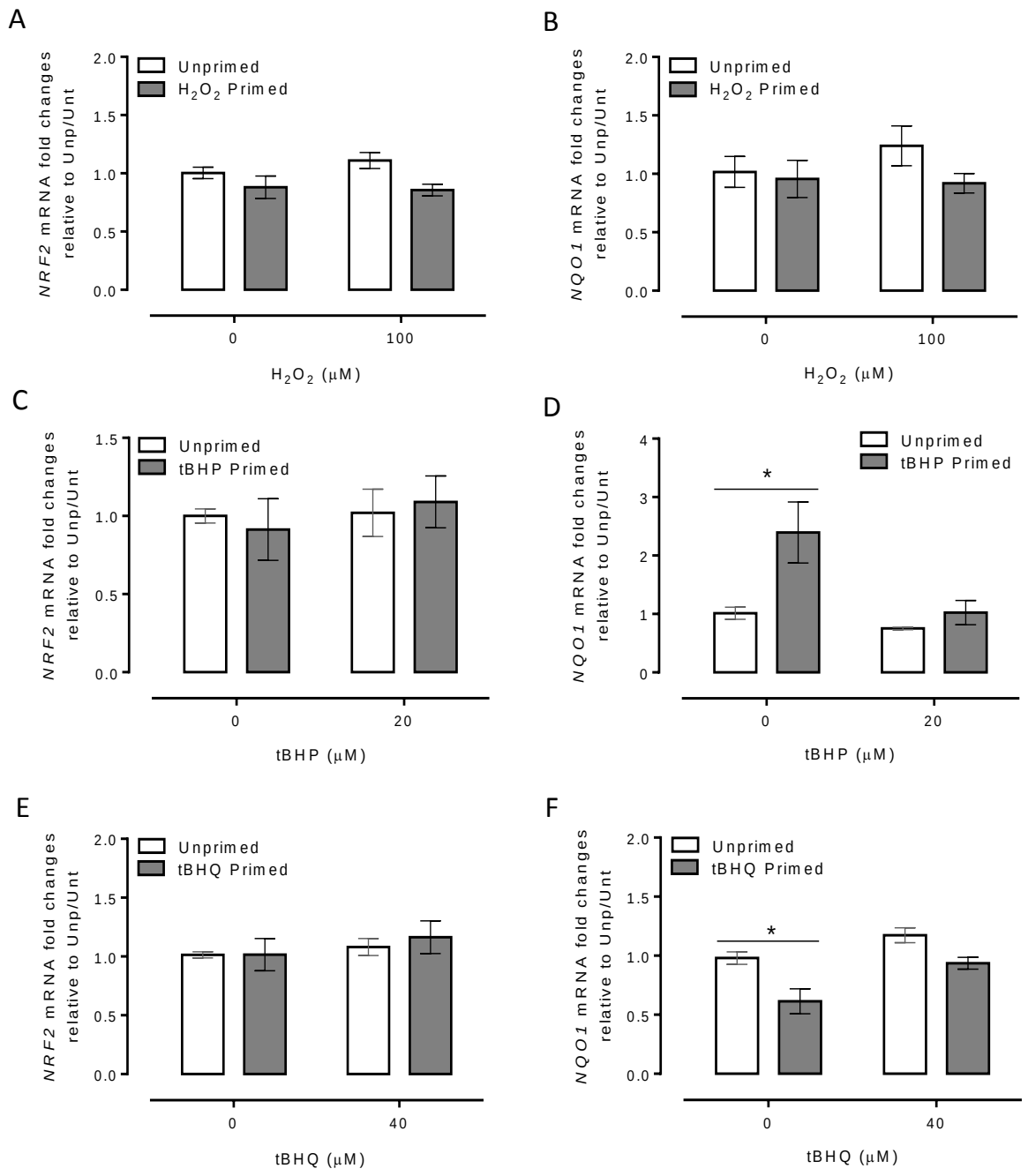

Supplementary Figure 4. *NRF2 and NQO1* mRNA level induced by double-hit-protocol in HeLa cell. Double-hit-protocol was applied to HeLa cells using H_2O_2, tBHQ or tBHP as stressors. (**A**) *NRF2* and (**B**) *NQO1* mRNA level were calculated using 100 µM H_2O_2 as a stressor. (**C**) *NRF2* and (**D**) *NQO1* mRNA level were calculated using 20 µM tBHP as a stressor. (**E**) *NRF2* and (**F**) *NQO1* mRNA level were calculated using 40 µM tBHQ as a stressor. Values are mean ± S.E.M. * $p< 0.05$, Unprimed Vs Primed condition. Two-way ANOVA, Bonferroni's multiple comparisons test. n=3.

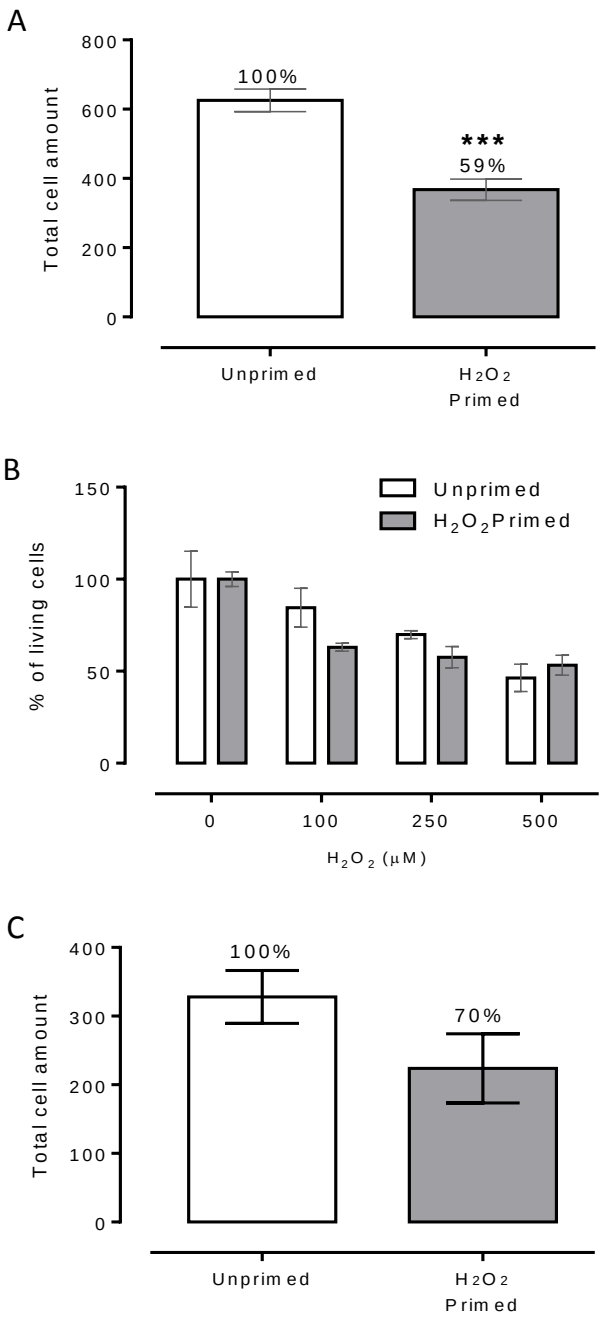

Supplementary Figure 5. H_2O_2 priming effect on cellular proliferation and on H_2O_2 high concentration resistance. (**A**) EA.hy926 cells ($3x10^5$) were seeded and incubated under proliferating condition for 24 h. The cells were then treated with H_2O_2 (100 µM, 3 h) and left proliferate for 21 h. Cells were trypsinized and counted by Trypan blue exclusion method. Values are mean ± S.E.M. *** $p< 0.001$, Unprimed *vs* Primed condition. Mann-Whitney test. n=6. (**B**) The H_2O_2 double-hit-protocol in EA.hy926 cells, where the second stress was made with 0, 100, 250, 500 µM H_2O_2 (6 h). Values are mean ± S.E.M. n= 3. (**C**) HeLa cells ($1x10^5$) were seeded and incubated under proliferating condition for 24 h. Then, cells were treated with H_2O_2 (100 µM, 3 h) and left proliferate for 21 h. Values are mean ± S.E.M. n= 3.

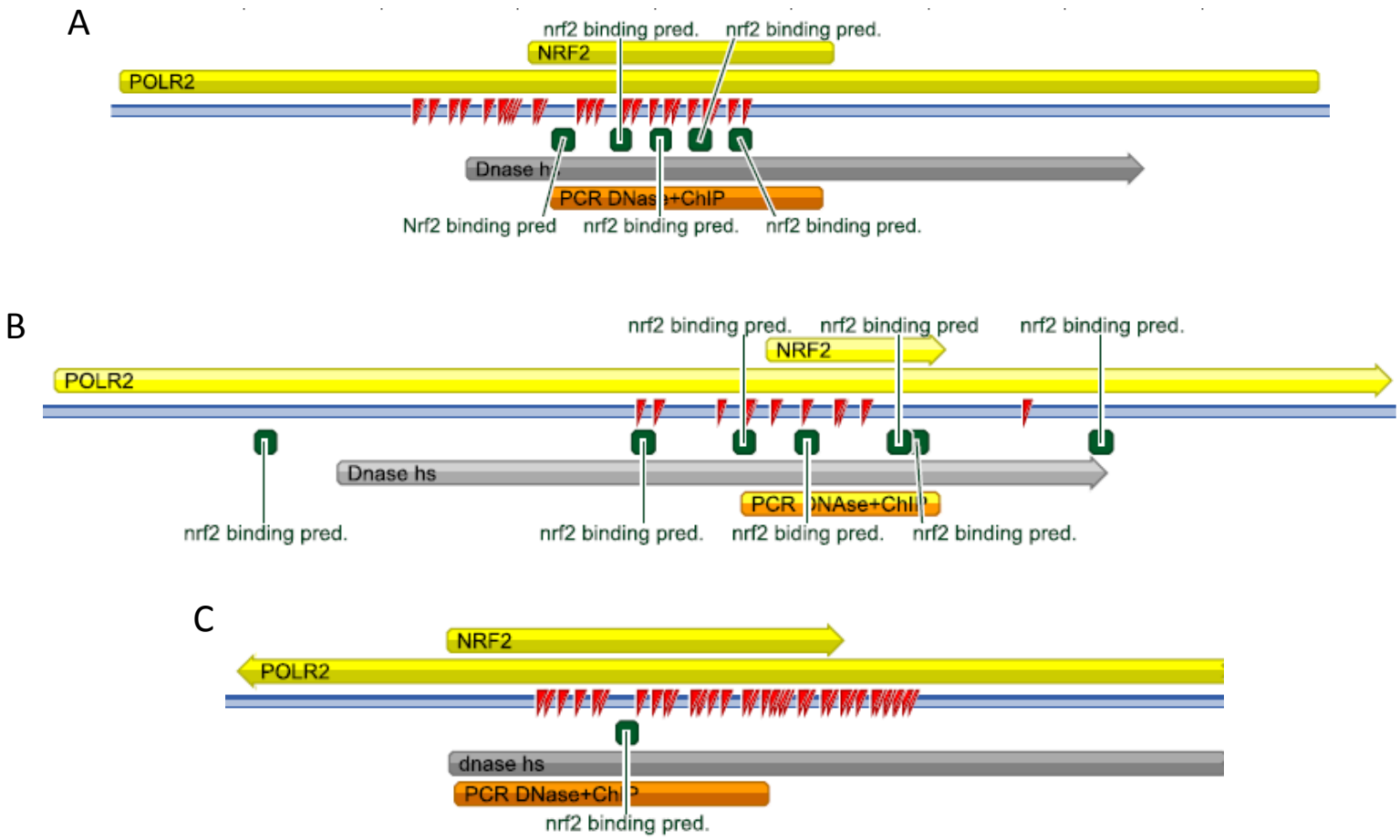

Supplementary Figure 6. CpGs and NRF2 binding sites at *HMOX1* regulatory regions. At **A)** Enhancer 2, **B)** Enhancer 1 and **C)** Core promoter (or TSS) are indicated RNAPII, NRF2 enrichment (Yellow bars) and DNase HS (grey bar) positions, as UCSC Genome Browser on Human Feb. 2009 (GRCh37/hg19) Assembly refers (*Genome Res.* 2002 Jun;12(6):996-1006). Orange bars show positions and sizes of PCR fragments amplified in our DNAse HS and ChIP assays. Red triangles indicate methylable CG dinucleotides. Green squares show the position of predicted ARE (NRF2 binding motif) described in Supplementary Table 2. Schemes were made with Geneious software (Biomatters Ltd.)

CHAPTER 4

GENERAL DISCUSSION.

GENERAL DISCUSSION

CHRONIC AND ACUTE OXIDATIVE STRESS INDUCE DIFFERENTIAL ADAPTATIONS IN ENDOTHELIAL CELLS

The results shown in Chapter 2 were obtained in primary cultures of endothelium from umbilical arteries of the offspring of women with pregestational obesity. As described previously, this is a model of chronic *in vivo* oxidative status. By the other hand Chapter 3 describes the mechanisms involved in the *in vitro* oxidative challenge in a human endothelial cell line. Although both Chapters try to unveil the molecular mechanisms involved in the chronic and acute adaptations to oxidative stress in human endothelium, for the purpose of highlighting the results observed in both models, the results will be discussed separately.

Chapter 2: Human umbilical artery endothelial cells from Large-for-Gestational-Age newborn from women with pregestational obesity have increased antioxidant efficiency and gene expression.

In this *in vivo* model of chronic exposure to oxidative stress, at a basal level we found that: 1) HUAEC from LGA newborn presented higher O_2^- levels, SOD activity, and H_2O_2 tone, compared to the control group; 2) reduced GSH:GSSG ratio *; 3)* increased *HMOX1* mRNA and reduced *NRF2* mRNA levels; 4) Increased *in situ* protein level of NOX4 and SOD1 and 5) an open state of chromatin in *GPX1* gene promoter. In a stimulated state LGA-HUAEC showed: 1) an enhanced *GPX1* expression, 2) a more efficient antioxidant machinery. Altogether the data indicate that LGA-HUAEC have an altered cellular and molecular antioxidant system.

A clear pro-oxidant environment was found in LGA-HUAEC evidenced by a high H_2O_2 tone and reduced GHS/GSSG ratio, suggesting the participation of oxidative stress in the NO-dependent endothelial dysfunction observed in placental arteries from LGA newborn[1]. Other reports showed that bovine aortic endothelial cells (BAEC) treated for 24 h with H_2O_2 showed reduced levels of tetrahydrobiopterin (BH_4), a limiting cofactor for eNOS activity, and its reducing enzyme dihydrofolate reductase (DHFR) [2], leading to eNOS uncoupling and shifting to a superoxide-producing enzyme[3]. Thus, we propose that the previously described pro-oxidant intrauterine environment in pregnancies with LGA from women with obesity [4], leads LGA-HUAEC to shift to an adapted oxidative status. Endothelial dysfunction also was found in genetic and chemically-induced oxidative stress, associated with a reduction of the GSH:GSSG ratio[5]; characterized by an uncoupled eNOS induced by its S-glutathionylation[5,6] and BH_4 oxidation to BH_2 [6]. Previous data in LGA-HUAEC indicated a reduction of eNOS activity[7].

In endothelial cells, two classical signaling pathways have been proved to be regulated by H_2O_2. One of them is VEGF and VEGF receptor 2 expression induced by H_2O_2, that induces cell growth, proliferation, and tube formation[8]. Also, physiological vascular relaxation is regulated by H_2O_2. Endothelial NOS activation can occur by stimulation via PI3K / Akt, ERK or p38 MAP kinases, which are activated by H_2O_2[9,10]. PKG1α kinase, considered one of the major cGMP-independent vascular relaxation regulators[11], can be activated by an H_2O_2-dependent disulfur-bond formation[12]. However, it is important to consider that H_2O_2-signaling has been described in a physiological state. Additionally, the H_2O_2 concentration threshold that unbalances the cell redox status has not been decoded.

Endothelial NOS (eNOS) transfers electrons from NADPH to O_2, which together with L-arginine, are key in nitric oxide ($NO^{\bullet}$) production[13]. In absence of its cofactors, L-arginine and tetrahydrobiopterin (BH4), eNOS shifts to its uncoupled state generating $O_2^{\bullet-}$ instead of $NO^{\bullet}$[14]. One of the mayor endothelial alterations in LGA newborn is the presence of endothelial dysfunction, which is defined as the reduced capacity of a vascular bed to relax in an eNOS-dependent manner[1]. The later can be explained by an uncoupled state of eNOS, induced by the oxidation of BH4 to BH2 by peroxynitrite ($ONOO^-$), a high reactive nitric species (RNS) formed by $NO^{\bullet}$ and $O_2^{\bullet-}$ during oxidative stress[15]; even though, it has been evidenced that BH2 competes with BH4 for eNOS interaction, reinforcing the uncoupled state of eNOS[16].

The main ROS produced by cells is $O_2^{\bullet-}$. There are three different SOD enzymes, encoded by different genes, that are highly compartmentalized[17]. SOD1, a homodimer that has copper and zinc in their catalytic center (CuZn-SOD), resides in the cytosol, nucleus, and lysosome[18–20]. SOD2, a homotetramer, is localized exclusively in the mitochondria, using manganese as a cofactor (Mn-SOD)[21]; and SOD3, a homotetramer that also possesses Cu and Zn, but is exported out of the cell (extracellular, EC-SOD)[22]. Our results evidenced an increased SODs activity and also elevated *in situ* protein level in LGA-HUAEC, compared to the control group. The latter could explain the elevated H_2O_2 tone indicated by Hyper since $O_2^{\bullet-}$ is dismutated to H_2O_2 by members of the superoxide dismutase (SOD) family[23]. In concordance with a systemic oxidative status described in women with pregestational obesity and the LGA-HUAEC response to an increment of superoxide anion production, the protein content of SOD and SOD activity is elevated in LGA umbilical cord blood[4].

NADPH oxidase 4 (NOX4) is the most abundant isoform of NOX in endothelial cells[24]. NOXs uses NAPDH as an electron donor, which is transferred across cellular membranes to molecular oxygen, generating $O_2^{\bullet-}$ [25]. Although, in this thesis, the mRNA and protein level of NOX4 were similar between Control and LGA-HUAEC, in a primary cell culture approach; the *in situ* protein levels were increased in LGA-HUAEC. Although there is no direct evidence of the relation between NOX4 and endothelial dysfunction in an obesogenic environment, other models demonstrate that ROS produced by NOX4 uncouples eNOS; thus, generating endothelial dysfunction.

In our model, the results obtained using the HyPer probe indicate that under basal conditions LGA-HUAEC have elevated level of H_2O_2. However, although there is a basal pro-oxidant status, this seems to be a mild-stress to which the cells can adapt. We propose that LGA endothelial cells adapt to overcome the intrauterine pro-oxidant status, increasing the efficiency of the whole antioxidant machinery, at least for H_2O_2. The latter is evidenced in the Hyper experiments, in which LGA cells were able not only to diminish the protein oxidation induced by an H_2O_2 bolus but also to reduce the oxidized proteins in a shorter period of time, once the stress was removed.

Antioxidant gene programming by the altered maternal metabolic and pro-oxidant environment

The model used, in chapter 2, were primary cell cultures of HUAEC from the offspring of women with pregestational obesity until passage number four. Therefore all the findings of this chapter, alterations of basal levels of *NRF2* and *HMOX1* mRNAs and increased *GPX1* gene expression in response to a new oxidative challenge, necessarily had to be inherited and

passed through several cell divisions. For this reason, we proposed the participation of epigenetic mechanisms in the "oxidative-stress memory". This proposal was further confirmed when the open chromatin state in the *GPX1* gene was evidenced in LGA-HUAEC.

If we consider the "double-hit hypothesis" of DOHAD when we analyze the overexpression of *GPX1* gene in challenged LGA-HUAEC, Epigenetic Transcriptional Memory (ETM) was considered as a potential mechanism which needed to be experimentally confirmed. The altered physiology of the maternal obesity-induced prooxidant milieu in LGA newborn served as first chronic stress for HUAEC.

A link between oxidative stress and epigenetic changes had been previously proposed. El-Osta et al. showed that ROS generated by hyperglycemia-induced the H3K4 monomethylation by Set7/9 methyltransferase at p65 gene[26]. Likewise, transient high glucose and elevated levels of O_2^-, were associated with CpG hypomethylation of the p66Shc gene promoter, favoring the overexpression of the pro-oxidant enzyme gene[27]. The hyperglycemic milieu induced an increase in acetylation of the histones at *HMOX1* gene promoter[28]. This result evidences a mechanism that induces a permanent shift in gene expression. However, it was not the case of the *GPX1* gene in LGA-HUAEC, in which the overexpression by stimulation was not associated with basal gene expression. More studies are necessary to depict obesity-induced hyperresponsiveness of the *GPX1* gene.

Chapter 3. Nrf2 pre-recruitment at enhancer2 is a hallmark of H2O2-induced epigenetic transcriptional memory in *HMOX1* in human endothelial cells.

Epigenetic transcriptional memory mechanism.

The epigenetic transcriptional memory (ETM) has been defined as "an adaptive system that permits a faster response of cells to episodic challenges such as heat stress, nutritional deprivation or infection"[29].

D´Urso and Brickner proposed a model of conserved and universal features of ETM, putting together findings from eukaryotic cells, from yeast and human[29]. They proposed that transcriptional memory requires the retention of the pre-initiation complex (PIC), mediator and poised RNAPII (unphosphorylated state) at the gene proximal promoter after the first transcription ending. The finding that CdK7 kinase is absent in this "memory complex", was reported as crucial since this kinase phosphorylates C- terminal repeat domain of subunit B1 RNAPII at serine 5[30], stimulating the mediator and PIC dissociation and promoting RNAPII escape[31]. These authors proposed a key role of mediator of Cdk8, facilitating the recruitment of a poised-RNAPII[32]; however, other reports indicate that Cdk8 as a critical component of paused-RNAPII released from *HIF1A* promoter under hypoxia[33].

In our model, the oxidative stress-induced ETM was associated with an open state of chromatin at the proximal promoter and Enhancer 2 of the *HMOX1* gene of primed cells. This relaxed chromatin in those regions was related to both paused-RNAPII (serine 5 phosphorylation of CTD) and NRF2 enrichment.

The *HMOX1* has a CpG island (from -97 to +163 bp, respect to TSS), which contains 35 methylable CpG. This is very relevant since Hendrix et al. associated the stalling of RNAPII to genes with an elevated rate of CG dinucleotide repeats at the pausing region[34]. In order to find a difference in the methylation status of the *HMOX1* CpG island that could help to explain the paused RNAPII enrichment in H_2O_2-primed cells, we sequenced that region after a DNA bisulfite conversion of both unprimed and H_2O_2-primed cells. We did not find any

change in methylation status between unprimed or H_2O_2-primed cells. Moreover, all the cytosines of the CpG island were unmethylated, in concordance with a previous report[28]. In our model, changes in the methylation pattern of the CpG island of the *HMOX1* gene is not a feature of RNAPII pausing.

Several DNA *cis*-regulatory elements have been related to RNAPII pausing, such as GAGA element[35], inverted GAGA, initiator and pause button elements[34]. In our model, none of them was found in the *HMOX1* gene promoter (data not showed).

Gene enhancers are not only involved in transcription induction but also have been involved in transcriptional memory mechanism. Murayama et al. showed that demethylation of a specific CpG of IL-2 gene enhancer favored OCT-1 transcription factor enrichment[36]. In a model of ETM of the *FOS* gene induced by a mitogenic stimulus, a long-range interaction by enhancer and the proximal promoter maintained by cohesins was found[37]. In our model, although paused-RNAPII enrichment in primed cells can explain a fast and stronger *HMOX1* expression with a second stimulus, it does not inform about the way that this enrichment occurs, and which is the role of NRF2 pre-recruitment at enhancer 2.

It is known that H_2O_2-dependent *HMOX1* gene induction is due to NRF2 activation[38]. The *HMOX1* has two regulatory regions, enhancer 2 (E2) and enhancer 1 (E1) at -9 kb and -4 kb from the transcription start site (TSS), respectively, in which NRF2 binds after its activation[39,40]. Using transcription binding motif predictor tool[41], we found that E2 and E1 have five ARE elements and that TSS has only one, similar to the amount proposed by Reichard et al.[40]. It can be deduced that those ARE elements could be related to ETM acquisition. Even more, four of the five ARE elements are non-canonical, and contains CG

nucleotides; perhaps the change in the methylation pattern of that specific CpGs could explain the NRF2 recruitment at enhancer 2.

The possible causality of NRF2 in ETM acquisition in the *HMOX1* gene is a hypothesis that requires confirmation. If this statement is true, ETM is a mechanism that crosses mitosis; so, it is possible to propose that the role of NRF2 enrichment in primed cells could be a bookmarking gene process. However, in stress-responsive genes, only *HSP70i* gene has been shown to be bookmarked, by the HSF2 transcription factor, during mitosis[42].

Further experiments are necessary, to completely depict the epigenetic mechanisms that are involved in the oxidative stress-induced ETM of *HMOX1* and possibly other genes.

Reductive stress could be part of endothelial dysfunction in LGA-HUAEC.

The findings exposed in this thesis indicate that i) LGA-HUAEC have a more efficient antioxidant system, which can both reduce H_2O_2 protein oxidation and accelerate their reduction, in concomitance with, an apparent epigenetic programmed over-responding *GPX1* gene., and ii) that an oxidative stress challenge is enough to induce an ETM-dependent *HMOX1* gene over-response, associated with NRF2 and paused-RNAPII pre-recruitment in upstream regulatory elements. However, from a classical point of view, an increase in the antioxidant capacity is associated with a healthy state; but in our model, it seems to be part of the vascular programming context. Then, a new question arises: *What is the relationship between an over-responding antioxidant system and the increased cardiovascular and metabolic risk, observed in individuals who are born as LGA from women with pregestational obesity?*

We propose that both mechanisms could be part of the same metabolic-induced alterations, which could result in a redox status unbalance. A more efficient antioxidant system, related

to over-responding genes could generate reductive stress in the cells. Reductive stress is defined as "*an abnormal increase of reducing equivalents in the presence of intact systems for oxidation and reduction*"[43], where an increment of GSH/GSSG or $NAD/NADH^{+}$ ratio or an elevation of antioxidant enzymes expression can lead to a pathophysiological ROS decline (**Figure 1)**

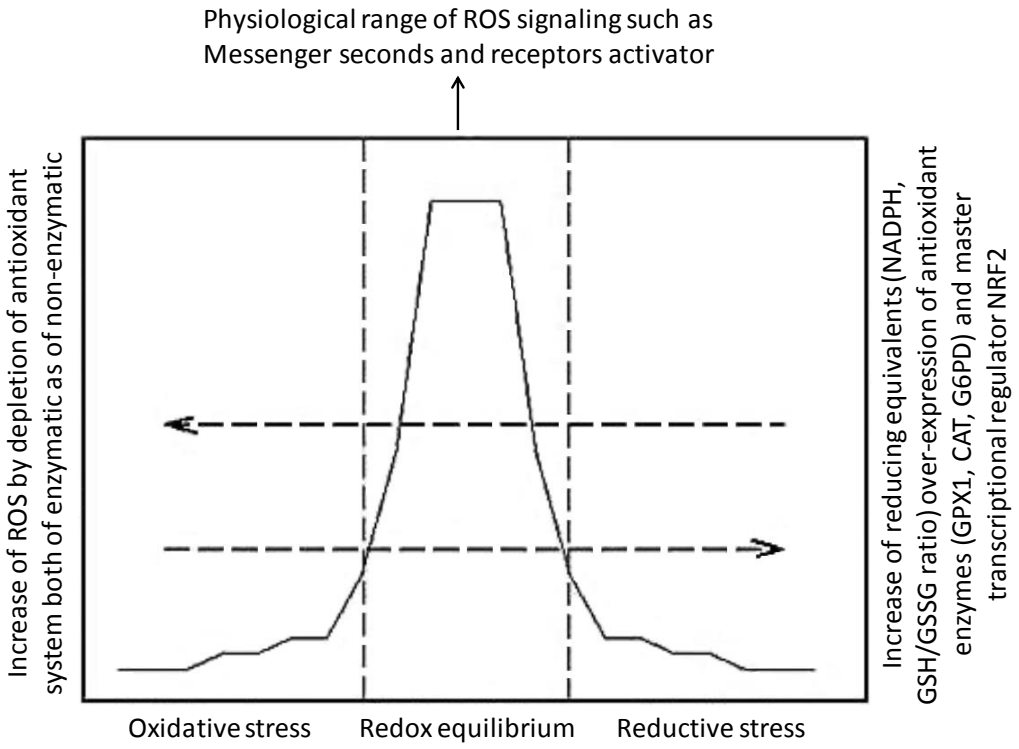

Figure 1. The redox equilibrium is essential for cellular homeostasis. Moderate reactive oxygen species (ROS) production leads to their effects as second messengers. However, ROS overproduction and/or depletion or the antioxidant enzymatic and non-enzymatic systems may lead to oxidative stress. Excess reducing equivalents such as reduced glutathione (GSH)/ oxidized glutathione (GSSG) ratio and reduced nicotinamide adenine dinucleotide (NADPH) can deplete all the ROS, leading to reductive stress by overexpression of an antioxidant enzymatic system. Moreover, chronic reductive stress may induce an oxidative stress and stimulated reductive stress by negative feedback regulation. Nevertheless, this process is not yet clearly understood. (Modified from [44])

Several reports show that an excessive reductive environment deregulates physiological functions, such as cell signaling. The over-expression of GPX1, Prx or catalase reduce the cell signaling generated by growth factor receptors and cellular proliferation[45,46]. The reductive stress is characterized by an excess of GSH availability, which can lead to an abnormal S-glutathionylation of cysteine residues[47], regulating the function of several proteins[48].

There is an important lack of knowledge regarding how the programmed cardiovascular and/or metabolic, of individuals born from mothers with obesity, system response to new stressors during the life span. And maybe there is not a failure of the antioxidant system but a stronger one.

Conclusion and perspectives

The original research question that guided this thesis was: *Do LGA-HUAEC from women with pregestational obesity have an altered redox balance?* In order to answer the question, several experimental approaches were designed. The main results that answer this question are summarized in Figure 2. Briefly, an elevated H_2O_2 basal level, high efficiency of H_2O_2 buffering and an augmented reduction capacity; also, an open state of the chromatin region in the core promoter of *GPX1* gene and overexpression of the *GPX1* gene after the stimulus, in comparison with control cells.

Thereafter, new questions arose such as *What are the cellular mechanisms and pathways, altered by oxidative stress, that induce endothelial dysfunction? What are the original stimuli and epigenetic mechanisms involved in the permanence of the altered redox balance through several cell cycles?* To answer the latter question we hypothesized that oxidative stress by itself can induce an epigenetic transcriptional memory in ARE-dependent genes. Opposing

to our expectations, the findings of ETM observed in primary cultured-HUAEC were not reproducible in an *in vitro* endothelial cell line exposed to chronic OxS stimuli, indicating that in the programming of antioxidant genes, in LGA-HUAEC from obese mother, additional factors participate, possibly acting in synergy with the evidenced redox imbalance.

Epigenetic transcriptional memory (ETM) can be induced by oxidative stress (OxS) in the *HMOX1* gene characterized by an overexpression of the gene after a second challenge (found in control-HUAEC, EA.hy926, and HeLa); an open state of the chromatin regions in Enhancer 2 and core promoter of the gene; an enrichment of NRF2 and a paused-RNAPII in Enhancer 2 and core promoter, respectively (Figure 2). OxS-ETM links a physiological cellular phenomenon with a mechanism which seems to be part of the epigenetic repertoire that underlies vascular programming. However, the mechanism involved in OxS-ETM seems to be more complex, probably involving molecules such as BRD4, or protein complexes, as Mediator. Several questions await to be answered, such as *Is the interaction between Enhancer 2 and core promoter of HMOX1 gene necessary for the acquisition of ETM? Is the NRF2 recruited to Enhancer 2, after the H_2O_2-priming, enough to transactivate gene transcription? Are there other genes that acquire ETM after an oxidative challenge?*

This thesis just offers a few pieces more to build the puzzle. The complete understanding about the mechanisms that underlie the early programming of vascular function in the offspring of women with pregestational obesity is far from being reached, but its comprehension is fundamental to offer better and opportune treatments and a better life and health to the future generations.

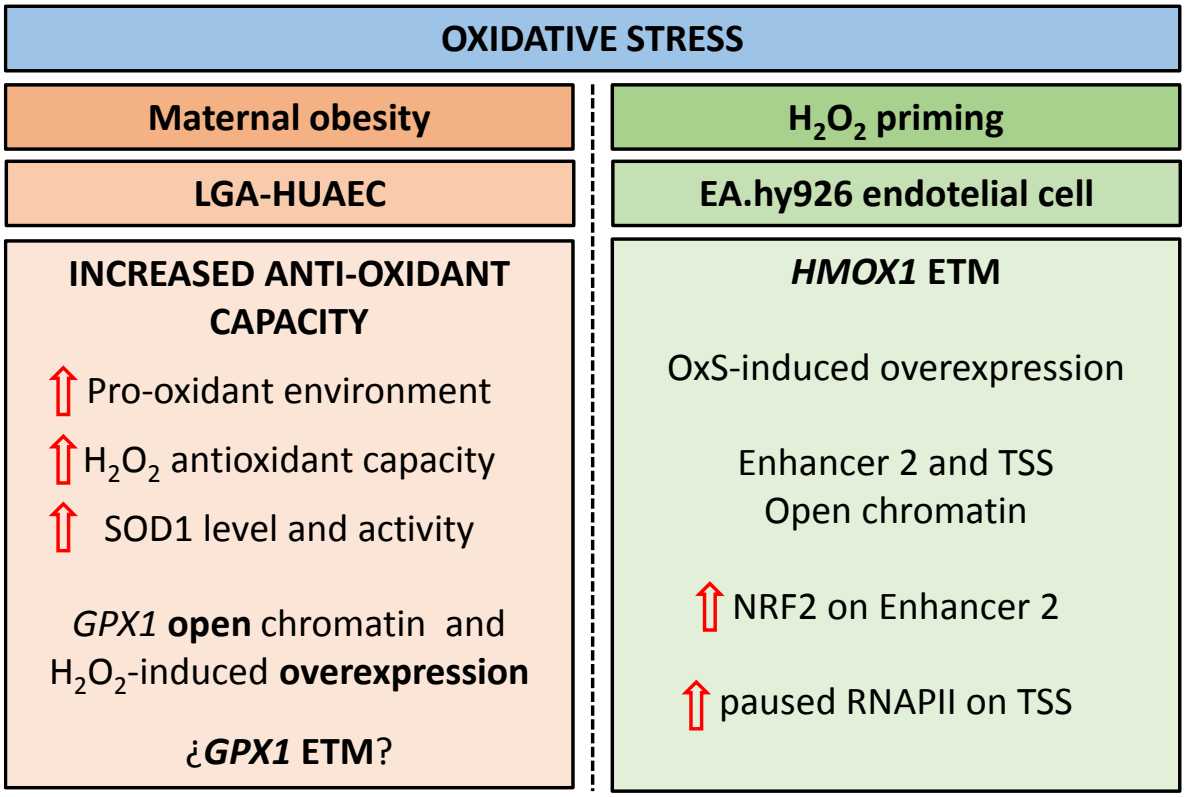

Figure 2. Summary of the results showed in this thesis. LGA-HUAEC from obese mothers showed an increased anti-oxidant capacity characterized by an elevated H_2O_2 basal level, high efficiency of H_2O_2 buffering and an augmented reduction capacity, both in response to an exogenous H_2O_2 bolus. Also, SOD1 was found increased at the protein level and enzymatic activity. In these cells, an open state of the chromatin region containing the core promoter of the *GPX1* gene was found, compared to control cells. After an H_2O_2 challenge, *GPX1* mRNA level was expressed at a higher level than stimulated control cells. On the other hand, using a double-hit-protocol in E.hy926 cells, H_2O_2 was able to induce epigenetic transcriptional memory in the *HMOX1* gene characterized by an overexpression after the second challenge. The priming with H_2O_2 induced relaxation of the chromatin structure at Enhancer 2 and the core promoter of *HMOX1*, which is maintained after cell divisions. Enrichment of the transcription factor NRF2 was observed in the enhancer 2 of *HMOX1* gene in primed cells. Also, the priming induced a pre-recruitment of paused-RNAPII in the core promoter of the *HMOX1* gene.

REFERENCES.

1. Schneider, D. *et al.* Oxidative stress as common trait of endothelial dysfunction in chorionic arteries from fetuses with IUGR and LGA. *Placenta* **36**, 552–558 (2015).
2. Chalupsky, K. & Cai, H. Endothelial dihydrofolate reductase: critical for nitric oxide bioavailability and role in angiotensin II uncoupling of endothelial nitric oxide synthase. *Proc. Natl. Acad. Sci. U. S. A.* **102**, 9056–61 (2005).
3. Förstermann, U. & Münzel, T. Endothelial nitric oxide synthase in vascular disease: From marvel to menace. *Circulation* **113**, 1708–1714 (2006).
4. Malti, N. *et al.* Oxidative stress and maternal obesity: Feto-placental unit interaction. *Placenta* (2014). doi:10.1016/j.placenta.2014.03.010
5. Espinosa-Díez, C. *et al.* Role of glutathione biosynthesis in endothelial dysfunction and fibrosis. *Redox Biol.* **14**, 88–99 (2018).
6. Crabtree, M. J., Brixey, R., Batchelor, H., Hale, A. B. & Channon, K. M. Integrated redox sensor and effector functions for tetrahydrobiopterin- and glutathionylation-dependent endothelial nitric-oxide synthase uncoupling. *J. Biol. Chem.* **288**, 561–569 (2013).
7. Muñoz-Muñoz, E., Krause, B. J., Uauy, R. & Casanello, P. LGA-newborn from patients with pregestational obesity present reduced adiponectin-mediated vascular relaxation and endothelial dysfunction in fetoplacental arteries. *J. Cell. Physiol.* **233**, 6723–6733 (2018).
8. Chua, C. C., Hamdy, R. C. & Chua, B. H. Upregulation of vascular endothelial growth factor by H2O2 in rat heart endothelial cells. *Free Radic. Biol. Med.* **25**, 891–7 (1998).
9. Cai, H. Akt-Dependent Phosphorylation of Serine 1179 and Mitogen-Activated Protein Kinase Kinase/Extracellular Signal-Regulated Kinase 1/2 Cooperatively Mediate Activation of the Endothelial Nitric-Oxide Synthase by Hydrogen Peroxide. *Mol. Pharmacol.* **63**, 325–331 (2003).
10. Bretón-Romero, R. *et al.* Critical role of hydrogen peroxide signaling in the sequential activation of p38 MAPK and eNOS in laminar shear stress. *Free Radic. Biol. Med.* **52**, 1093–1100 (2012).
11. Surks, H. K. cGMP-Dependent Protein Kinase I and Smooth Muscle Relaxation: A Tale of Two Isoforms. *Circ. Res.* **101**, 1078–1080 (2007).
12. Burgoyne, J. R. Cysteine Redox Sensor in PKGIa Enables Oxidant-Induced Activation. *Initiatives* **1393**, 1393–1398 (2007).
13. Palmer, R. M. J., Ashton, D. S. & Moncada, S. Vascular endothelial cells synthesize nitric oxide from L-arginine. *Nature* **333**, 664–666 (1988).
14. Landmesser, U. *et al.* Oxidation of tetrahydrobiopterin leads to uncoupling of endothelial cell nitric oxide synthase in hypertension. *J. Clin. Invest.* **111**, 1201–9 (2003).
15. Kuzkaya, N., Weissmann, N., Harrison, D. G. & Dikalov, S. Interactions of peroxynitrite, tetrahydrobiopterin, ascorbic acid, and thiols: Implications for uncoupling endothelial nitric-oxide synthase. *J. Biol. Chem.* **278**, 22546–22554 (2003).
16. Crabtree, M. J., Smith, C. L., Lam, G., Goligorsky, M. S. & Gross, S. S. Ratio of 5,6,7,8-tetrahydrobiopterin to 7,8-dihydrobiopterin in endothelial cells determines glucose-elicited changes in NO vs. superoxide production by eNOS. *AJP Hear. Circ. Physiol.* **294**, H1530–H1540 (2008).
17. Zelko, I. N., Mariani, T. J. & Folz, R. J. Superoxide dismutase multigene family: a comparison of the CuZn-SOD (SOD1), Mn-SOD (SOD2), and EC-SOD (SOD3) gene structures, evolution, and expression. *Free Radic. Biol. Med.* **33**, 337–349 (2002).
18. Keller, G. A., Warner, T. G., Steimer, K. S. & Hallewell, R. A. Cu,Zn superoxide dismutase is a peroxisomal enzyme in human fibroblasts and hepatoma cells. *Proc. Natl. Acad. Sci. U. S. A.* **88**, 7381–5 (1991).
19. Crapo, J. D., Oury, T., Rabouille, C., Slot, J. W. & Chang, L. Y. Copper,zinc superoxide dismutase is primarily a cytosolic protein in human cells. *Proc. Natl. Acad. Sci. U. S. A.* **89**,

10405–9 (1992).
20. Liou, W. *et al.* Distribution of CuZn superoxide dismutase in rat liver. *Free Radic. Biol. Med.* **14**, 201–207 (1993).
21. Weisiger, R. A. & Fridovich, I. Mitochondrial superoxide simutase. Site of synthesis and intramitochondrial localization. *J. Biol. Chem.* **248**, 4793–6 (1973).
22. Marklund, S. L. Human copper-containing superoxide dismutase of high molecular weight. *Proc. Natl. Acad. Sci. U. S. A.* **79**, 7634–8 (1982).
23. McCord, J. & Fridovich, I. Superoxide Dismutase An enzymic function for erythrocuprein (Hemocuprein). *J. Biol. Chem.* **244**, 6049–6055 (1969).
24. Ago, T. *et al.* Nox4 as the major catalytic component of an endothelial NAD(P)H oxidase. *Circulation* **109**, 227–33 (2004).
25. Bedard, K. & Krause, K.-H. The NOX Family of ROS-Generating NADPH Oxidases: Physiology and Pathophysiology. *Physiol. Rev.* **87**, 245–313 (2007).
26. Assam El-Osta , Daniella Brasacchio , Dachun Yao , Alessandro Pocai , Peter L. Jones , Robert G. Roeder, M. E. C. and M. B. Transient high glucose causes persistent epigenetic changes and altered gene expression during subsequent normoglycemia. *J. Exp. Med.* **205**, 2409–17 (2008).
27. Paneni, F. *et al.* Gene silencing of the mitochondrial adaptor p66Shc suppresses vascular hyperglycemic memory in diabetes. *Circ. Res.* **111**, 278–289 (2012).
28. Pirola, L. *et al.* Genome-wide analysis distinguishes hyperglycemia regulated epigenetic signatures of primary vascular cells. *Genome Res.* **21**, 1601–1615 (2011).
29. D'Urso, A. & Brickner, J. H. Mechanisms of epigenetic memory. *Trends Genet.* 1–7 (2014). doi:10.1016/j.tig.2014.04.004
30. Watanabe, Y. *et al.* Modulation of TFIIH-associated kinase activity by complex formation and its relationship with CTD phosphorylation of RNA polymerase II. *Genes to Cells* **5**, 407–423 (2000).
31. Wong, K. H., Jin, Y. & Struhl, K. TFIIH Phosphorylation of the Pol II CTD Stimulates Mediator Dissociation from the Preinitiation Complex and Promoter Escape. *Mol. Cell* **54**, 601–612 (2014).
32. D'Urso, A. *et al.* Set1/COMPASS and mediator are repurposed to promote epigenetic transcriptional memory. *Elife* **5**, 1–29 (2016).
33. Galbraith, M. D. *et al.* XHIF1A employs CDK8-mediator to stimulate RNAPII elongation in response to hypoxia. *Cell* **153**, 1327–1339 (2013).
34. Hendrix, D. A., Hong, J.-W., Zeitlinger, J., Rokhsar, D. S. & Levine, M. S. Promoter elements associated with RNA Pol II stalling in the Drosophila embryo. *Proc. Natl. Acad. Sci. U. S. A.* **105**, 7762–7 (2008).
35. Shopland, L. S., Hirayoshi, K. & Fernandes, M. HSF access to heat shock elements in criticallv on Promoter vivo de ~ ends TFIID , and RNA polymerase I1. *Genes Dev.* 2756–2769 (1995). doi:10.1101/gad.9.22.2756
36. Murayama, A. *et al.* A specific CpG site demethylation in the human interleukin 2 gene promoter is an epigenetic memory. *EMBO J.* **25**, 1081–1092 (2006).
37. Wong, M. M. *et al.* Promoter-Bound p300 Complexes Facilitate Post-Mitotic Transmission of Transcriptional Memory. *PLoS One* **9**, e99989 (2014).
38. Jian, Z. *et al.* Heme oxygenase-1 protects human melanocytes from H2O2-induced oxidative stress via the Nrf2-ARE pathway. *J. Invest. Dermatol.* **131**, 1420–7 (2011).
39. Chorley, B. N. *et al.* Identification of novel NRF2-regulated genes by ChIP-Seq: influence on retinoid X receptor alpha. *Nucleic Acids Res.* **40**, 7416–29 (2012).
40. Reichard, J. F., Motz, G. T. & Puga, A. Heme oxygenase-1 induction by NRF2 requires inactivation of the transcriptional repressor BACH1. *Nucleic Acids Res.* **35**, 7074–86 (2007).
41. Tsunoda, T. & Takagi, T. Estimating transcription factor bindability on DNA. *Bioinformatics* **15**, 622–630 (1999).

42. Xing, H. *et al.* Mechanism of hsp70i gene bookmarking. *Science* **307**, 421–423 (2005).
43. Singh, F. *et al.* Reductive stress impairs myoblasts mitochondrial function and triggers mitochondrial hormesis. *Biochim. Biophys. Acta - Mol. Cell Res.* **1853**, 1574–1585 (2015).
44. Pérez-Torres, I., Guarner-Lans, V. & Rubio-Ruiz, M. E. Reductive stress in inflammation-associated diseases and the pro-oxidant effect of antioxidant agents. *Int. J. Mol. Sci.* **18**, 1–26 (2017).
45. Handy, D. E. & Loscalzo, J. Responses to reductive stress in the cardiovascular system. *Free Radic. Biol. Med.* **109**, 114–124 (2017).
46. Lubos, E., Loscalzo, J. & Handy, D. E. Glutathione Peroxidase-1 in Health and Disease: From Molecular Mechanisms to Therapeutic Opportunities. *Antioxid. Redox Signal.* **15**, 1957–1997 (2011).
47. Ali, Z. A. *et al.* Oxido-reductive regulation of vascular remodeling by receptor tyrosine kinase ROS1. *J Clin Invest.* **124**, 5159–5174 (2014).
48. Xiong, Y., Uys, J. D., Tew, K. D. & Townsend, D. M. S-Glutathionylation: From Molecular Mechanisms to Health Outcomes. *Antioxid. Redox Signal.* **15**, 233–270 (2011).